Norwegian
Meteorological
Institute

No. 21/2021
ISSN 2387-4201
Meteorology

METreport

Sensitivity experiments with microphysics parameters in MUSC

A study of sensitivity tests to identify target parameters for stochastic parameterisation approaches in AROME-Arctic

Petter Ekrem, Teresa Valkonen, Marvin Kähnert, Harald Sodemann

Title Sensitivity experiments with microphysics parameters in MUSC	**Date** 21 December 2021
Section Meteorology	**Report no.** No. 21/2021
Author(s) Petter Ekrem, Teresa Valkonen, Marvin Kähnert, Harald Sodemann	**Classification** ● Free ○ Restricted
Client(s) Norwegian Research Council	**Client's reference** Project number 280573 ‘Advanced models and weather prediction in the Arctic: enhanced capacity from observations and polar process representations (ALERTNESS)

Abstract

Cloud microphysics schemes in operational forecast models contain many parameters that are only weakly constrained from observations. Such parameters can be suitable targets for stochastic parameterisation approaches. This report summarises a set of sensitivity studies which were conducted with the operational weather forecasting model AROME-Arctic in its single-column version (MUSC). Analysis covered the impacts of changing model parameters on a summer situation with persistent low level (stratocumulus/stratus) clouds over the Barents Sea during July 20, 2018 (YOPP SOP2). The profile was initialised from a HARMONIE-AROME cy43 run. The sensitivity experiments have been made for two vertical profiles with different humidity distribution. Tested parameters were VIGQSAT, RADGR, RSC_H, RZL_INF, RFRMIN(10), and RFRMIN(11), accessible either via the namelist, or implemented as namelist variables. At a second location, in addition the parameters XCCR, RFRMIN(9), and RFRMIN(21) were included in the sensitivity analysis. The sensitivity results can be categorized into 3 outcomes: (i) linear response of cloudiness, hydrometeors, and cloud water, (ii) non-linear response, (iii) no apparent response.

Keywords

Single-column modelling, Parameter sensitivity, MUSC, AROME-Arctic

Disciplinary signature

Responsible signature

Abstract

Cloud microphysics schemes in operational forecast models contain many parameters that are only weakly constrained from observations. Such parameters can be suitable targets for stochastic parameterisation approaches. This report summarises a set of sensitivity studies which were conducted with the operational weather forecasting model AROME-Arctic in its single-column version (MUSC). Analysis covered the impacts of changing model parameters on a summer situation with persistent low level (stratocumulus/stratus) clouds over the Barents Sea during July 20, 2018 (YOPP SOP2). The profile was initialised from a HARMONIE-AROME cy43 run. The sensitivity experiments have been made for two vertical profiles with different humidity distribution. Tested parameters were VIGQSAT, RADGR, RSC_H, RZL_INF, RFRMIN(10), and RFRMIN(11), accessible either via the namelist, or implemented as namelist variables. At a second location, in addition the parameters XCCR, RFRMIN(9), and RFRMIN(21) were included in the sensitivity analysis. The sensitivity results can be categorized into 3 outcomes: (i) linear response of cloudiness, hydrometeors, and cloud water, (ii) non-linear response, (iii) no apparent response.

Meteorologisk institutt	Oslo	Bergen	Tromsø	
Meteorological Institute	P.O. Box 43 Blindern	Allégaten 70	P.O. Box 6314, Langnes	
Org.no 971274042	0313 Oslo, Norway	5007 Bergen, Norway	9293 Tromsø, Norway	
post@met.no	T. +47 22 96 30 00	T. +47 55 23 66 00	T. +47 77 62 13 00	www.met.no

Table of contents

1 Summary

Persistent summertime fog is an important target for high-impact weather at high latitudes. Cloud microphysics contain many parameters that are only weakly constrained from observations. Such parameters can be suitable for stochastic parameterisation approaches, in order to obtain larger spread in model simulations. In order to select potential parameters for perturbation experiments, and to find a suitable perturbation range, a set of sensitivity studies were conducted with the operational weather forecasting model AROME-Arctic in its single-column version (MUSC).

Specifically, the tasks were to (i) conduct sensitivity experiments of the cloud microphysics and other parameterisations, using the 1D version of AROME-Arctic (MUSC), and (ii) to create suitable visualisations and statistic measures to quantify the model sensitivity for different parameters.

Analysis focused first on the impacts of changing model parameters on a summer situation with persistent low level (stratocumulus/stratus) clouds over the Barents Sea during July 20, 2018 (YOPP SOP2). The profile was initialised from a HARMONIE-AROME cy43 run. The sensitivity experiments have been made for two very different vertical profiles, the first one with a relatively thin layer of stratocumulus and the second with a vertically thick cloud layer that is basically wet though the whole troposphere (at least at the initial profile).

At the first location (Bjørnøya Meteorological Station), tested parameters were VIGQSAT, RADGR, RSC_H, RZL_INF, RFRMIN(10), and RFRMIN(11). These parameters were accessible either via the namelist, or implemented as namelist variables. Starting from the default value, the parameters were perturbed within the range recommended by experts, and beyond. The results of these sensitivity experiments are presented in Section 3.

Since no solid precipitation was present at location 1, a second location was chosen that included solid precipitation (Section 4). At that location, in addition to the above parameters, the parameters XCCR, RFRMIN(9), and RFRMIN(21) were included in the sensitivity analysis described in more detail below.

From the sensitivity runs, there can be impacts with regard tocloudiness (L, M, H), hydrometeors (liquid/solid precipitation), and cloud condensate (liquid/ice). These results are summarized in Table 1.

In general, the sensitivity results can be categorized into 3 outcomes:

- Approximately linear response regarding cloudiness, hydrometeros, and cloud water.
- Non-linear response.
- No apparent response for some or all target variables. At location 1, this is the case for RADGR and RFRMIN(11). At location 2, this is the case for RADGR, RFRMIN(11), and RZC_H.

Table 1: Response of different microphysics parameters with regard to cloud cover, hydrometers, and cloud water from MUSC sensitivity experiments. Response is characterized as none, linear, or non-linear.

Parameter	**cloudiness**	**hydrometeors**	**cloud water**
VSIGQSAT	non-linear	non-linear	non-linear
RZC_H	-	-	(linear)
RZL_INF	non-linear	(linear)	non-linear
RFRMIN(10)	-	linear	linear
RFRMIN(9)	-	(linear)	-
XCCR	-	linear	linear
RFRMIN(21)	linear	linear	linear
RFRMIN(11)	-	-	-
RADGR	-	-	-

In conclusion from the sensitivity experiments, the following perturbations to 3D model runs with summertime fog are recommended as a next step:

1. Perturb VSIGQSAT within a range of 0.01-0.06 or slightly higher. Impacts condensate and cloudiness.
2. Perturb RZL_INF within a range of 20-500. Impacts condensate and precipitation and cloudiness.

3. Perturb RFRMIN(10) within a range of 1-100. Impacts condensate and precipitation.
4. Perturb XCCR within a range of 8e5 to 8e8. Impacts condensate and precipitation.
5. Perturb RFRMIN(21) within a range of 0-5. Impacts condensate, precipitation and cloudiness.
6. Perturb RFRMIN(9) within a range of 0.1-10. Impacts precipitation.

From these 3D sensitivity experiments, a candidate for the implementation of SPP should be determined.

Table 2: Parameters that have been perturbed, with default value, accepted range, and tested range.

Parameter	**Default**	**Range**	**Tested**	**Description**
VSIGQSAT	0.02	0-0.06	0.01-0.18	Saturation limit sensitivity
RADGR	0.5	0-1	0.1-3.0	Graupel impact on radiation
RZC_H	0.11	0.1-0.25	0.11-0.6	Stable conditions length scale
RZL_INF	40	20-300	20-500	Asymptotic free atmospheric length scale
RFRMIN(21)	1	0-2	0-6	Cloud ice content impact on cloud thickness
RFRMIN(10)	10	1-50	1-100	Kogan autoconversion speed
RFRMIN(11)	1	0.01-1	0.01-2	Kogan subgrid scale(cloud fraction) sensitivity
RFRMIN(9)	1	0.1-10	0.1-20	Ice nuclei
XCCR	8e6	8e6-8e8	8e5-8e9	rain intercept parameter N0, shifts the distribution from larger to smaller raindrops

2 Radiosonde observations for comparison

Vertical profiles from radiosondes released from the meteorological station at Bjørnøya, have been plotted and examined for the period 30.06-31.07.2018. An example plot from 30.06.2018 can be found below. Plot files are named using the format “YYYY-MM-DD-HH_MM_SS”. All individual launches were examined to find a useful initial condition for the single column model initialisation. Finally, 20 July 2018, a day during YOPP SOP2, was chosen as the first initial time. Figure 2.1 shows the radiosonde launch at 2018-07-19 23:14 UTC.

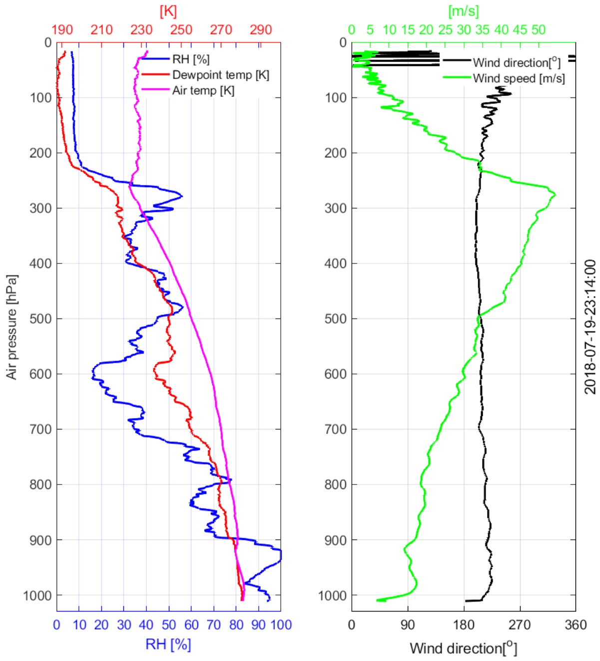

Figure 2.1: Left panel; Vertical profiles from radiosonde observations of relative humidity (%; blue), air temperature (K; magenta) and dewpoint temperature (K, red). Right panel; Vertical profiles from radiosonde observations of wind direction (degrees; black) and wind speed (m/s; green). The date and time can be found on the right y-axis.

3 Parameter sensitivity experiments at Bjørnøya

In this section, all shown results are responses from perturbing different parameters within multiple MUSC runs. All runs were performed for the same 6 hour period. The initialisation point was chosen to represent Bjørnøya Meteorological Station (74.5°N, 19.0°E). MUSC runs were started from the analysis time, with no hydrometeors present in the vertical column. Examined variables were total, low-level, medium, and high-level cloud cover; solid and liquid precipitation; cloud mixing ratio, and specific humidity.

Table 3 provides a summary of the mean and standard deviation values calculated after 3 hours of simulation time to the end of the simulation with a total simulation time of 6 hours. The Figure 3 and similar within this section, and in Section 2 correspond to the numbers given here.

Table 3. Mean values and standard deviation of precipitation amounts during 3-6 hours from model runs with perturbed parameter values. The results are from experiments using the parameters; VSIGQSAT (Saturation limit sensitivity), RZC_H (Stable conditions length scale), RZL_INF (Asymptotic free atmospheric length scale) and RFRMIN(10).

VSIGQSAT	0.01	0.02	0.04	0.06	0.08	0.10	0.12	0.18		
Mean (kg/kg10^{-4})	2.5	2.2	1.4	1.0	1.1	0.9	0.8	1.2		
SD (kg/kg10^{-4})	1.6	1.5	1.1	0.5	0.5	0.4	0.3	0.2		
RZC_H	0.11	0.13	0.15	0.17	0.20	0.23	0.25	0.40	0.60	
Mean (kg/kg10^{-4})	2.2	1.6	1.4	1.3	0.1	0.1	0.1	0	0	
SD (kg/kg10^{-4})	1.5	1.4	1.3	1.2	0.1	0.1	0.1	0	0	

RZL_INF	20	40	60	80	100	150	200	250	300	500
Mean (kg/kg10^{-4})	3.2	2.1	1.7	1.8	1.8	1.4	0.6	0.5	1.4	1.5
SD (kg/kg10^{-4})	1.7	1.5	1.4	1.4	1.4	1.2	0.6	0.3	1.2	1.2
RFRMIN(10)	1	2	5	10	20	30	50	100		
Mean (kg/kg10^{-4})	1.8	1.8	2	2.1	2.5	2.8	3.5	5		
SD (kg/kg10^{-4})	1.4	1.4	1.4	1.5	1.6	1.7	1.8	2.1		

3.1 VSIGQSAT (Saturation limit sensitivity)

This section shows different variable responses from perturbing the parameter VSIGQSAT. Default value 0.02, range by physics experts 0-0.06, tested range 0.01-0.18. Values above 0.06 exceed the range given by physics experts (red below).

Parameter values:

VSIGQSAT	**0.01**	**0.02**	**0.04**	**0.06**	**0.08**	**0.10**	**0.12**	**0.18**

Analysis of the variation of parameter VSIGQSAT showed:

- No changes in cloud cover, except when VSIGQSAT=0.18.
- Lower values (0.01, 0.02, 0.04) give sudden precipitation peaks (Figure 3.2b)
- Reduction in mean and SD liquid precipitation with increasing value in the range suggested by physics experts (Figure 3.3).
- Values larger or equal to 0.06 gives approximately the same precipitation (Figure 3.3)
- VSIGQSAT has a large impact on the amount of cloud water and thickness of cloud cover. The smallest value gives least cloud water and most concentrated cloud layer (Figures 3.4-3.5)

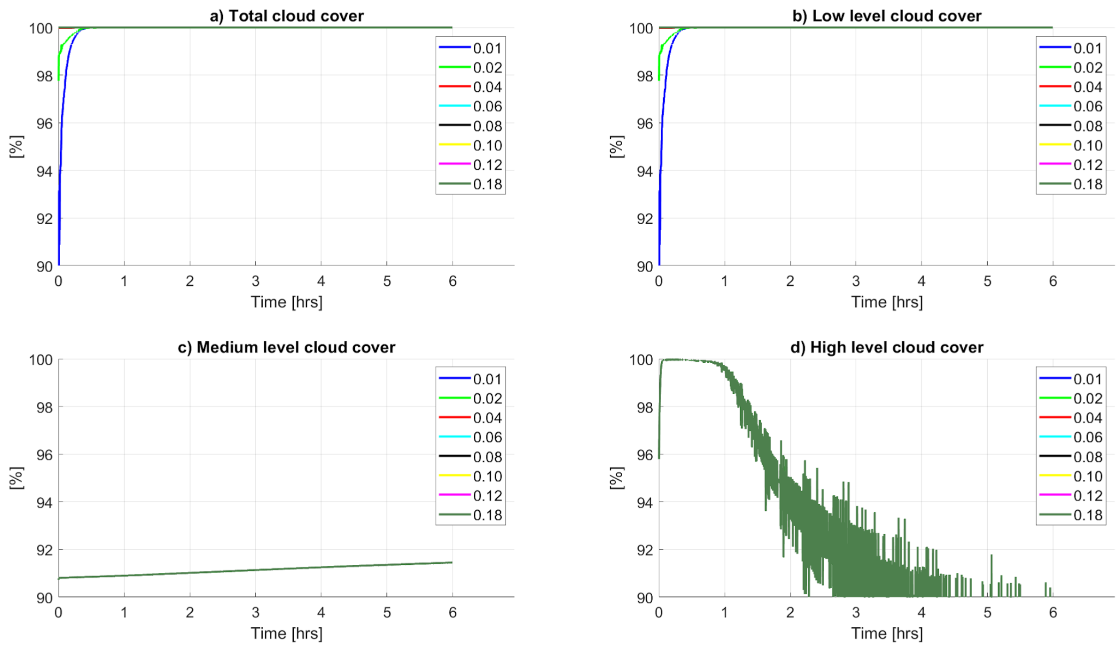

Figure 3.1. Time series of impact on a) total cloud cover, b) low level cloud cover, c) medium level cloud cover, d) high level cloud cover [%] from perturbing the parameter VSIGQSAT. The timeperiod is for 6 hours of simulation time and at the location 74.5°N, 19.0°E. Legend shows color of line plots and corresponding value for the parameter VSIGSAT. The run with VSIGQSAT=0.18 is the only one that shows a response in high level cloud cover (panel d).

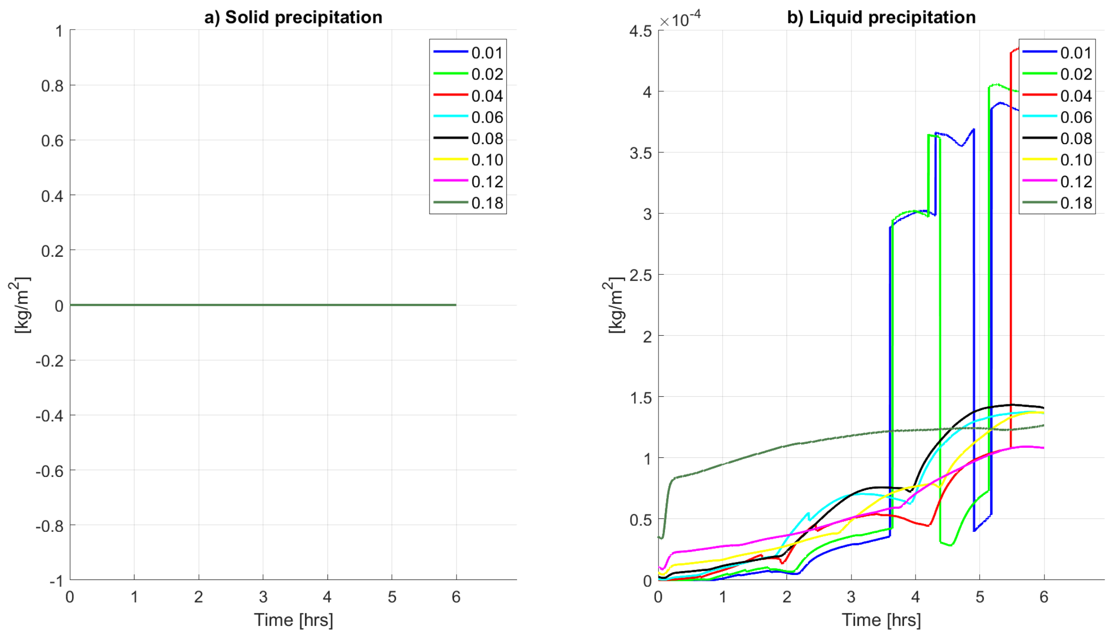

Figure 3.2. As Figure 3.1 but for impact on a) solid precipitation and b) liquid precipitation [kg/m^2] from perturbing the parameter VSIGQSAT. The precipitation has been summed

together for all 66 model layers. A sudden change in liquid precipitation (b) can be identified at 3.5 hours from all the runs with values below the suggested range (0.06).

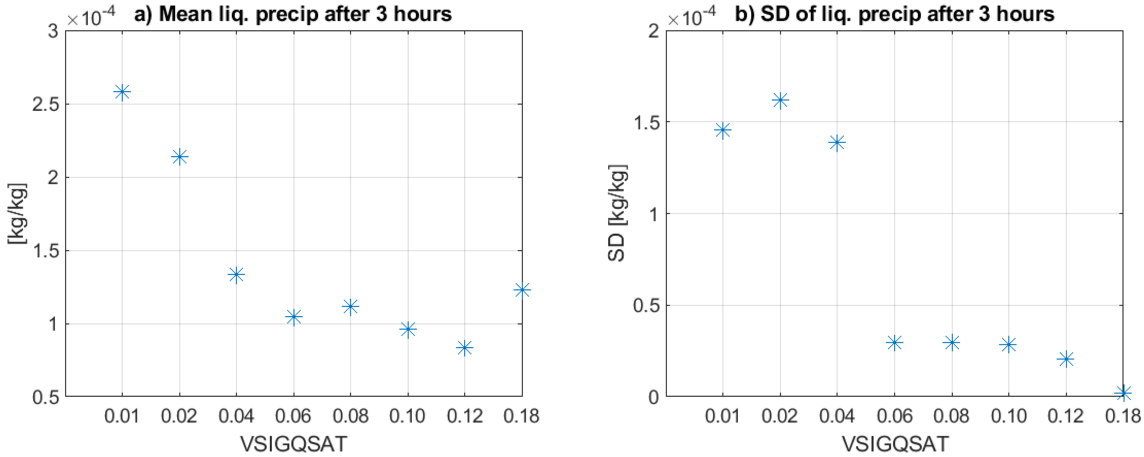

Figure 3.3. Parameter sensitivity after 3h simulation time. a) Mean of liquid precipitation after 3 hours to 6 hours of simulation time. b) standard deviation of liquid precipitation after 3 hours to 6 hours of simulation time. After 3 hours, a sudden increase in precipitation was seen in figure 1.2.

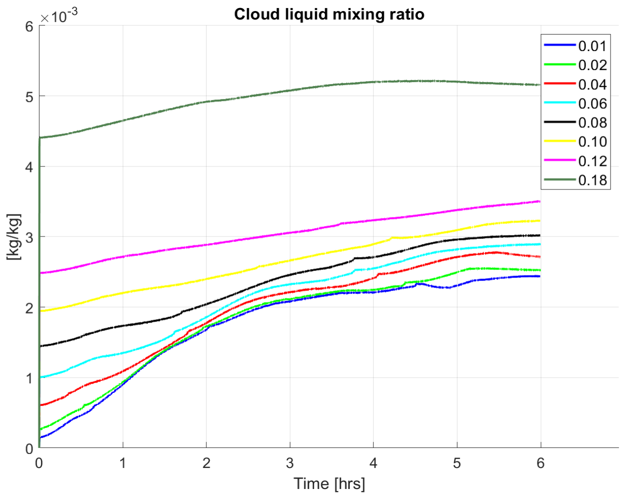

Figure 3.4. As Figure 3.1, but for the impact on cloud liquid mixing ratio [kg/kg] from perturbing the parameter VSIGQSAT. The cloud liquid mixing ratio has been summed together for all 66 model layers.

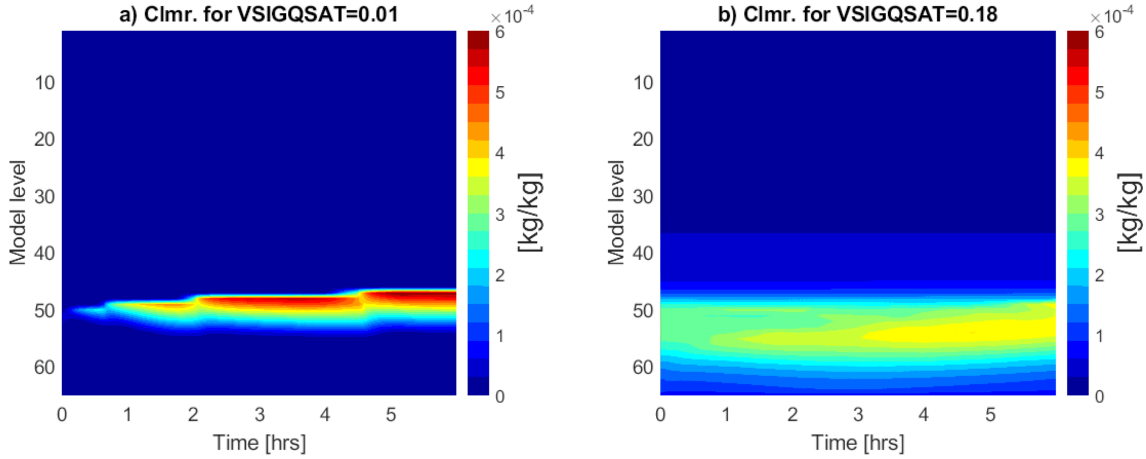

Figure 3.5. Vertical distribution of cloud liquid mixing ratio [kg/kg] with regard to time, with a) VSIGQSAT = 0.01 and b) VSIGQSAT = 0.18.

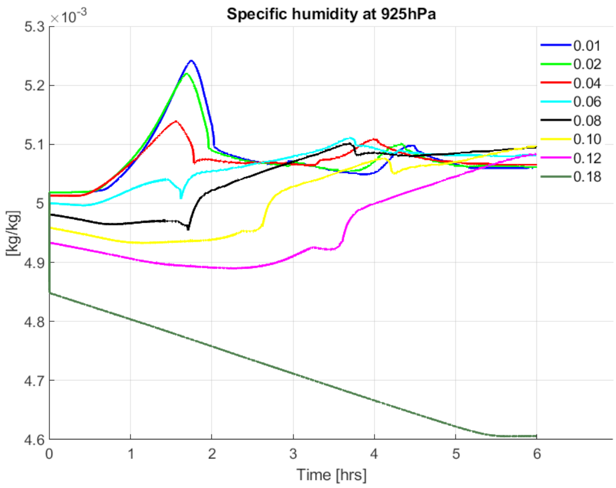

Figure 3.6. As Figure 3.1, but for impact on specific humidity at 925 hPa [kg/kg] from perturbing the parameter VSIGQSAT.

Initial vertical profiles from MUSC output have been inspected to determine if there is a pre-existing difference from different parameter values. Indeed, the model column attains different values for liquid precipitation (Fig. 3.7). The initial state was also explored in terms of cloud liquid mixing ratio (Fig. 3.8) and the initial vertical profiles (Fig. 3.9).

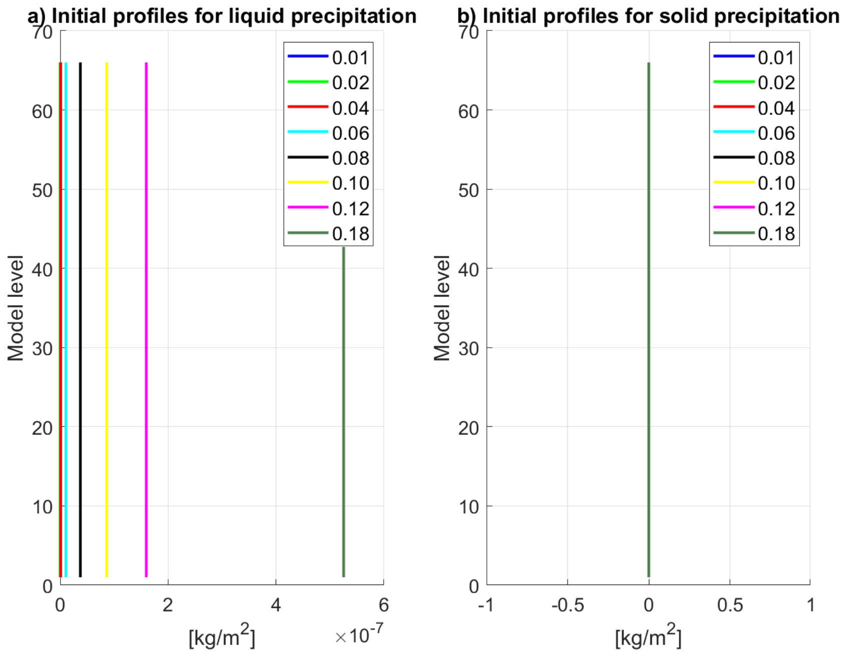

Figure 3.7. Initial vertical profiles of a) liquid precipitation [kg/m^2] and b) solid precipitation [kg/m^2]. The profiles are plotted for the first timestep of the model simulation. In panel b), only one line is shown since all the initial profiles are identical.

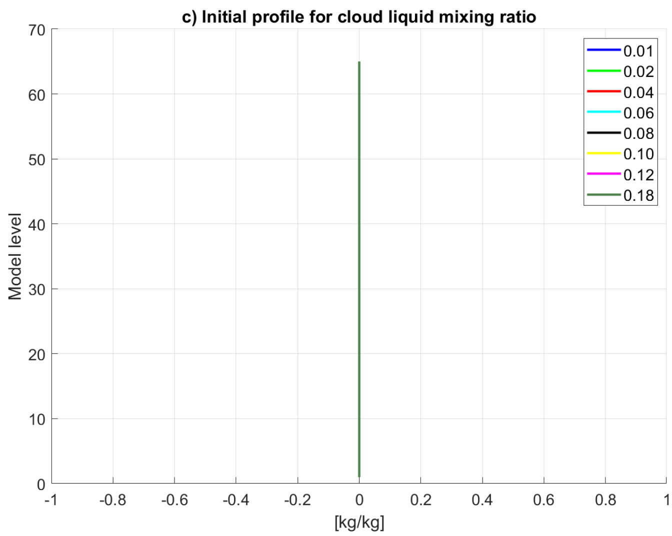

Figure 3.8. As figure 3.7, but for cloud liquid mixing ratio [kg/kg].

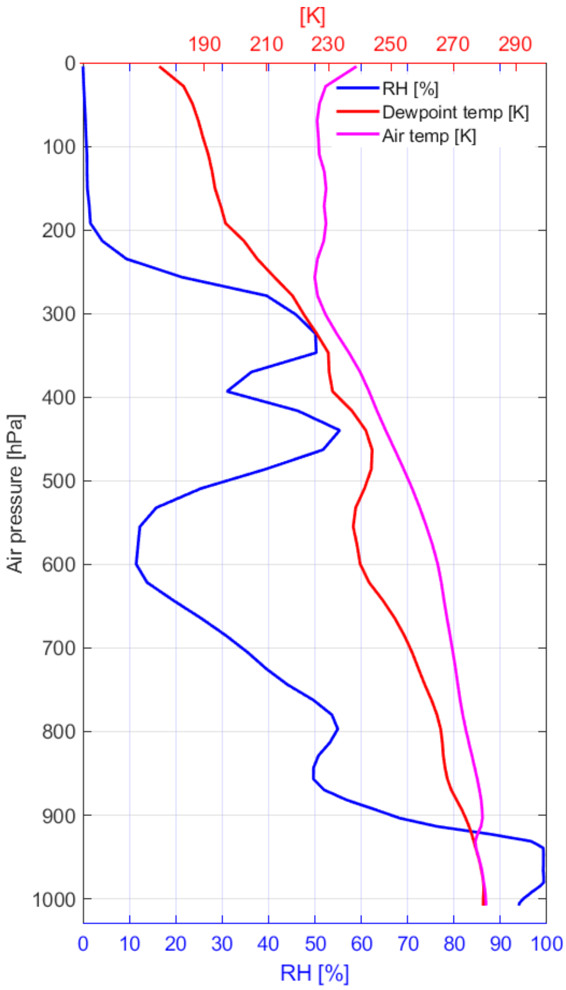

Figure 3.9. Vertical profiles from MUSC of relative humidity (%; blue), air temperature (K; magenta) and dewpoint temperature (K,red) at the initial timestep of the model simulation (20 July 2018 00 UTC).

The dewpoint temperature in Fig. 3.9 has been calculated using the Arden-Buck equation:

$$T_d(T, RH) = \frac{1}{a}\left(b(T, RH) - \sqrt{b(T, RH)^2 + 2ac(T, RH)}\right)$$

Eq.1

Where T_d is the dewpoint temperature, T is the air temperature and RH is the relative humidity. Hereby, the following expressions were used:

$$\alpha(T) = \frac{(18.678 - \frac{T}{234.5})T}{257.14 + T}$$

$$b(T, RH) = 18.678 - \beta(T, RH)$$

$$c(T, RH) = -256.14 \times \beta(T, RH)$$

$$\beta(T, RH) = lnRH + \alpha(T)$$

3.2 RADGR *(Graupel impact on radiation)*

Parameter values:

RADGR	**0.1**	**0.3**	**0.5**	**0.7**	**0.9**	**1.0**	**1.5**	**2.0**	**3.0**

This parameter showed no response in any of the variables investigated. This is most likely due to the fact that there was no solid precipitation occurring during the time period of the model simulation.

3.3 RZC_H *(Stable conditions length scale)*

This section shows the impact from perturbing RZC_H on different variables. Default value 0.11, range by physics experts 0.1-0.25, tested range 0.11-0.60. Values above 0.25 exceed the range given by physics experts (shown in red below).

Parameter values:

RZC_H	**0.11**	**0.13**	**0.15**	**0.17**	**0.20**	**0.25**	**0.40**	**0.60**

Analysis of the variation of parameter RZC_H shows that:

- There are no changes in cloud cover. This is the case for all remaining experiments.
- Liquid precipitation has two regimes: 0.11-0.17 and 0.20-0.60. The lower values 0.11-0.17 produces periodic peaks of precipitation and decreasing amounts with increasing RZH_H values, while the higher values 0.20-0.60 give precipitation close to 0 (Figures 3.11-3.12)
- The smallest RZC_H gives the highest cloud water and the highest RZC_H gives the lowest cloud water (Figure 3.13).
- The larger the RZC_H value is, the faster the response (Figure 3.15)
- Higher stable conditions length scale induces stronger entrainment on top of cloud layer (stable layer) and thus makes the cloud thinner.

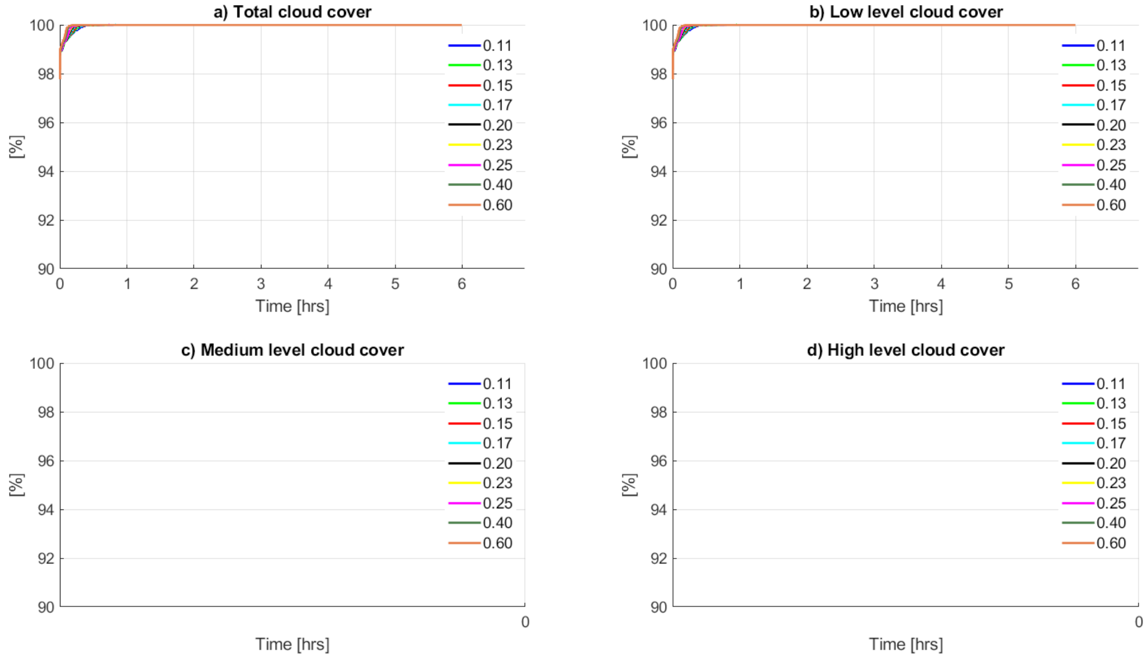

Figure 3.10. Sensitivity of a) total cloud cover, b) low level cloud cover, c) medium level cloud cover, d) high level cloud cover [%] from perturbing the parameter RZC_H. The time period is for 6 hours of simulation time and at 74.5°N, 19.0°E. Legend shows color of line plots and corresponding value for the parameter RZC_H.

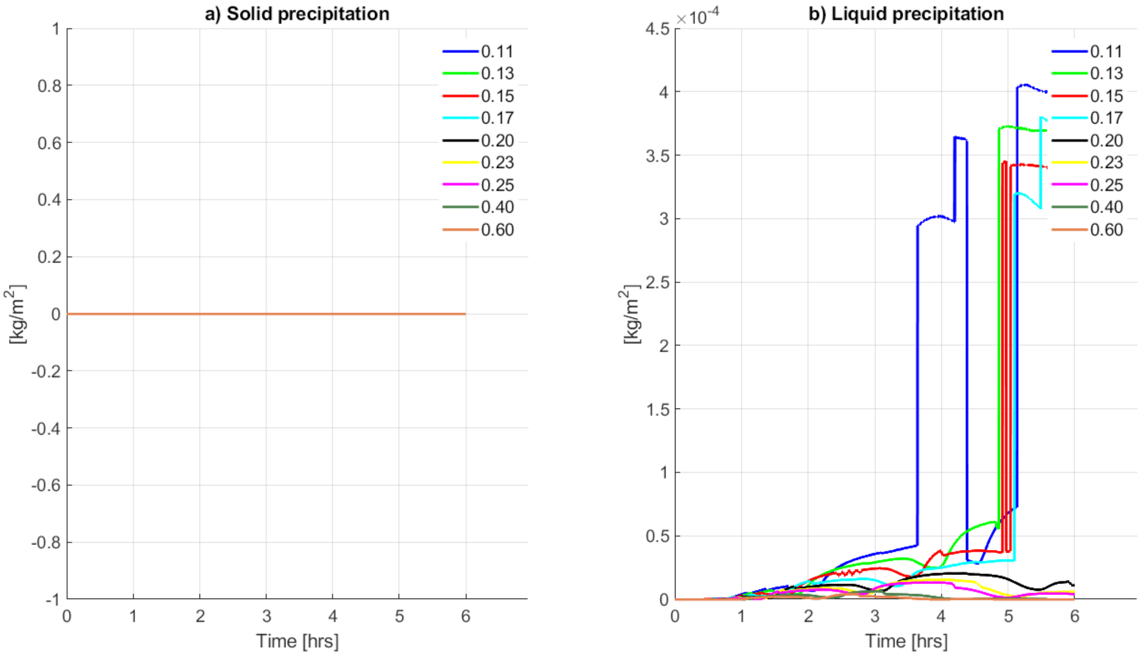

Figure 3.11. As for Figure 3.10, but for the impact on a) solid precipitation and b) liquid precipitation [kg/m^2] from perturbing the parameter RZC_H. The precipitation has been summed together for all 66 model layers. A sudden change in liquid precipitation (b) can be identified at 3.5 hours from all the runs with values below 0.20.

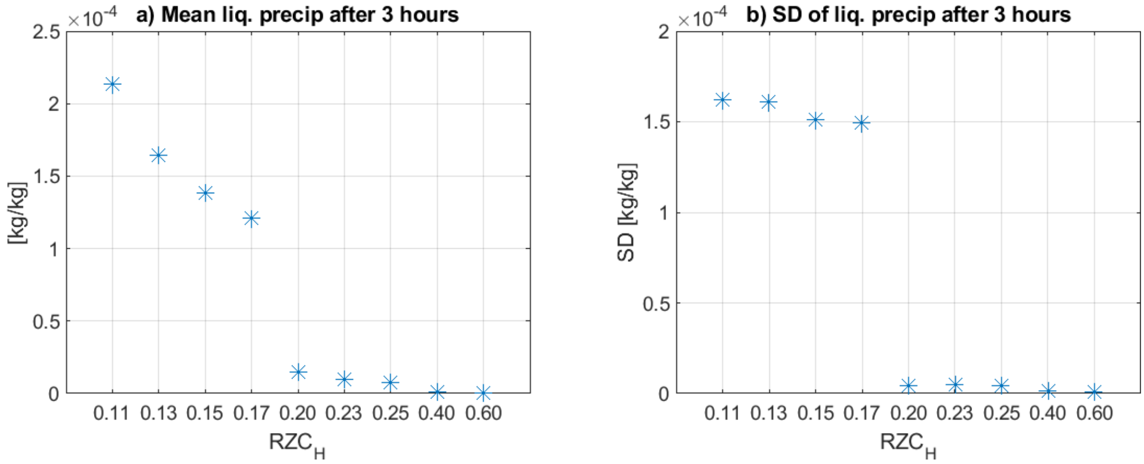

Figure 3.12. Sensitivity of a) mean of liquid precipitation after 3 hours to 6 hours of simulation time. b) standard deviation of liquid precipitation after 3 hours to 6 hours of simulation time. After 3 h simulation time, a sudden increase in precipitation in Figure 3.11.

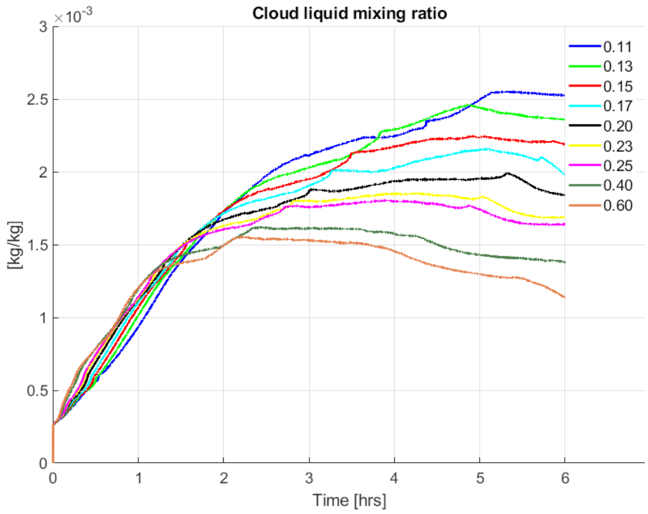

Figure 3.13. As Figure 3.10, but for a time series on responses on cloud liquid mixing ratio [kg/kg] from perturbing the parameter RZC_H. The cloud liquid mixing ratio has been summed for all 66 model layers.

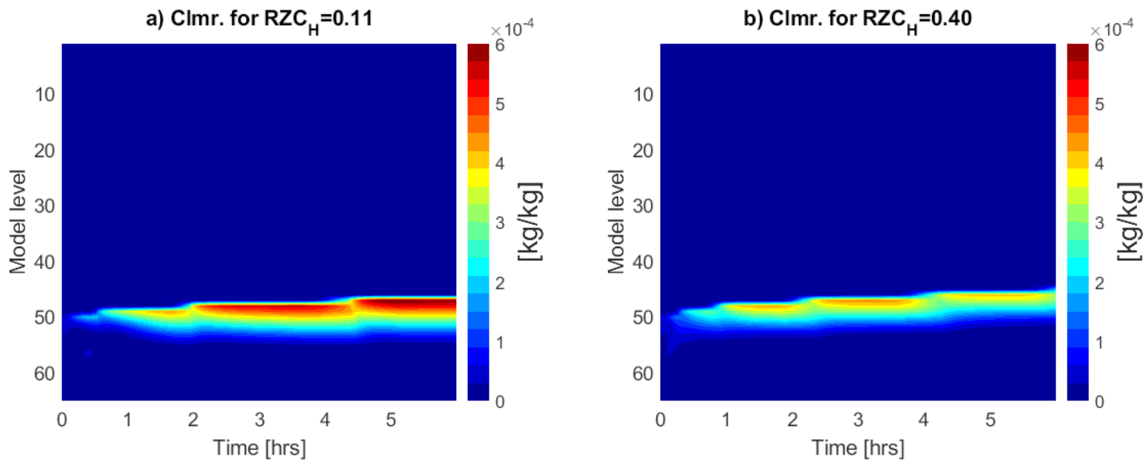

Figure 3.14. Vertical distribution of cloud liquid mixing ratio [kg/kg] from MUSC with a) RZC_H = 0.11 and b) RZC_H = 0.40.

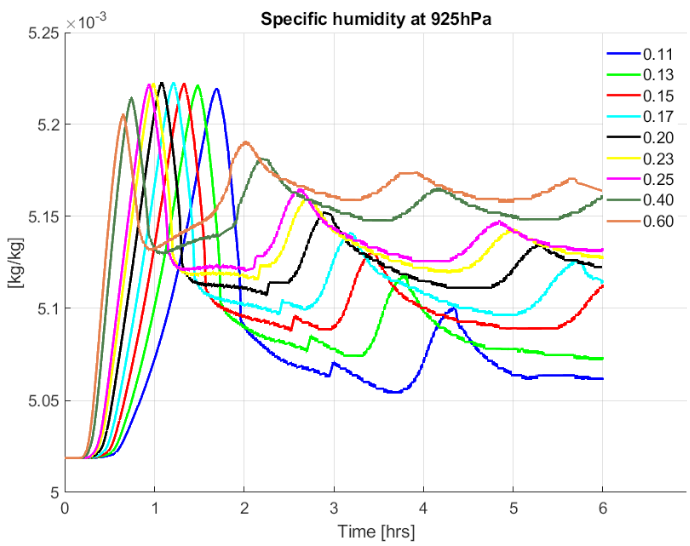

Figure 3.15. As Figure 3.10, but for the impact on specific humidity at 925 hPa [kg/kg] from perturbing the parameter RZC_H.

Initial profiles for liquid precipitation, solid precipitation, and cloud liquid mixing ratio are zero for all values of RZL_H (not shown).

3.4 RZL_ING *(Asymptotic free atmospheric length scale)*

Plots of different variable responses from perturbing the parameter, RZL_INF. The values used in perturbing RZL_INF can be found in the tables listed on the first page. Default value 40, range by physics experts 20-300, tested range 20-500. Values above 300 exceed the range given by physics experts.

Parameter values:

RZL_INF	20	40	60	80	100	150	200	250	300	500

Analysis of variations of parameter RZL_INF showed:

- Precipitation peaks for some of the experiments after 3.5 hours, experiments with lower value of RZL_INF give more precipitation, but the impact is non-linear (Fig. 3.20)
- Numerical oscillations in precipitation and cloud liquid mixing ratio for some of experiments with high RZL_INF (Figures 3.19, 3.21)
- Asymptotic free atmospheric length scale impacts the mixing higher in the atmosphere, not directly in the cloud layer, and impact on the cloud is indirect.
- It is not entirely clear whether the asymptotic free atmospheric length scale acts only in spatial or also in a temporal dimension, although spatial mixing appears more likely.
- Cross-section of cloud water shows “breaks” in cloud water which are not connected to the precipitation events (Figure 3.21). It may be possible to understand this better from inspecting cloud ice (Section 2).

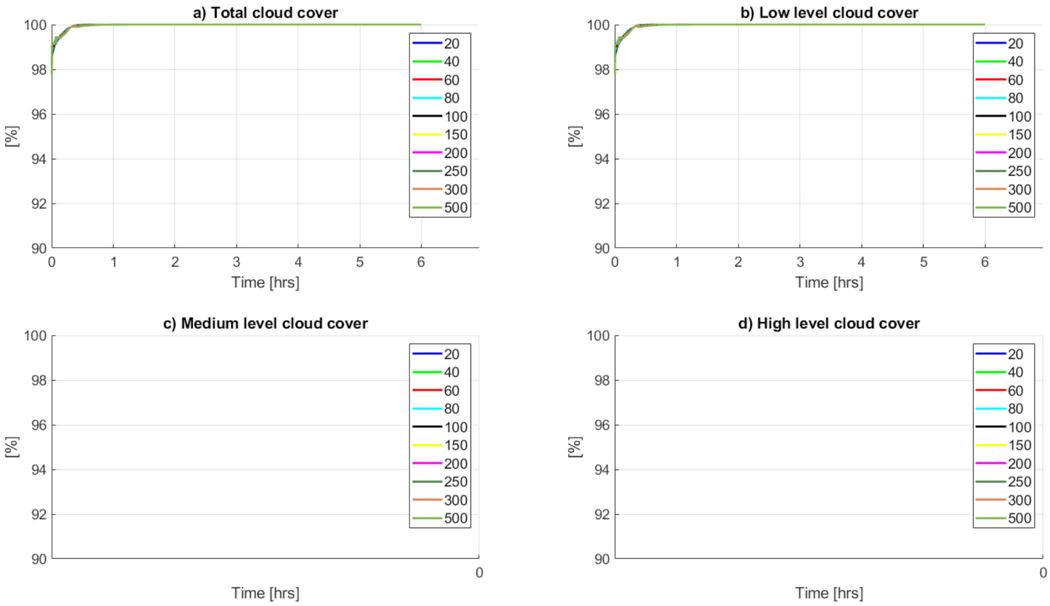

Figure 3.18. Sensitivity of a) total cloud cover, b) low level cloud cover, c) medium level cloud cover, d) high level cloud cover [%] from perturbing the parameter RZL_INF.

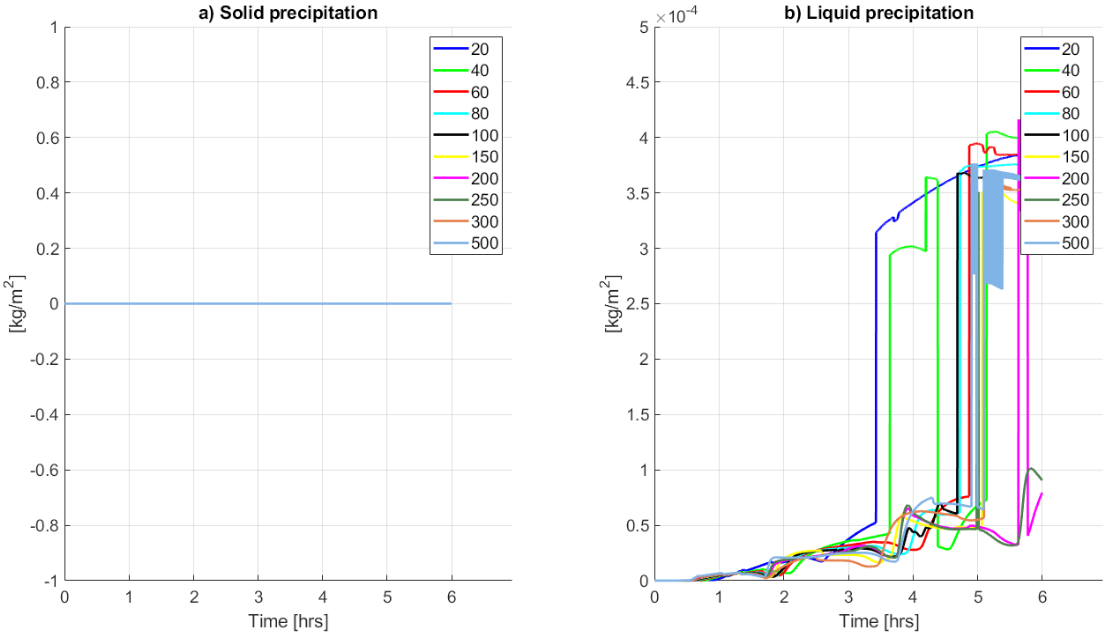

Figure 3.19. As Figure 3.18, but for impact on a) solid precipitation and b) liquid precipitation [kg/m^2] from perturbing the parameter RZL_INF. The precipitation has been summed together for all 66 model layers. A sudeen change in liquid precipitation can be identified at 3.5 hours (panel b).

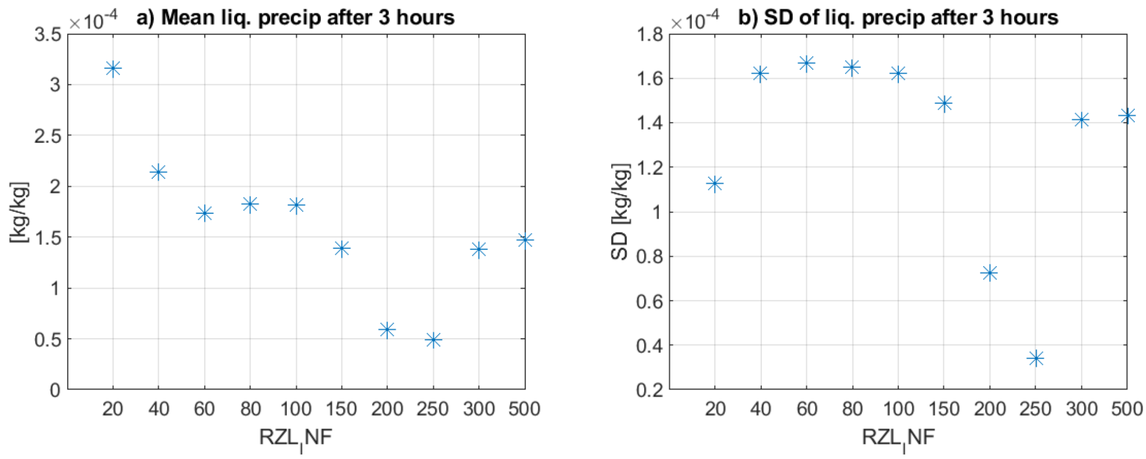

Figure 3.20. Sensitivity of a) mean of liquid precipitation after 3 hours to 6 hours of simulation time. b) standard deviation of liquid precipitation after 3 hours to 6 hours of simulation time, where a sudden increase in precipitation occurred.

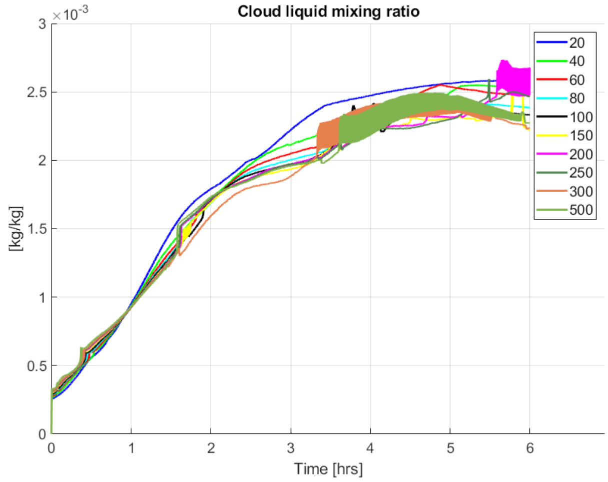

Figure 3.21. As Figure 3.18, but for a time series on responses on cloud liquid mixing ratio [kg/kg] from perturbing the parameter RZL_INF. The cloud liquid mixing ratio has been summed over all model layers. Some oscillations are apparent for RZL_INF larger then 200.

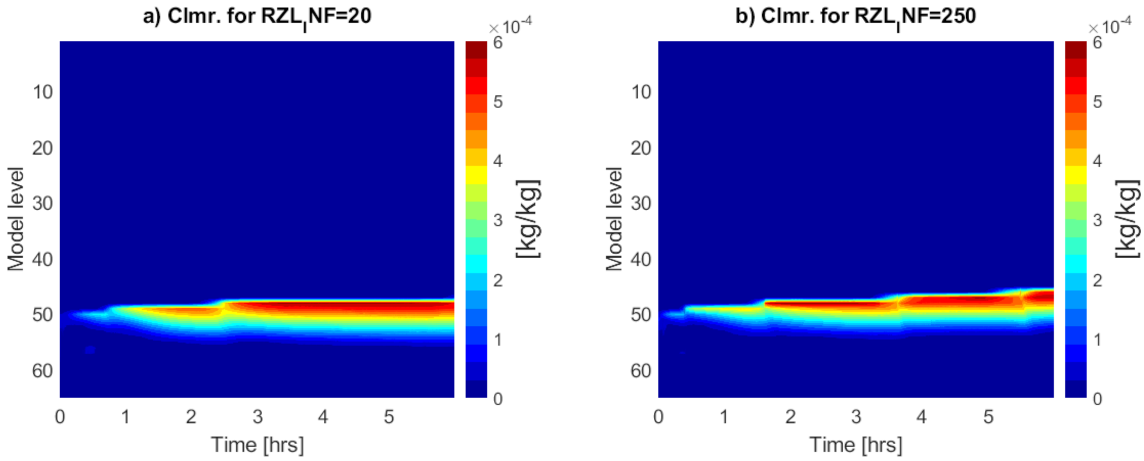

Figure 3.21. Vertical distribution of cloud liquid mixing ratio [kg/kg] from MUSC with a) RZL_INF = 20 and b) RZL_INF = 250.

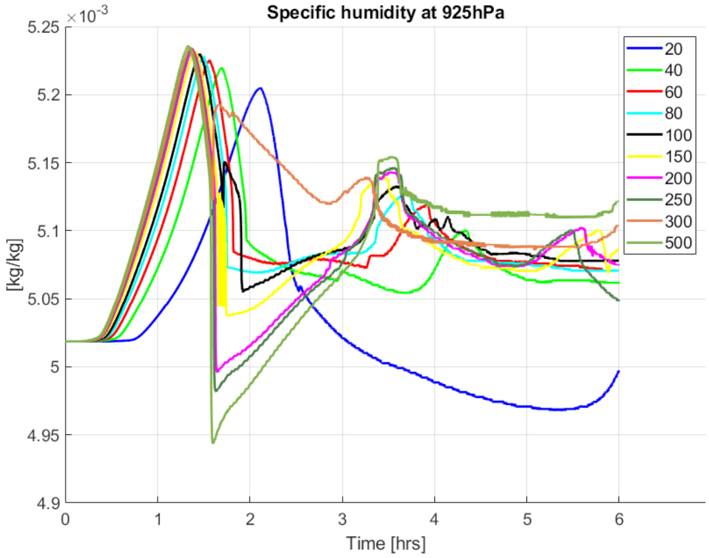

Figure 3.22. As Figure 3.18, but showing the impact on specific humidity at 925 hPa [kg/kg] from perturbing the parameter RZL_INF.

Initial profiles for liquid precipitation, solid precipitation, and cloud liquid mixing ratio are zero for all values of RZL_INF (not shown).

3.5 RFRMIN(10) *(Kogan autoconversion speed)*

This section presents the response of different variables to perturbations of the parameter RFRMIN(10). Default value 10, range by physics experts 2-50, tested range 1-100. Values above 50 exceed the range given by physics experts.

Parameter values:

RFRMIN(10)	**1**	**2**	**5**	**10**	**20**	**30**	**50**	**100**

Analysis of variations of parameter RFRMIN(10) showed:

- Autoconversion describes the formation of rain from cloud droplets through the collision-coalescence.
- Experiments with lower parameter values (1-30) create a sudden increase in precipitation at 3.5 hours. The experiments with the highest values (50-100) don't have peaks, but show in general higher precipitation.
- The higher the parameter value the higher the precipitation, matching with intuition (Figure 3.28)
- The higher the autoconversion value, the less cloud water (Figure 3.29), because more cloud water is formed into rain when autoconversion speed is high.

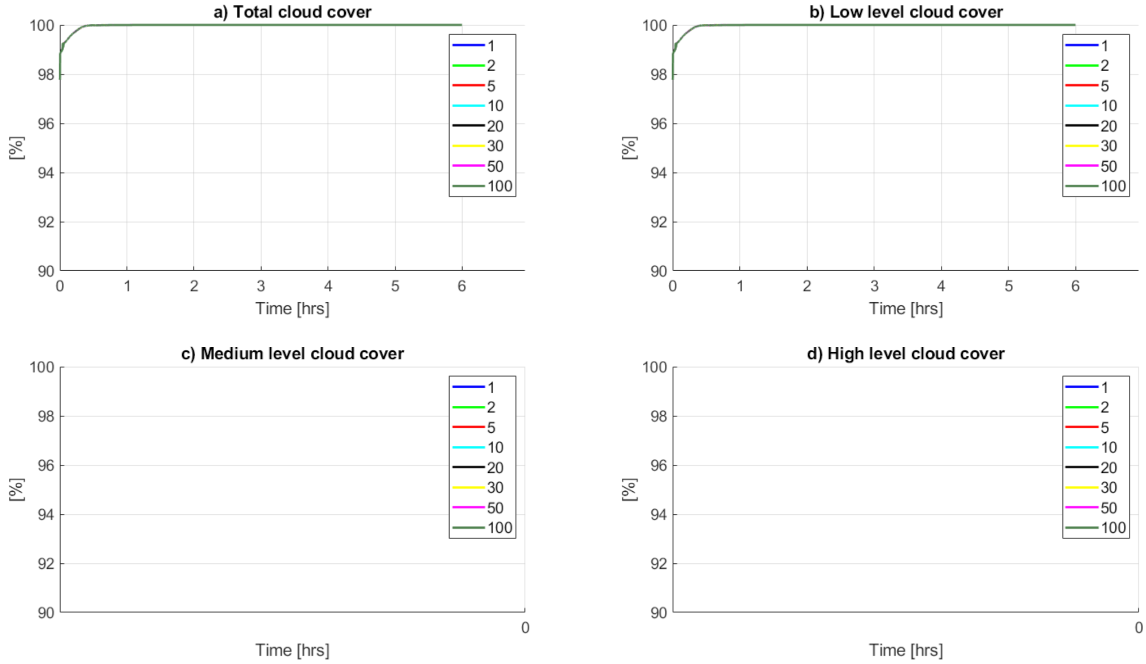

Figure 3.26. Impact on a) total cloud cover, b) low level cloud cover, c) medium level cloud cover, d) high level cloud cover [%] from perturbing the parameter RFRMIN(10).

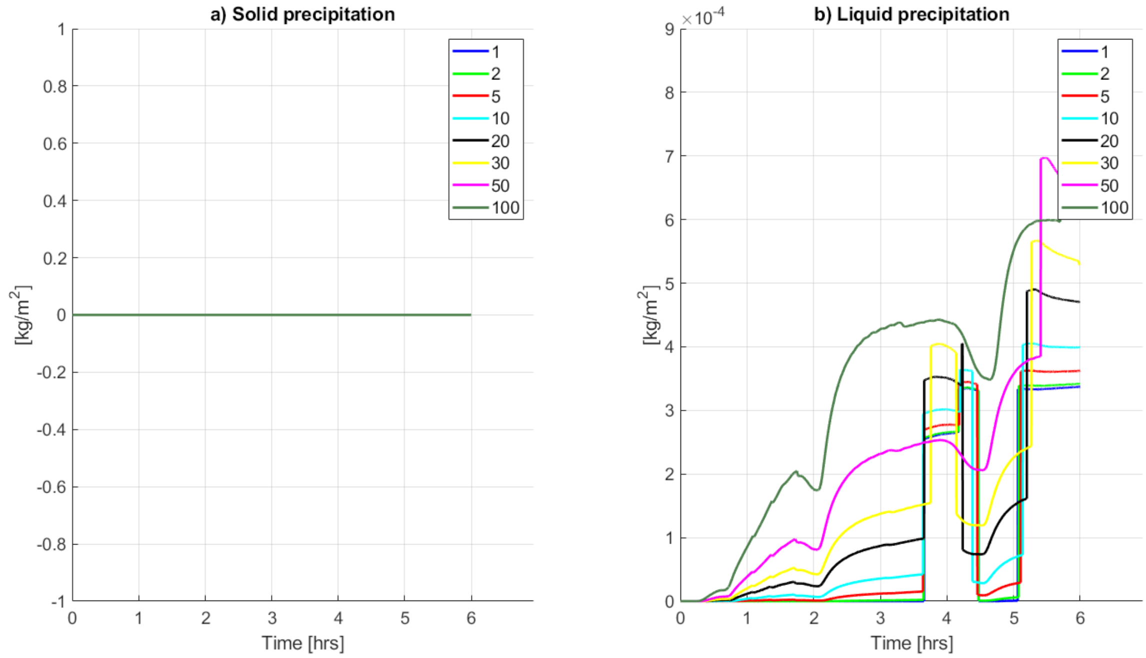

Figure 3.27. As for Figure 3.26, but for impact on a) solid precipitation and b) liquid precipitation [kg/m^2] from perturbing the parameter RFRMIN(10). The precipitation has been summed over all 66 model layers. The runs with RFRMIN(10) above 20 show larger amounts of precipitation, and an earlier onset. This early increase can not be identified in the other experiments (other parameters).

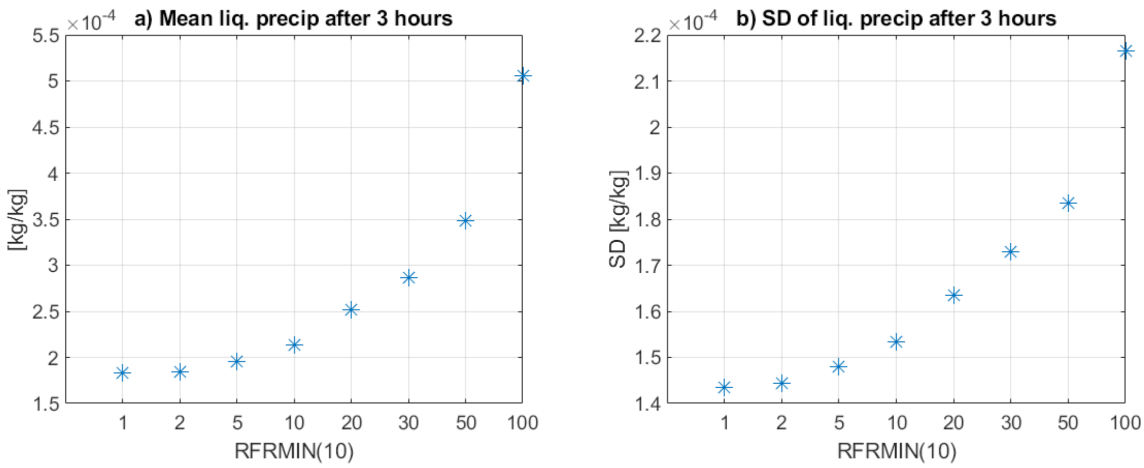

Figure 3.28. Sensitivity of a) mean of liquid precipitation after 3 hours to 6 hours of simulation time. b) standard deviation of liquid precipitation after 3 hours to 6 hours of simulation time.

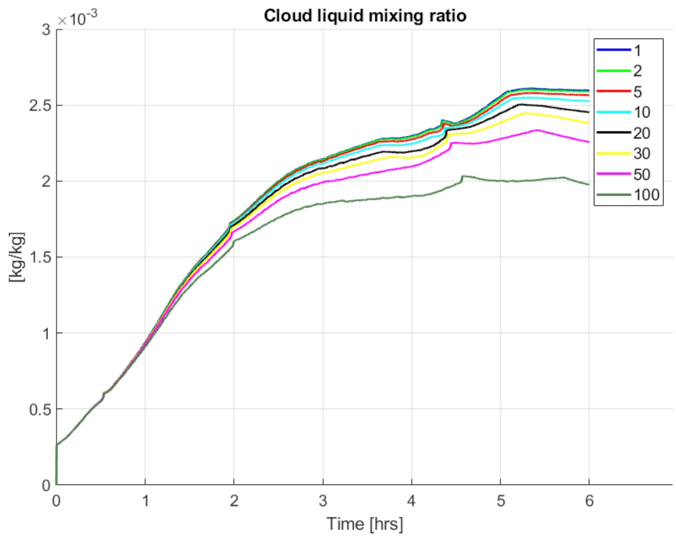

Figure 3.29. As Figure 3.26, but for the impact on cloud liquid mixing ratio [kg/kg] from perturbing the parameter RFRMIN(10). The cloud liquid mixing ratio has been summed from all 66 model layers.

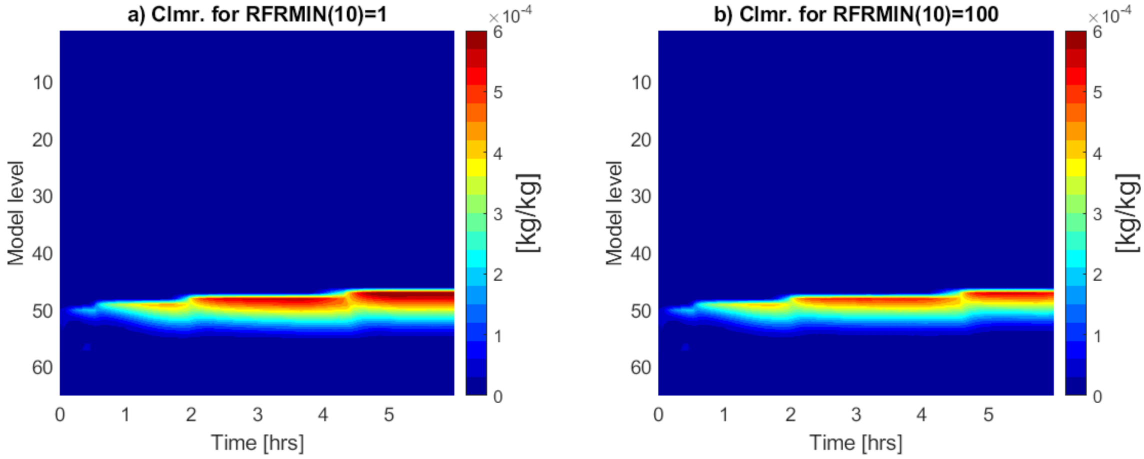

Figure 3.30. Vertical distribution of cloud liquid mixing ratio [kg/kg] from MUSC with a) RFRMIN(10)=1 and b) RFRMIN(10)=100.

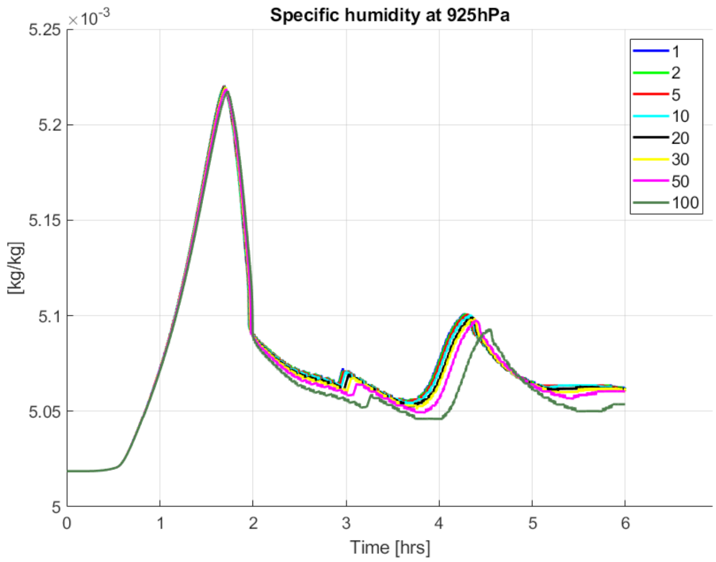

Figure 3.31. As Figure 3.26, but for the impact on specific humidity at 925 hPa [kg/kg] from perturbing the parameter RFRMIN(10).

Initial profiles for liquid precipitation, solid precipitation, and cloud liquid mixing ratio are zero for all values of RFRMIN(10) (not shown).

3.6 RFRMIN(11) *(Kogan subgrid scale(cloud fraction) sensitivity)*

This section shows the response of different variables to perturbations of the parameter RFRMIN(11). Default value 1, range by physics experts 0.01-1, tested range 0.01-2. Values above 1 exceed the range given by physics experts. Note that only runs with parameter values above the max range given by physics experts (>1) shows a response, as can be seen below.

Parameter values:

RFRMIN(11)	0.01	0.1	0.3	0.5	0.7	0.9	1	1.5	2

Analysis of variations of parameter RFRMIN(11) showed:

- Only values > 1 give responses.
- It remains unclear what this parameter actually does, and how it is related to cloud and precipitation processes.

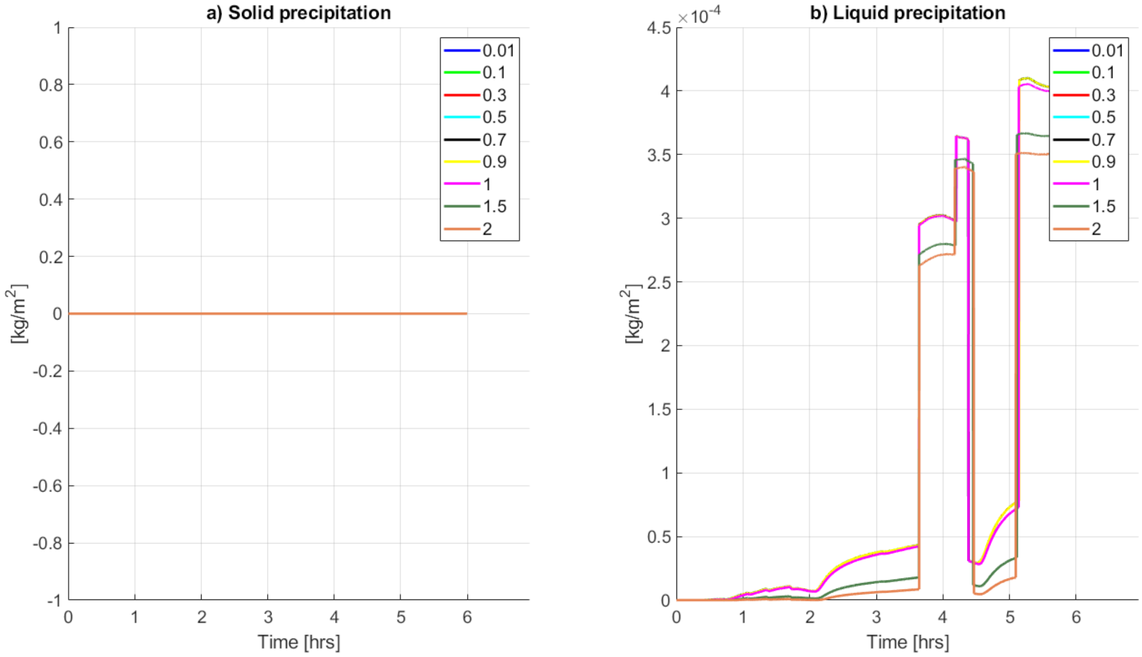

Figure 3.34. Impact on a) solid precipitation and b) liquid precipitation [kg/m^2] from perturbing the parameter RFRMIN(11). The precipitation has been summed together for all 66 model layers. Only runs with RFRMIN(11) values above 1 show responses, the other runs have no precipitation.

4 Parameter sensitivity experiments at location 80ºN 4ºW

The main purpose of this section is to study the impact on solid precipitation and ice. Therefore, a different location has been selected, that includes both solid precipitation and ice in the initial conditions. To this end, a grid point west of Svalbard (80ºN, 4ºW) has been selected (Fig. 4.13). The same 3D HARMONIE-AROME run as before was used, and the initial profile extracted for the new location. MUSC runs were started from the analysis time, with no hydrometeors present in the vertical column.

The MUSC experiments presented in this section include additional perturbed model variables. First, parameters that have been perturbed in these experiments included as previously the parameters VSIGQSAT, RADGR, RZC_H, RZL_INF, RFRMIN(10), RFRMIN(11). In addition, here the sensitivity to the parameters XCCR, FRFMIN(21) and RFRMIN(9) has been evaluated.

VSIGQSAT (Saturation limit sensitivity) showed a small impact on cloud cover, and a slightly surprising impact on solid precipitation. While it was expected that VSIGQSAT has a direct impact on cloud cover, it appeared to also or instead have an impact through redistribution of moisture and/or radiation. The question remains what role VSIGQSAT actually plays in the model. Other sensitivity runs showed responses that were more in line with expectations, though partly with an overall small impact, especially regarding RADGR.

In an expert judgement, Jenny Engdal shared her view on other important parameters and processes. In the revised microphysics scheme of HARMONIE-AROME (Engdal et al., 2020), stricter conditions apply to ice nucleation, which have a large impact within their MUSC runs. Furthermore, the efficiency of collection processes was previously set to 1, which is too efficient. Lastly, the size distribution of the rain was changed, which is a rather simple parameter in the code.

Regarding variables to focus on for the further perturbation analysis, the following variables are possibly most useful to detect changes:

- Cloud water (mixing ratio at certain level / cloud water path)
- Cloud ice (mixing ratio at certain level / cloud ice path)
- Liquid precipitation
- Solid precipitation
- Vertically integrated water vapor

4.1 *VSIGQSAT (Saturation limit sensitivity)*

Plots of different variable responses from perturbing the parameter, VSIGQSAT. The values used in perturbing VSIGQSAT can be found in Section 1. Values above 0.06 exceed the range given by physics experts.

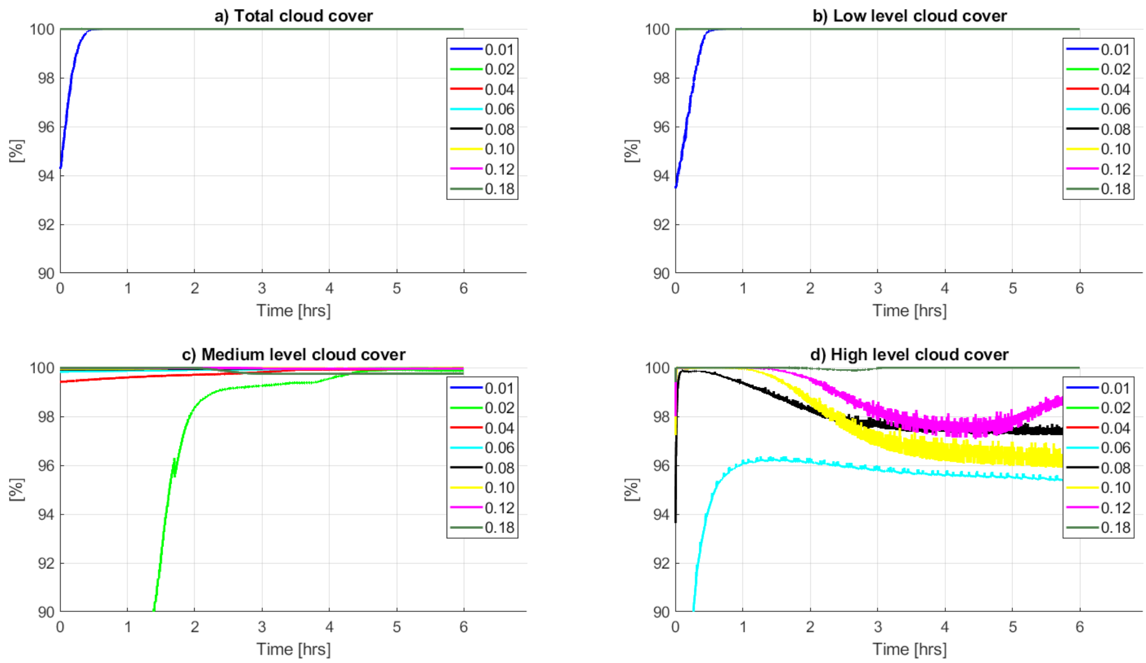

Figure 4.1: Impact on a) total cloud cover, b) low level cloud cover, c) medium level cloud cover, d) high level cloud cover [%] from perturbing the parameter VSIGQSAT. The time period is for 6 hours of simulation time and at the location 80ºN, 4ºW. Legend shows color of line plots and corresponding value for the parameter VSIGSAT.

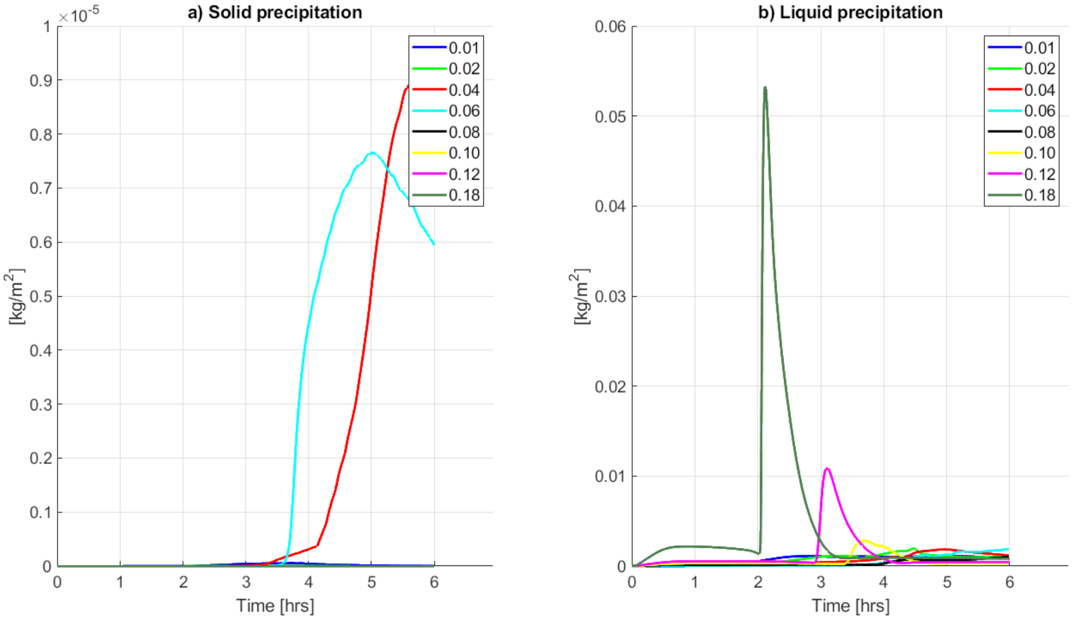

Figure 4.2: As Figure 4.1 but for impact on a) solid precipitation and b) liquid precipitation [kg/m^2] from perturbing the parameter VSIGQSAT. The precipitation has been summed for all 66 model layers. Note the difference in scale on the y-axis in panel a) and b).

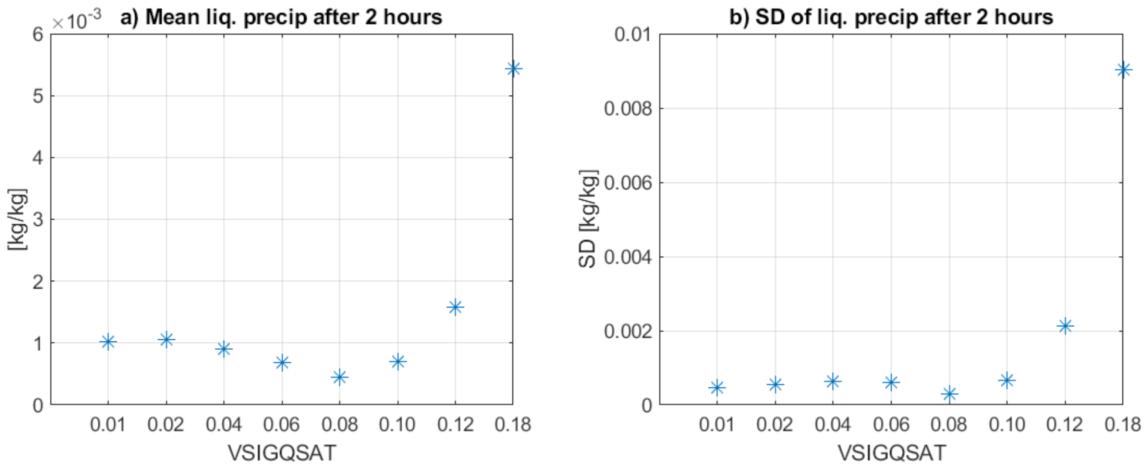

Figure 4.3: Sensitivity of a) mean of liquid precipitation during 2 to 6 hours of simulation time. b) standard deviation of liquid precipitation during 2 to 6 hours of simulation time. After 2 h, a sudden increase in liquid precipitation is apparent in Figure 4.2.

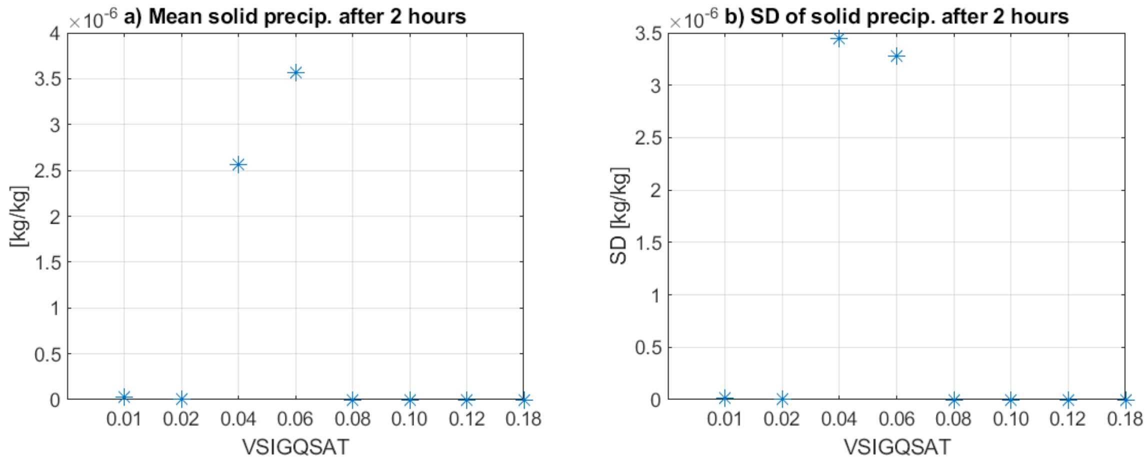

Figure 4.4: Sensitivity of a) mean of solid precipitation during 2 to 6 hours of simulation time. b) standard deviation of solid precipitation during 2 to 6 hours of simulation time. After 2 h, a sudden increase in liquid precipitation appears in Figure 4.2.

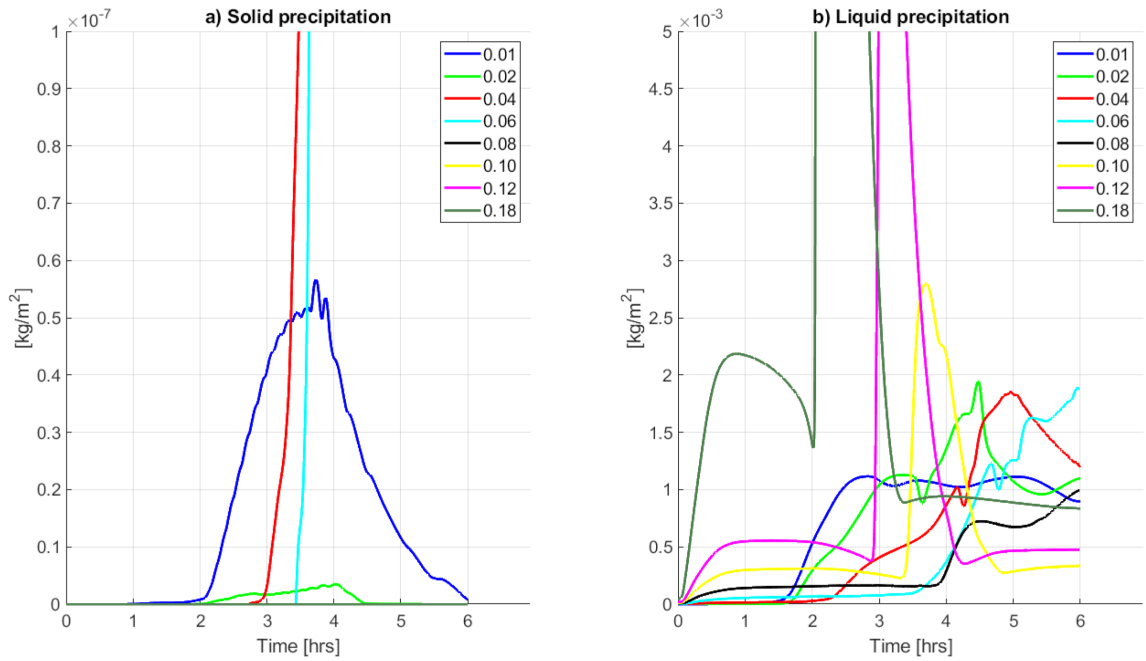

Figure 4.5: As Figure 4.2, but the scale on the y-axis has been changed to emphasize the results the from runs with a less extreme response.

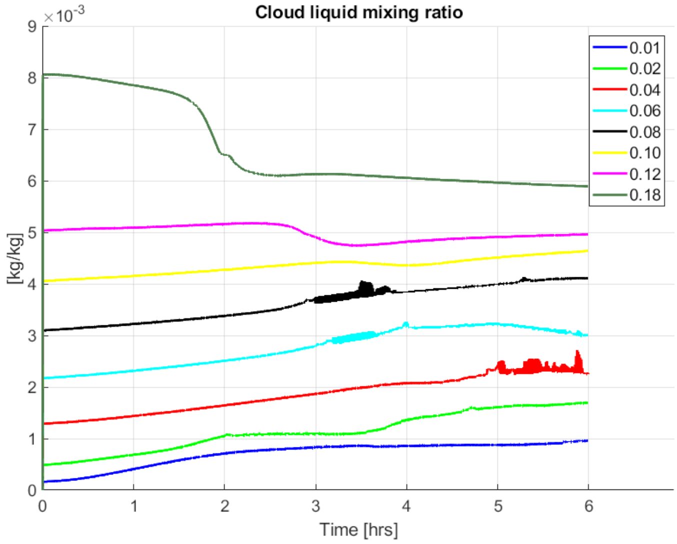

Figure 4.6: As Figure 4.1, but for the impact on cloud liquid mixing ratio [kg/kg] from perturbing the parameter VSIGQSAT. The cloud liquid mixing ratio has been summed for all 66 model layers.

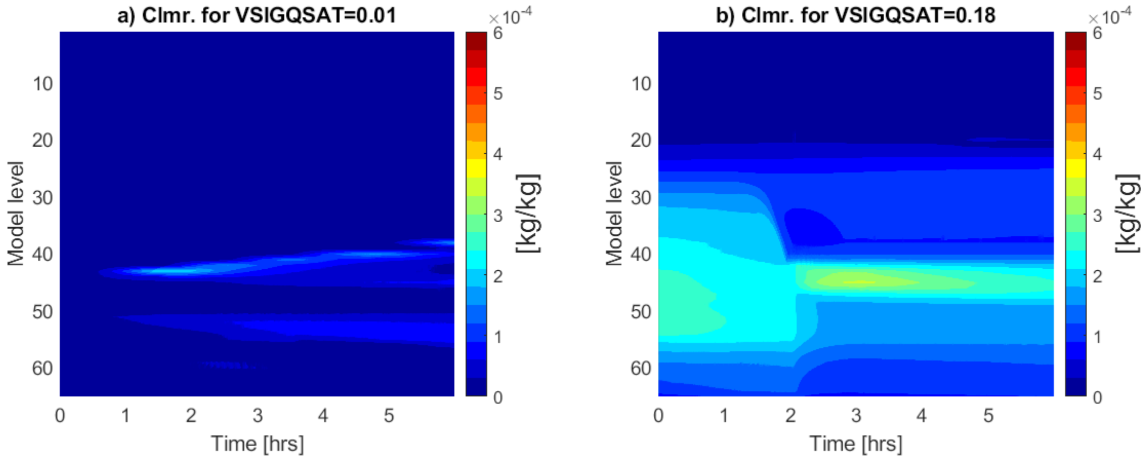

Figure 4.7: Vertical distribution of cloud liquid mixing ratio [kg/kg] from MUSC with a) VSIGQSAT = 0.01 and b) VSIGQSAT = 0.18.

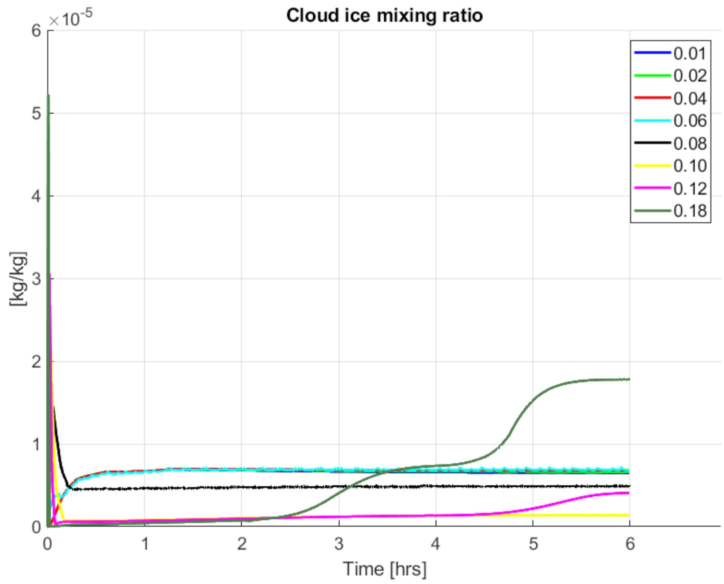

Figure 4.8: As Figure 4.1, but for a time series of cloud ice mixing ratio [kg/kg] from perturbing the parameter VSIGQSAT. The cloud ice mixing ratio has been summed for all 66 model layers.

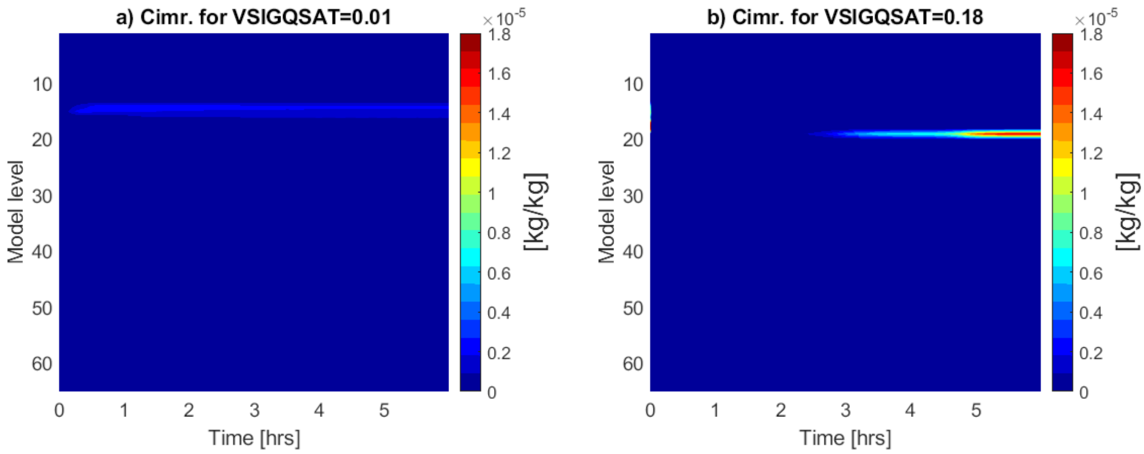

Figure 4.9: Vertical distribution of cloud lice mixing ratio [kg/kg] from MUSC with a) VSIGQSAT = 0.01 and b) VSIGQSAT = 0.18. The ice mixing ratio is overall lower in figure a) (values in the range $0.0 - 0.4 \times 10^{-5} kg/kg$), but the values do seem to change throughout the period. The ice mixing ratio from panel b) is close to zero during the first 2 hours of simulation time but then increases from $0.0 - 1.8 \times 10^{-5} kg/kg$towards the end of the simulation. This pattern in the ice mixing ratio in panel b) is also located lower in the model layers compared to panel a).

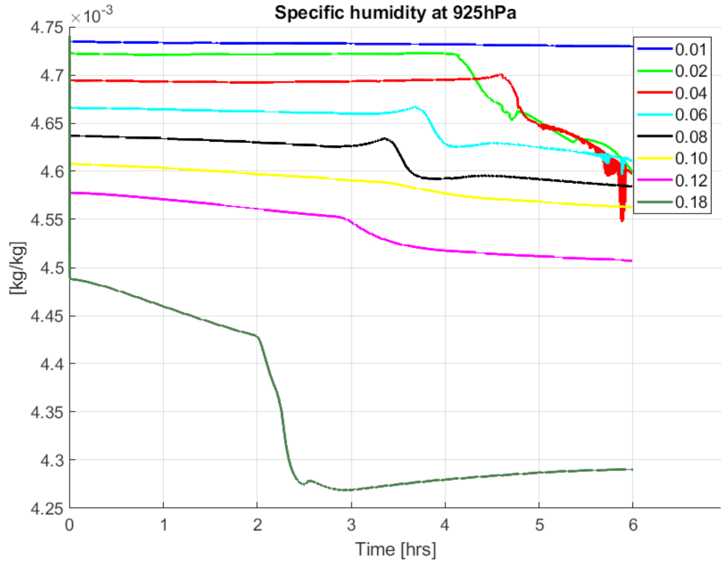

Figure 4.10: As Figure 4.1, but for the impact on specific humidity at 925 hPa [kg/kg] from perturbing the parameter VSIGQSAT.

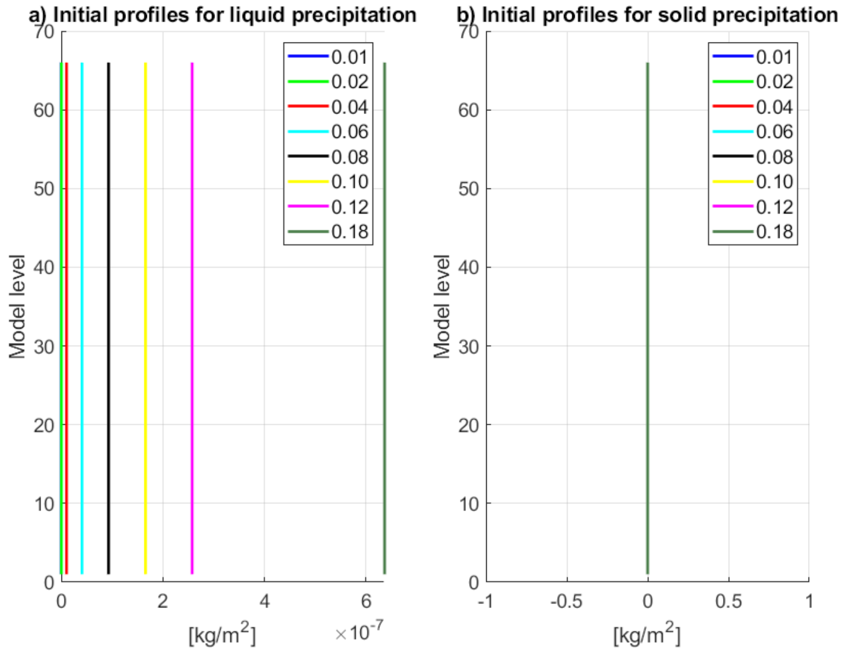

Figure 4.11: Initial vertical profiles of a) liquid precipitation [kg/m^2] and b) solid precipitation [kg/m^2] for the location 80 deg N, 4 deg W. The profiles are plotted for the first timestep of the model simulation. On figure b), only one line is shown because all the initial profiles are identical.

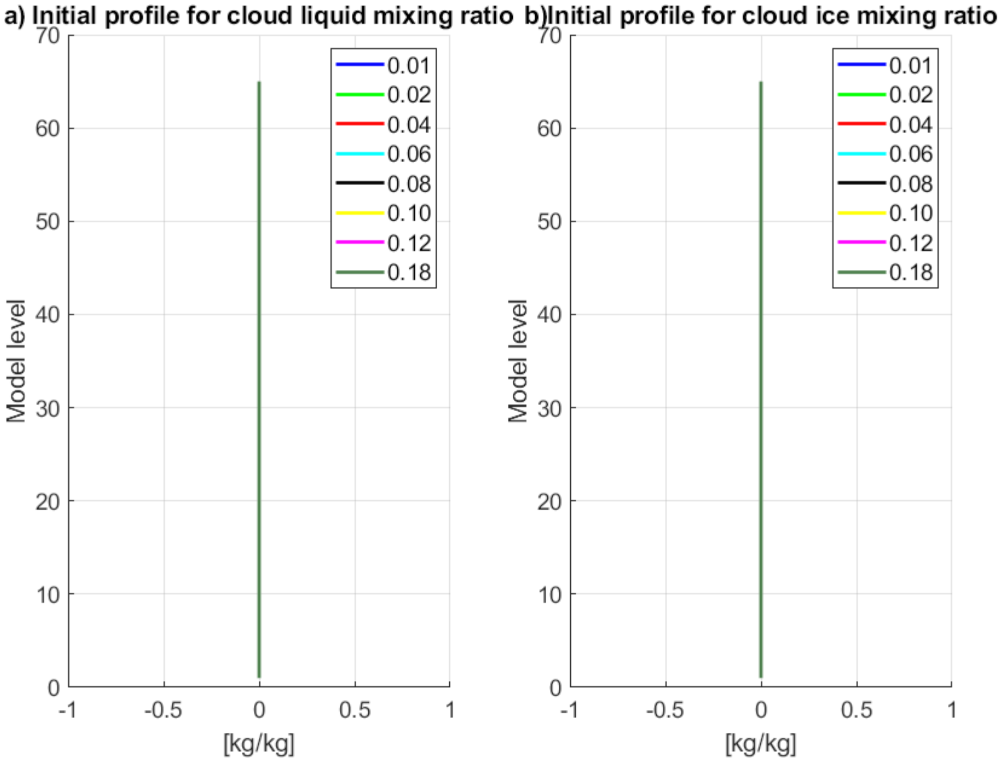

Figure 4.12: Initial vertical profiles of a) cloud liquid mixing ratio [kg/kg] and b) cloud ice mixing ratio [kg/kg] for the location 80ºN, 4ºW. The profiles are plotted for the first timestep of the model simulation. Only one line is shown because all the initial profiles are identical.

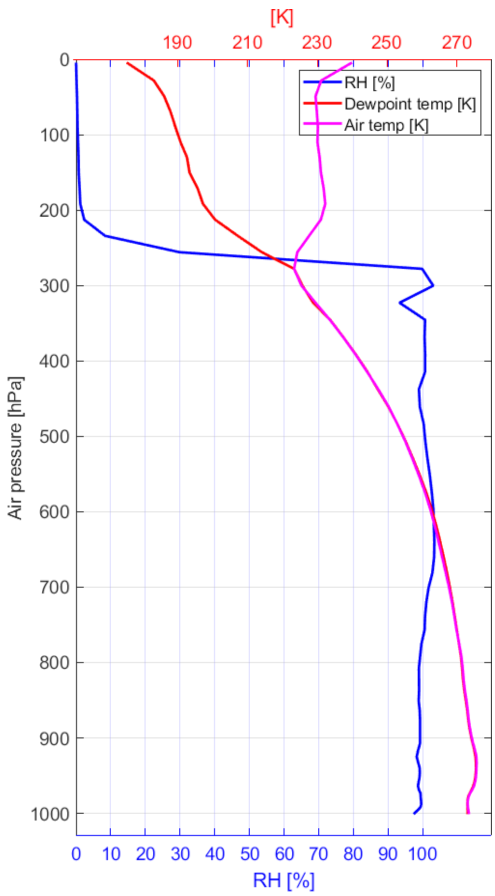

Figure 4.13: Vertical profiles from MUSC of relative humidity (%; blue), air temperature (K; magenta) and dewpoint temperature (K,red) at the initial timestep of the model simulation.

4.2 RADGR (Graupel impact on radiation)

This section presents the response from perturbing the parameter RADGR. The values used in perturbing RADGR can be found in Section 1. Values above 1 exceed the range given by physics experts.

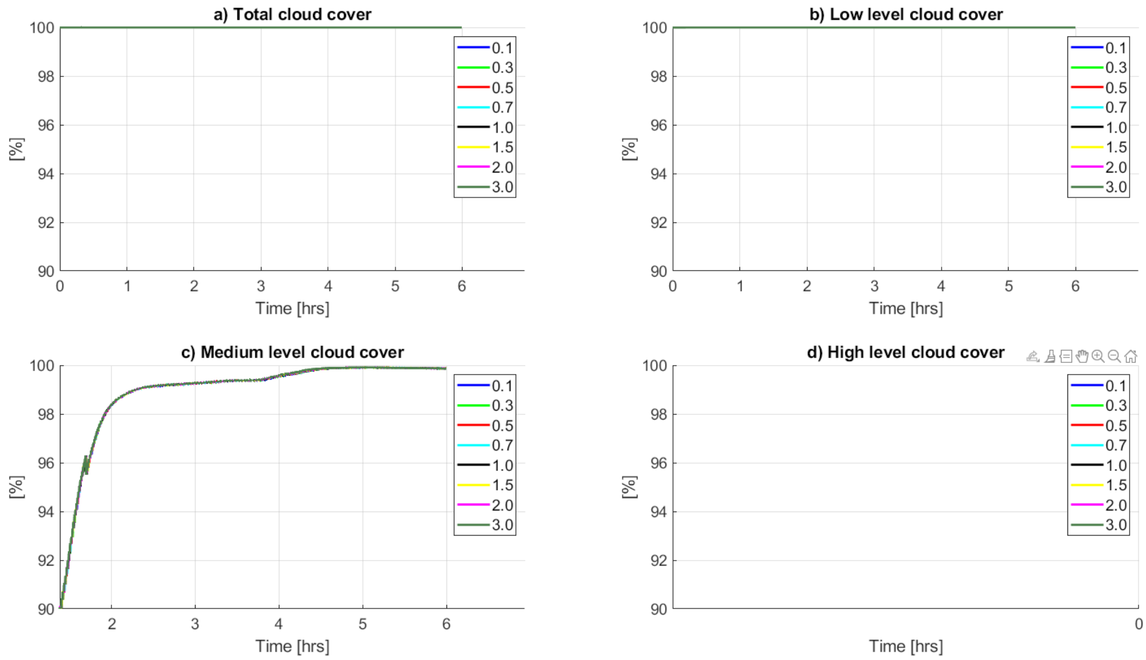

Figure 4.14: Impact on a) total cloud cover, b) low level cloud cover, c) medium level cloud cover, d) high level cloud cover [%] from perturbing the parameter RADGR. The time period is for 6 hours of simulation time and at the location is 80ºN, 4ºW. Legend shows color of line plots and corresponding value for the parameter RADGR.

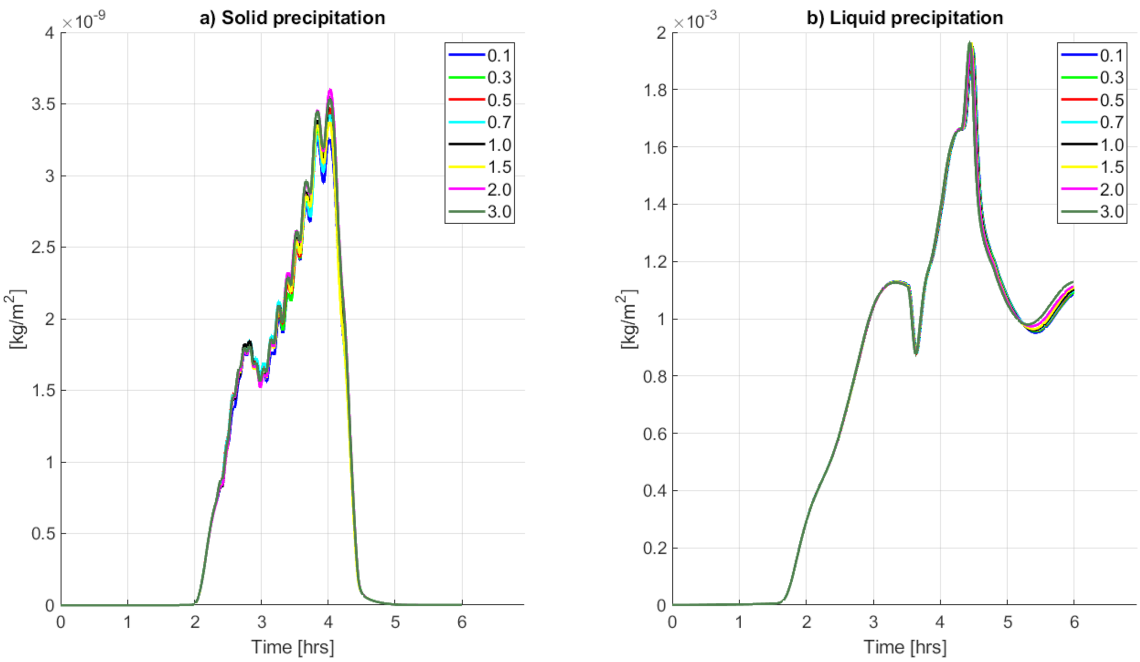

Figure 4.15: As Figure 4.1, but for impact on a) solid precipitation and b) liquid precipitation [kg/m^2] from perturbing the parameter RADGR. The precipitation has been summed for all 66 model layers. Note the difference in scale on the y-axis on panel a) and b).

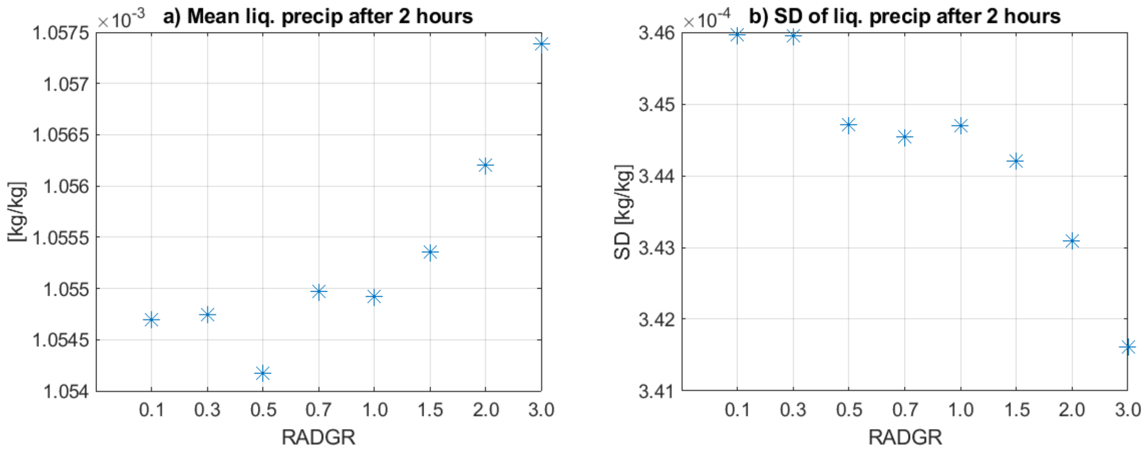

Figure 4.16: Sensitivity of a) mean of liquid precipitation during 2 to 6 hours of simulation time, and b) standard deviation of liquid precipitation during 2 to 6 hours of simulation time. After 2 h, a sudden increase in precipitation is apparent in Figure 4.2.

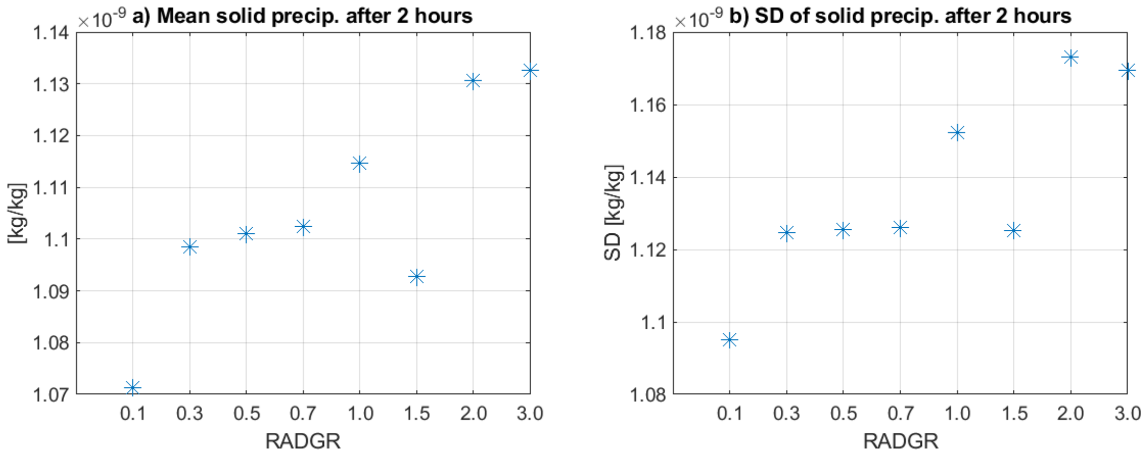

Figure 4.17: Sensitivity of a) mean of solid precipitation during 2 to 6 hours of simulation time, and b) standard deviation of solid precipitation during 2 to 6 hours of simulation time. After 2 h, a sudden increase in precipitation is apparent in Figure 4.2.

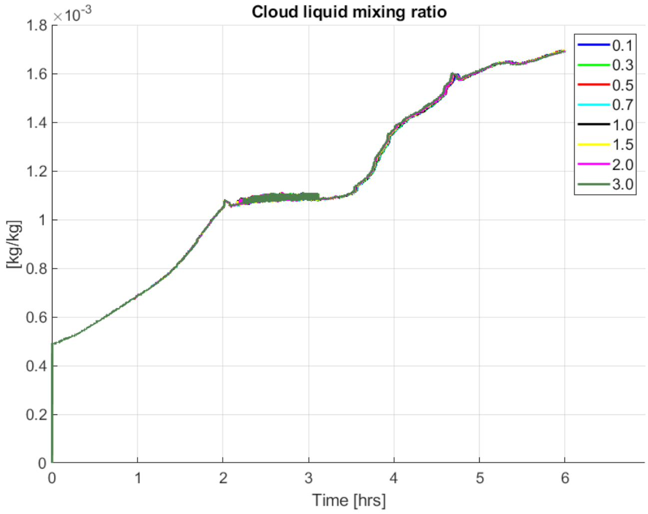

Figure 4.18: As Figure 4.14, but for the impact on cloud liquid mixing ratio [kg/kg] from perturbing the parameter RADGR. The cloud liquid mixing ratio has been summed for all 66 model layers.

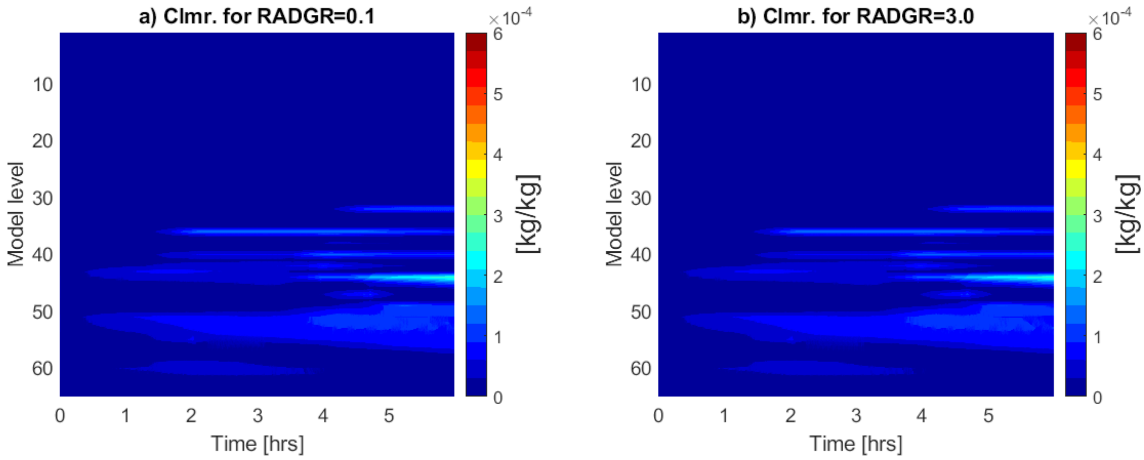

Figure 4.19: Vertical distribution of cloud liquid mixing ratio [kg/kg] with a) RADGR=0.1 and b) RADGR=3.0.

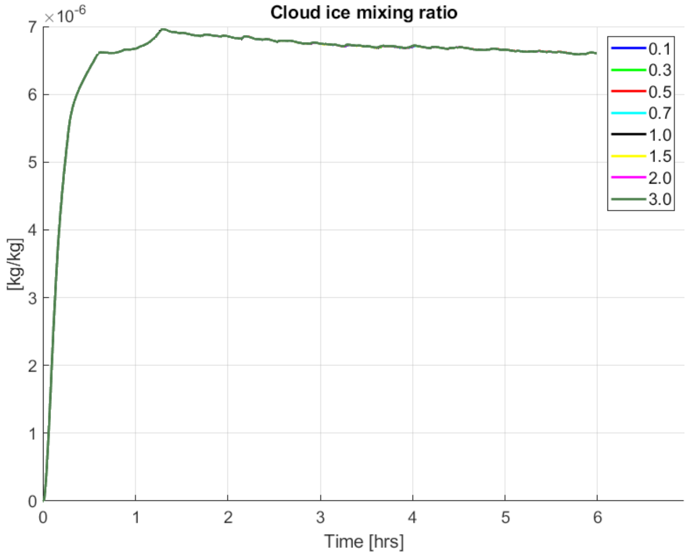

Figure 4.20: As Figure 4.14, but for the impact on cloud ice mixing ratio [kg/kg] from perturbing the parameter RADGR. The cloud liquid mixing ratio has been summed for all 66 model layers. Only one line is visible because the values are identical for all RADGR values.

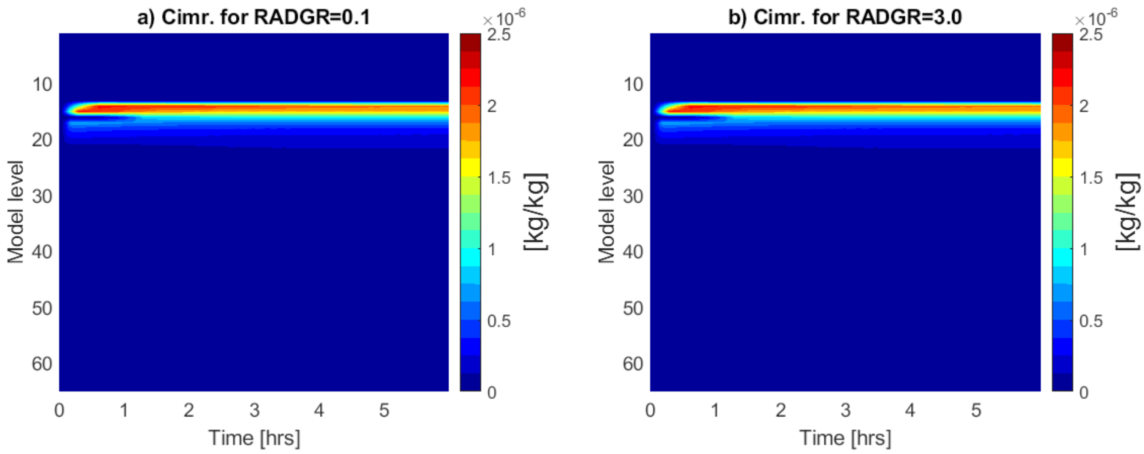

Figure 4.21: Vertical distribution of cloud ice mixing ratio [kg/kg] from MUSC with a) RADGR=0.1 and b) RADGR=3.0.

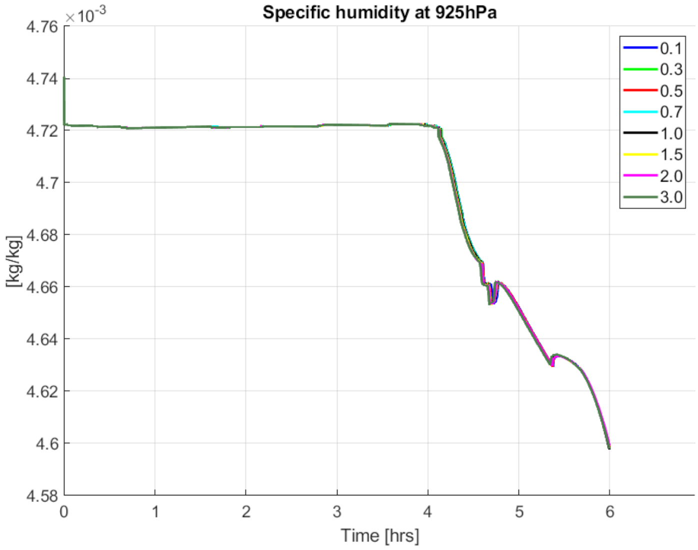

Figure 4.22: As Figure 4.14, but for impact on specific humidity [kg/kg] at 925 hPa [kg/kg] from perturbing the parameter RADGR.

Initial profiles for liquid precipitation, solid precipitation, and cloud liquid mixing ratio are zero for all values of RADGR (not shown).

4.3 RZC_H (Stable conditions length scale)

This section presents the responses from perturbing the parameter RZC_H. The values used in perturbing RZC_H can be found in Section 1. Values above 0.25 exceed the range given by physics experts.

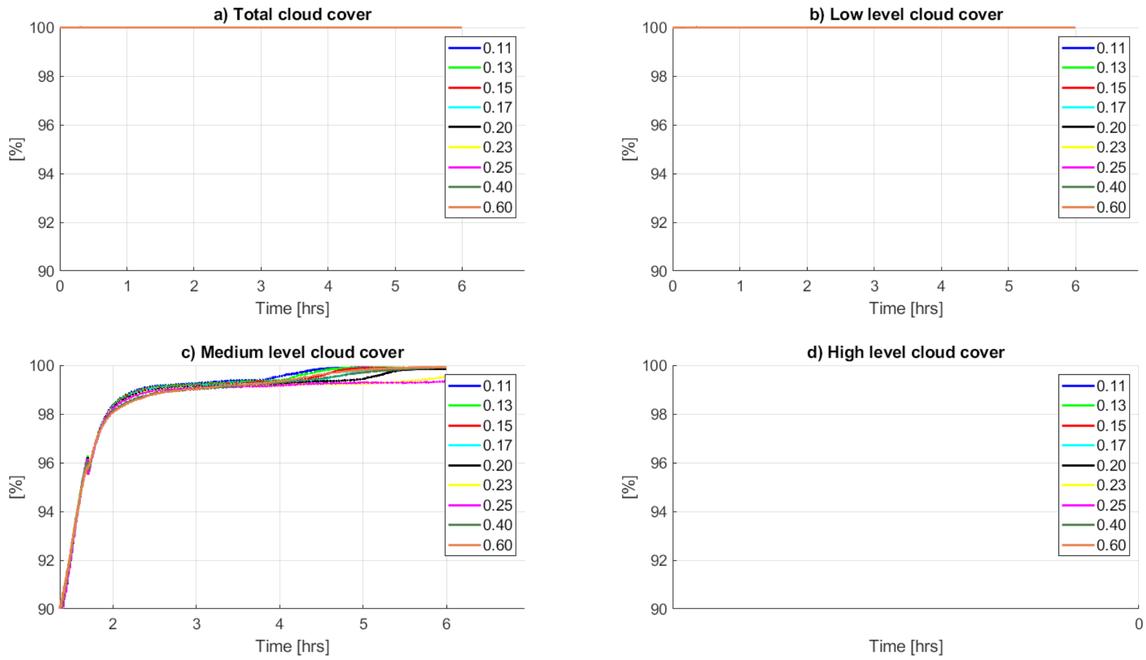

Figure 4.25: Impact of a) total cloud cover [%], b) low level cloud cover [%], c) medium level cloud cover [%] and d) high level cloud cover from perturbing the parameter RZC_H.

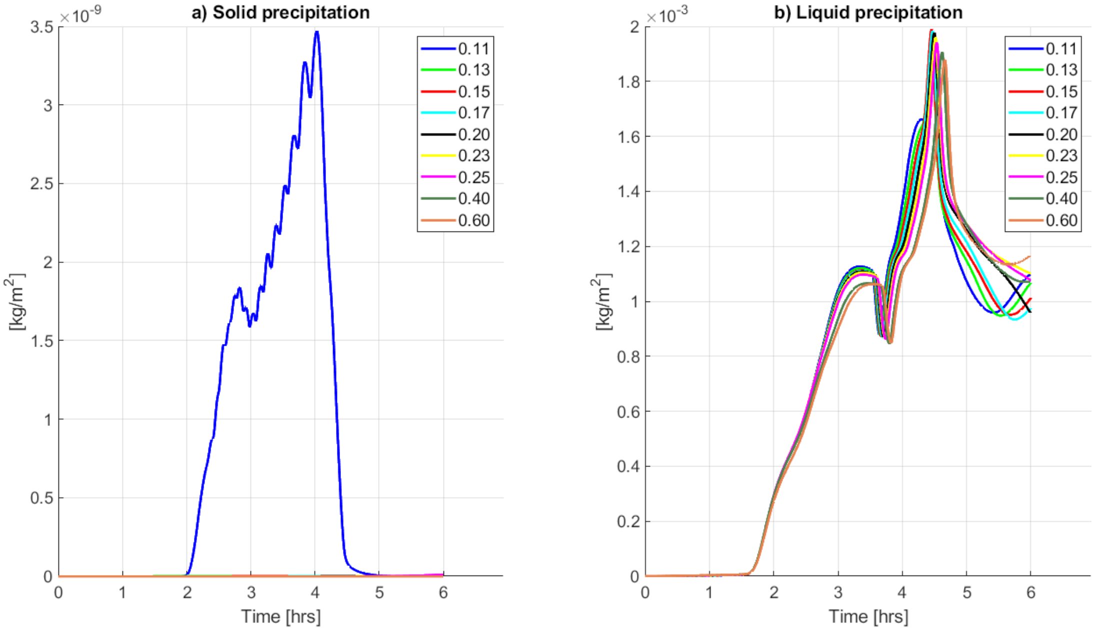

Figure 4.26: As Figure 4.25, but for the impact on a) solid precipitation and b) liquid precipitation from perturbing the parameter RZC_H.

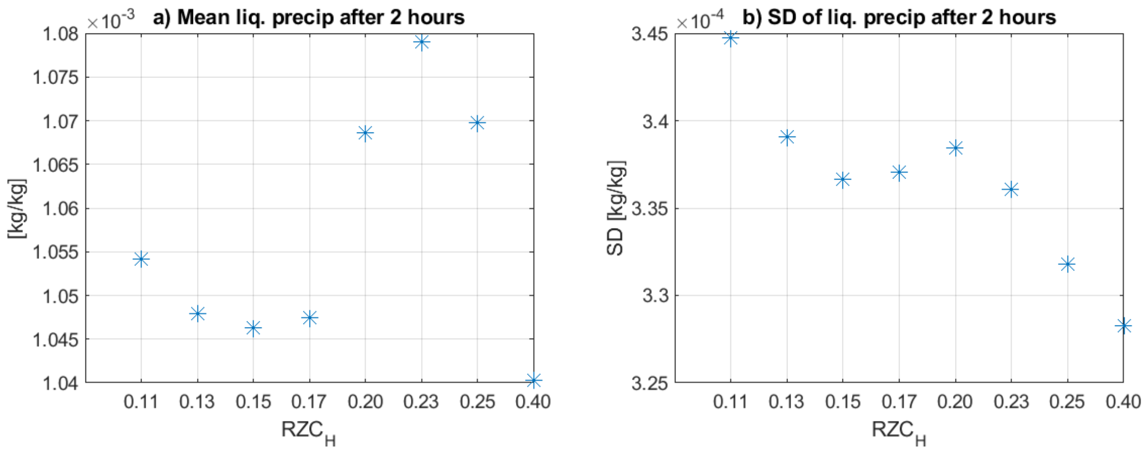

Figure 4.27: Sensitivity of a) mean of liquid precipitation during 2 to 6 hours of simulation time, and b) standard deviation of liquid precipitation during 2 to 6 hours of simulation time. After 2 h, a sudden increase in liquid precipitation is apparent in Figure 4.2.

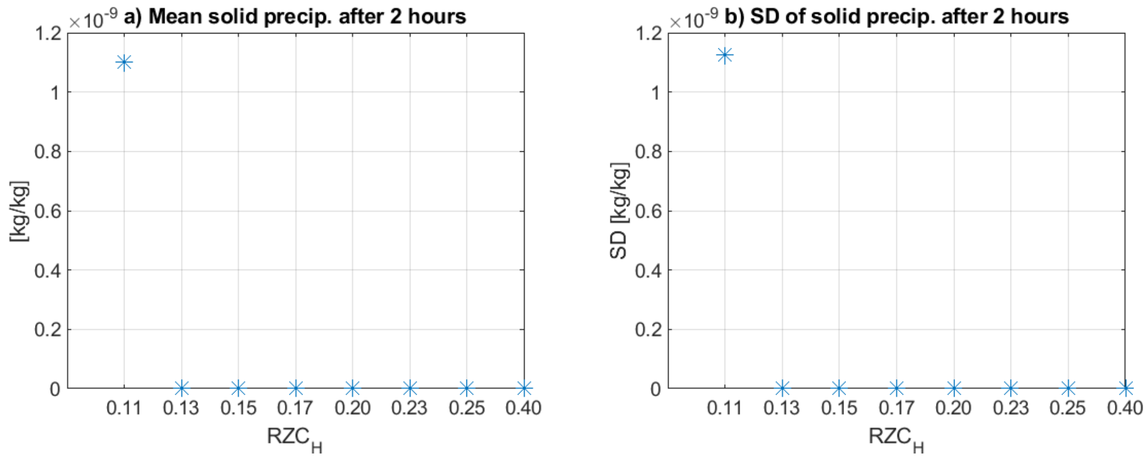

Figure 4.28: Sensitivity of a) mean of solid precipitation during 2 to 6 hours of simulation time, and b) standard deviation of solid precipitation during 2 to 6 hours of simulation time. After 2 h, a sudden increase in liquid precipitation is apparent in Figure 4.2. Panel a) only shows a response with RZC_H=0.11, since that run has a much greater solid precipitation amount compared to the other runs. However, the remaining runs do not show zero precipitation amount, only much lower values.

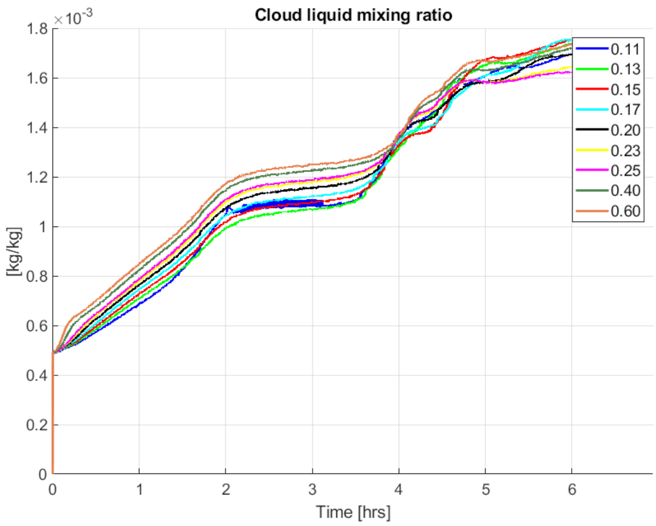

Figure 4.29: As Figure 4.25, but for the impact on cloud liquid mixing ratio [kg/kg] from perturbing the parameter RZC_H. The cloud liquid mixing ratio has been summed for all 66 model layers.

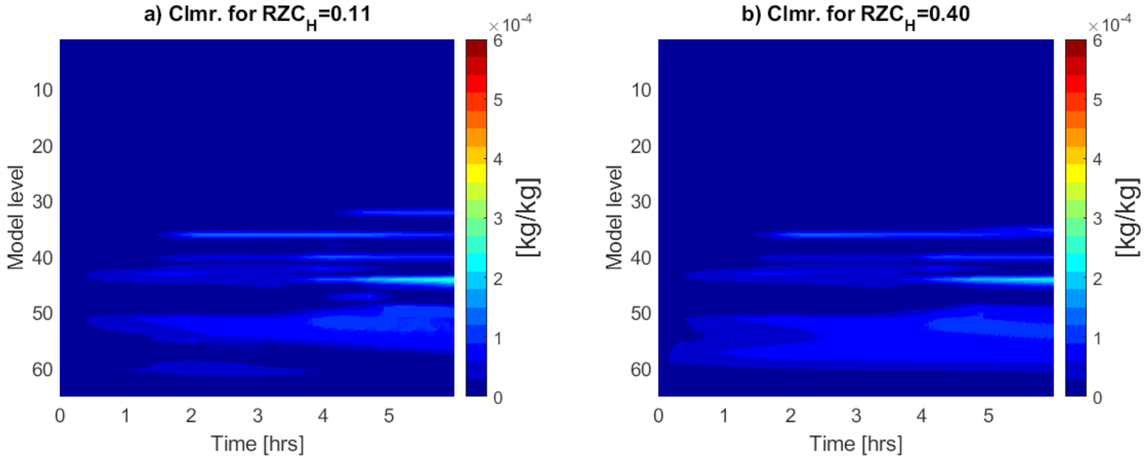

Figure 4.30: Vertical distribution of cloud liquid mixing ratio [kg/kg] with a) RZC_H=0.11 and b) RZC_H=0.40.

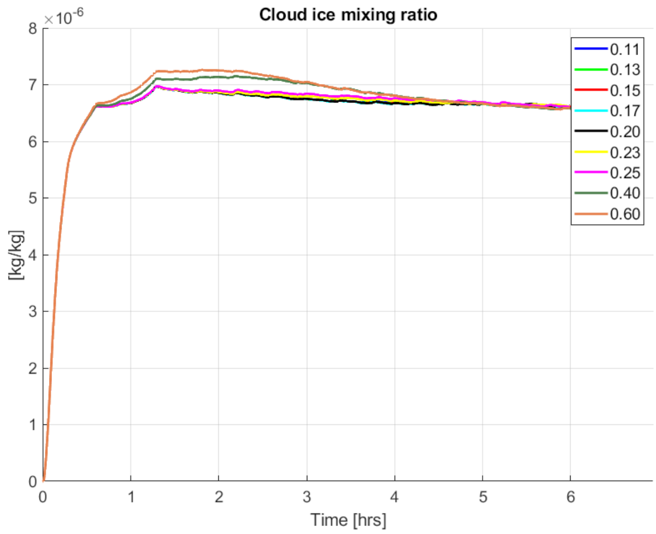

Figure 4.31: As Figure 4.25, but for the impact on cloud ice mixing ratio [kg/kg] from perturbing the parameter RZC_H. The cloud liquid mixing ratio has been summed for all 66 model layers.

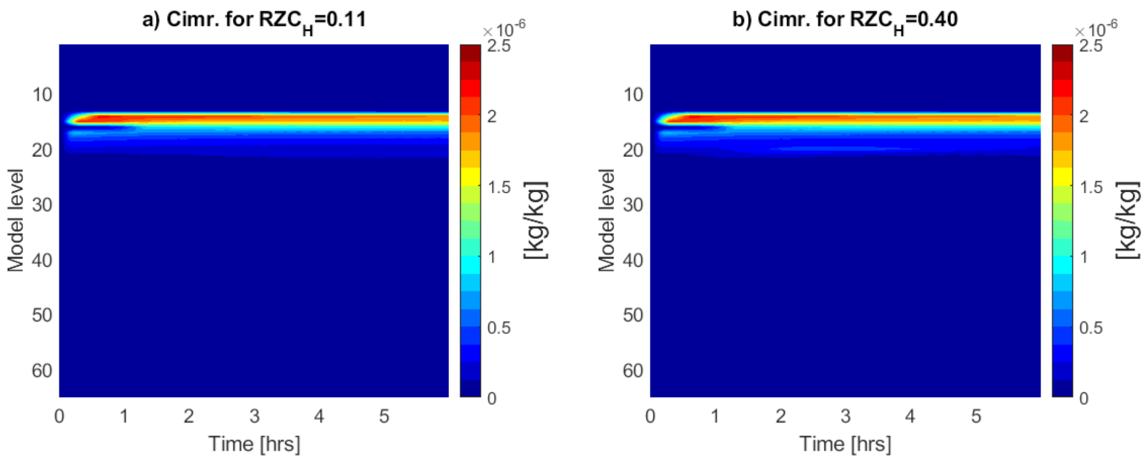

Figure 4.32: Vertical distribution of cloud ice mixing ratio [kg/kg] from MUSC with a) RZC_H=0.11 and b) RZC_H=0.40.

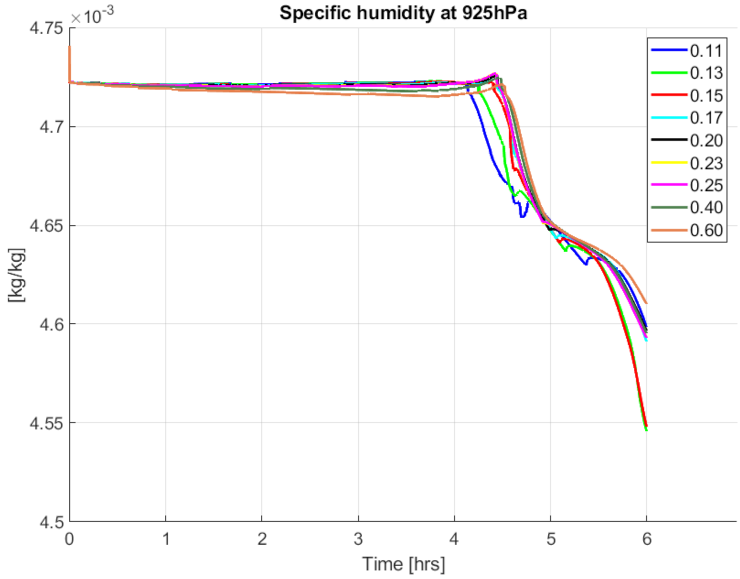

Figure 4.33: As Figure 4.25, but for the impact on specific humidity [kg/kg] at 925 hPa [kg/kg] from perturbing the parameter RZC_H.

Initial profiles for liquid precipitation, solid precipitation, and cloud liquid mixing ratio are zero for all values of RZC_H (not shown).

4.4 RZL_INF (Asymptotic free atmospheric length scale)

This section presents the responses from perturbing the parameter RZL_INF. The values used in perturbing RZL_INF can be found in Section 1.4. Values above 300 exceed the range given by physics experts.

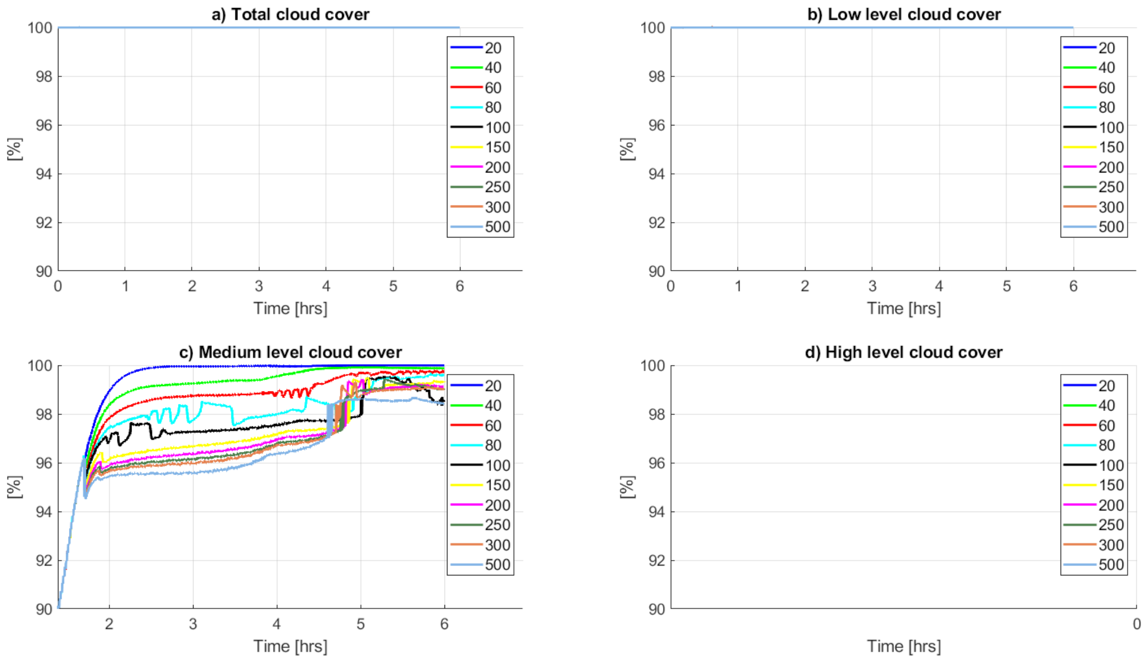

Figure 4.35: Impact on a) total cloud cover, b) low level cloud cover, c) medium level cloud cover, d) high level cloud cover [%] from perturbing the parameter RZL_INF.

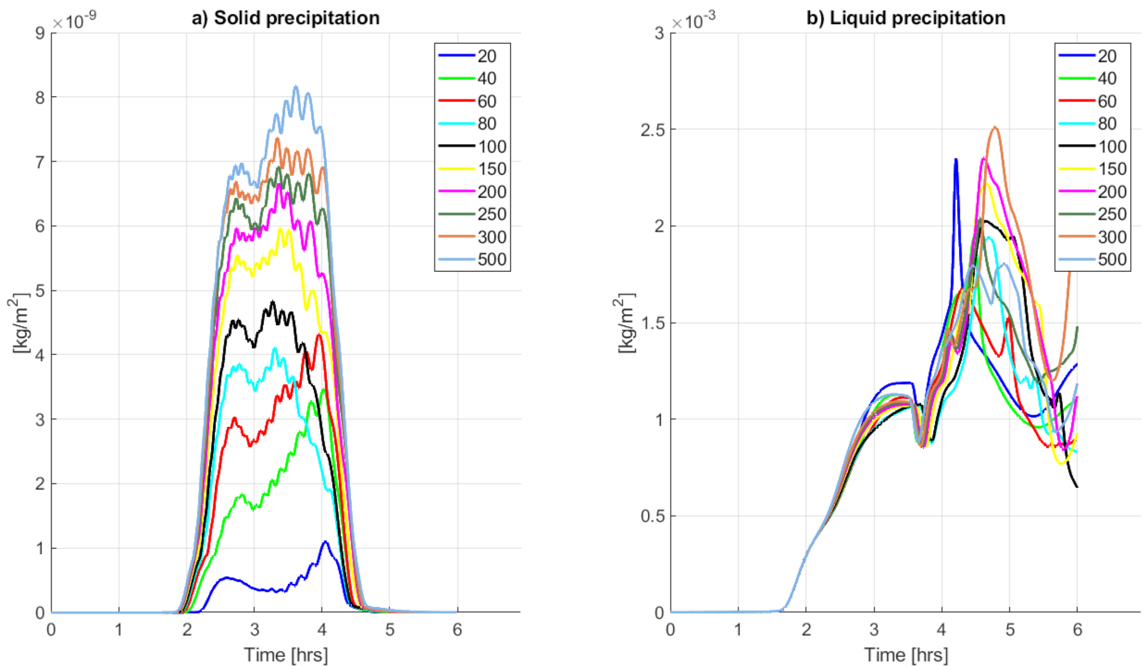

Figure 4.36: As Figure 4.35, but for the impact on a) solid precipitation and b) liquid precipitation [kg/m^2] from perturbing the parameter RZL_INF. The precipitation has been summed for all 66 model layers.

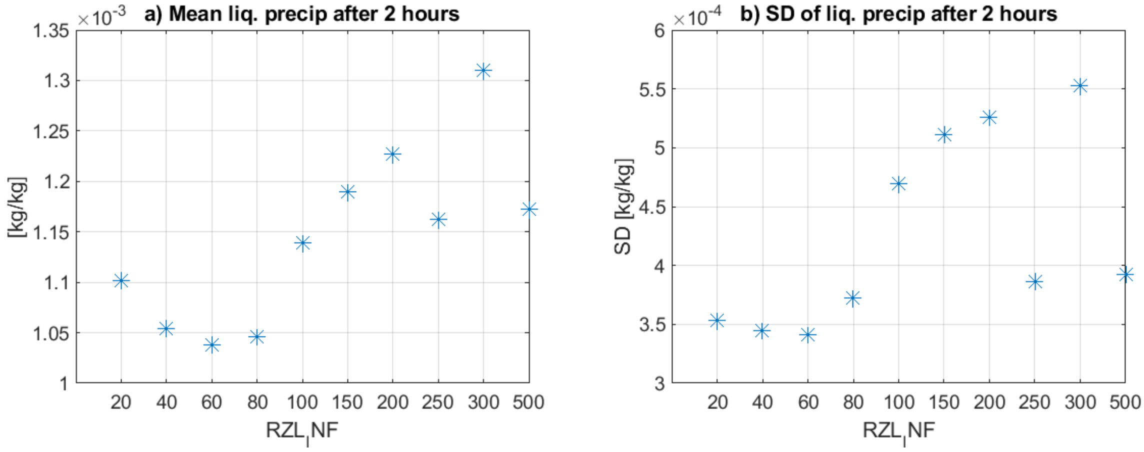

Figure 4.37: Mean of liquid precipitation during 2 to 6 hours of simulation time. b) standard deviation of liquid precipitation during 2 to 6 hours of simulation time. After 2 h, a sudden increase in precipitation is apparent in Figure 4.36.

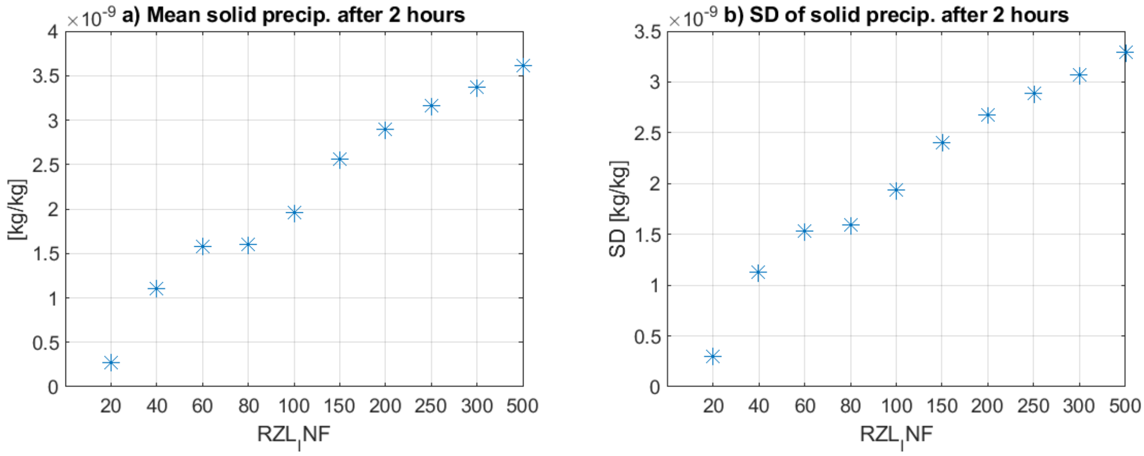

Figure 4.38: Mean of solid precipitation during 2 to 6 hours of simulation time. b) standard deviation of solid precipitation during 2 to 6 hours of simulation time. After 2 h, a sudden increase in precipitation in Figure 4.36.

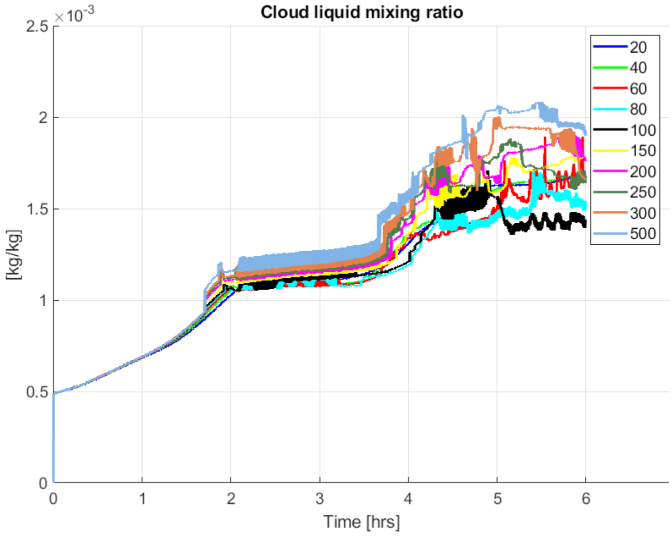

Figure 4.39: As Figure 4.35, but for a time series on responses on cloud liquid mixing ratio [kg/kg] from perturbing the parameter RZL_INF. The cloud liquid mixing ratio has been summed for all 66 model layers.

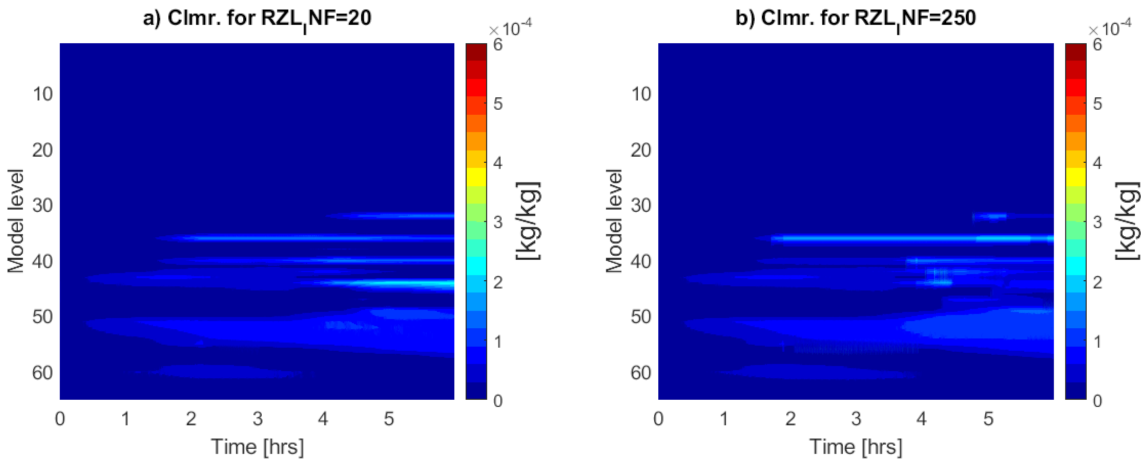

Figure 4.40: Vertical distribution of cloud liquid mixing ratio [kg/kg] from MUSC with a) RZL_INF = 20 and b) RZL_INF = 250.

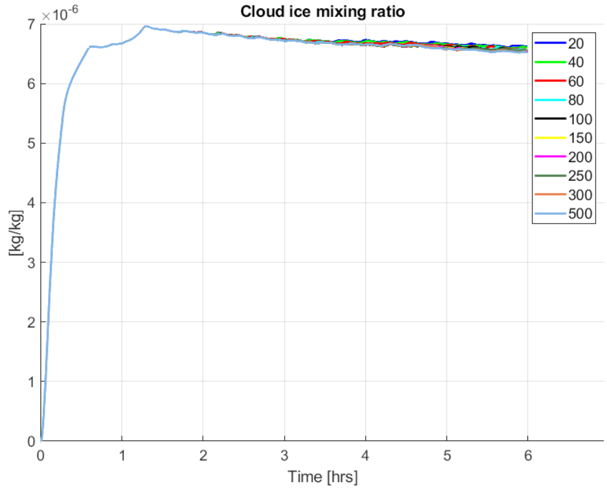

Figure 4.41: As Figure 4.35, but for a time series on responses on cloud ice mixing ratio [kg/kg] from perturbing the parameter RZL_INF. The cloud ice mixing ratio has been summed for all 66 model layers.

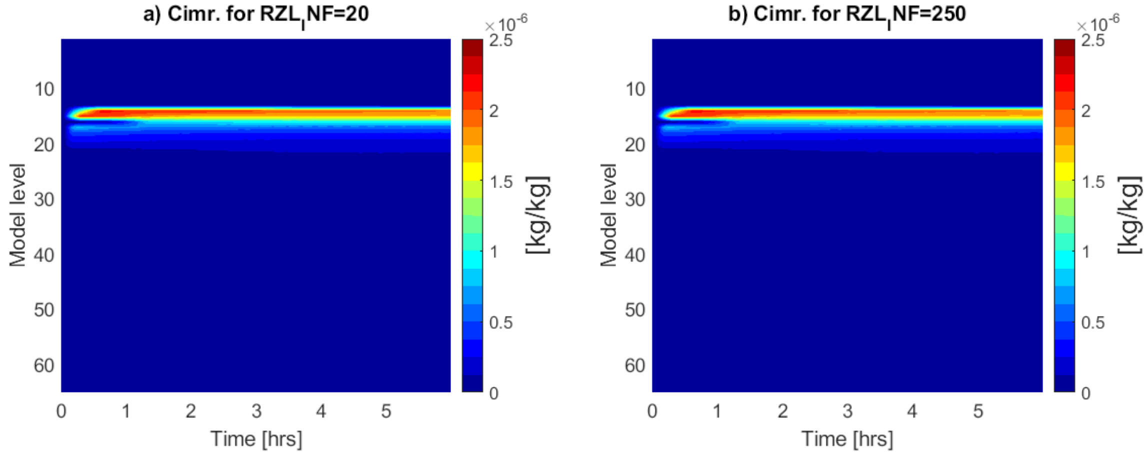

Figure 4.42: Vertical distribution of cloud ice mixing ratio [kg/kg] from MUSC with a) RZL_INF = 20 and b) RZL_INF = 250.

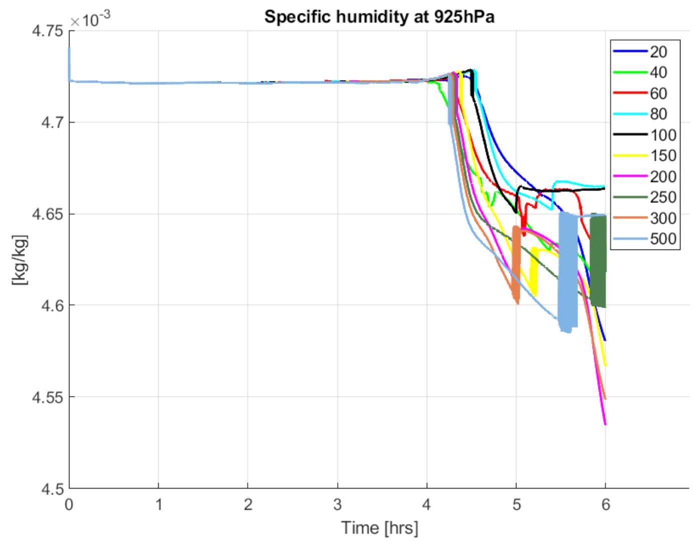

Figure 4.43: As Figure 4.35, but for the impact on specific humidity at 925 hPa [kg/kg] from perturbing the parameter RZL_INF.

Initial profiles for liquid precipitation, solid precipitation, and cloud liquid mixing ratio are zero for all values of RZL_INF (not shown).

4.5 RFRMIN(10) (Kogan autoconversion speed)

This section presents responses from perturbing the parameter RFRMIN(10). The values used in pertrubing RFRMIN(10) can be found in Section 1.5. Values above 50 exceed the range given by physics experts.

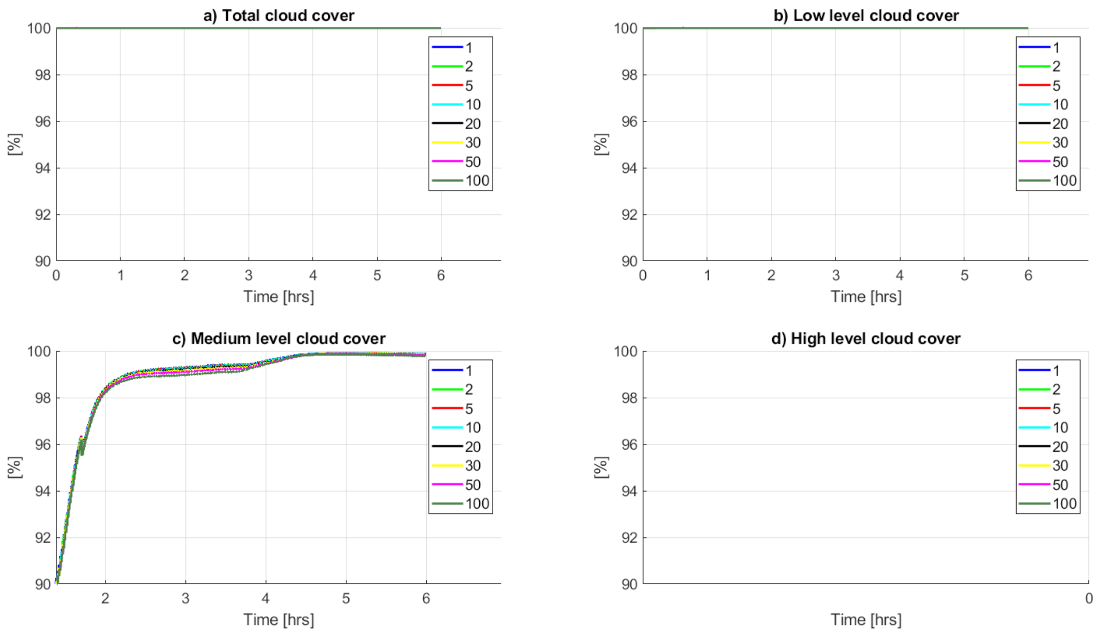

Figure 4.46: Impact on a) total cloud cover, b) low level cloud cover, c) medium level cloud cover, d) high level cloud cover [%] from perturbing the parameter RFRMIN(10). The time period is for 6 hours of simulation time.

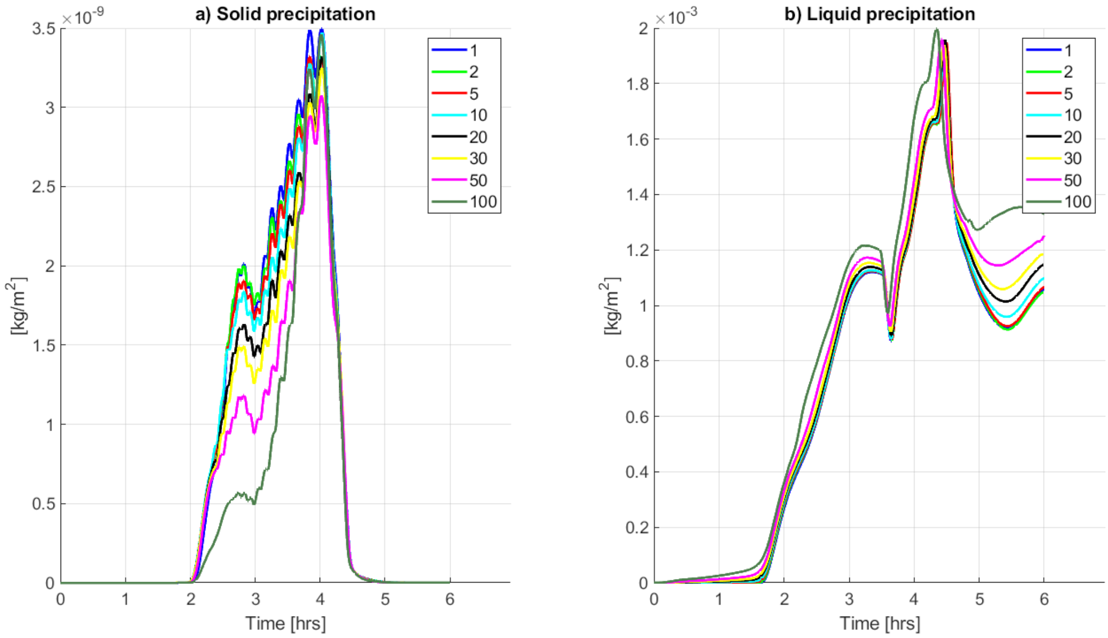

Figure 4.47: As Figure 4.46, but for impact on a) solid precipitation and b) liquid precipitation [kg/m^2] from perturbing the parameter RFRMIN(10). The precipitation has been summed for all 66 model layers.

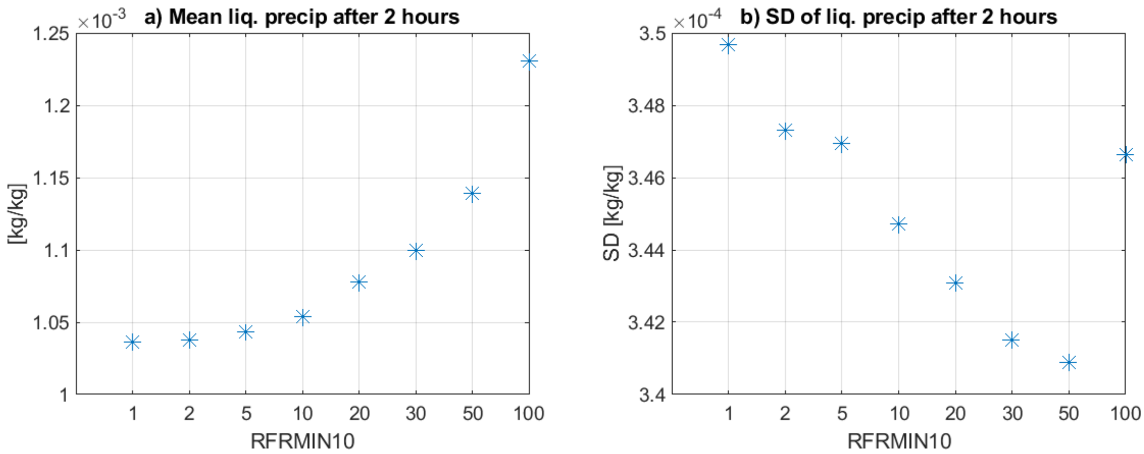

Figure 4.48: Sensitivity of a) mean of liquid precipitation during 2 to 6 hours of simulation time, and b) standard deviation of liquid precipitation during 2 to 6 hours of simulation time. After 2 h, an increase in precipitation is apparent in Figure 4.47.

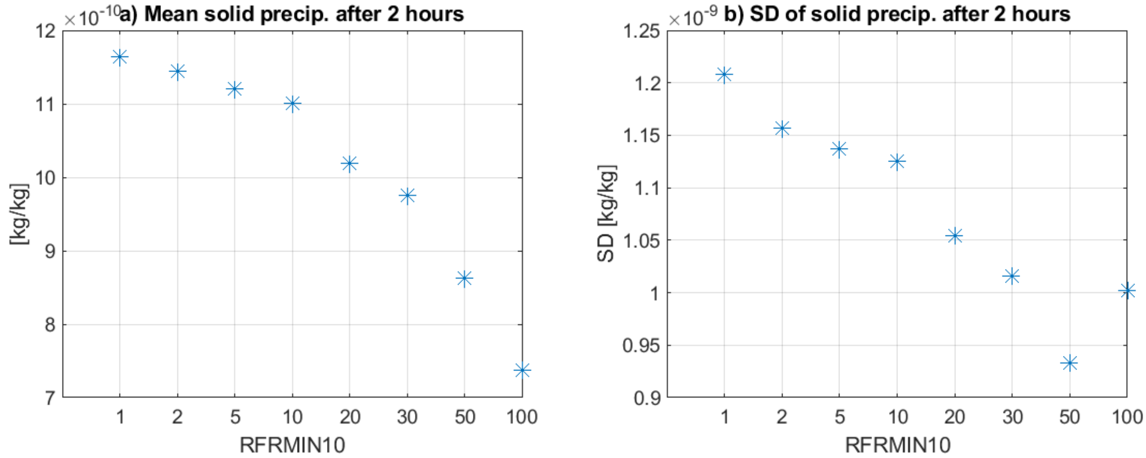

Figure 4.49: Sensitivity of a) mean of solid precipitation during 2 to 6 hours of simulation time, and b) standard deviation of solid precipitation during 2 to 6 hours of simulation time. After 2h, an increase in precipitation is detected in Figure 4.47.

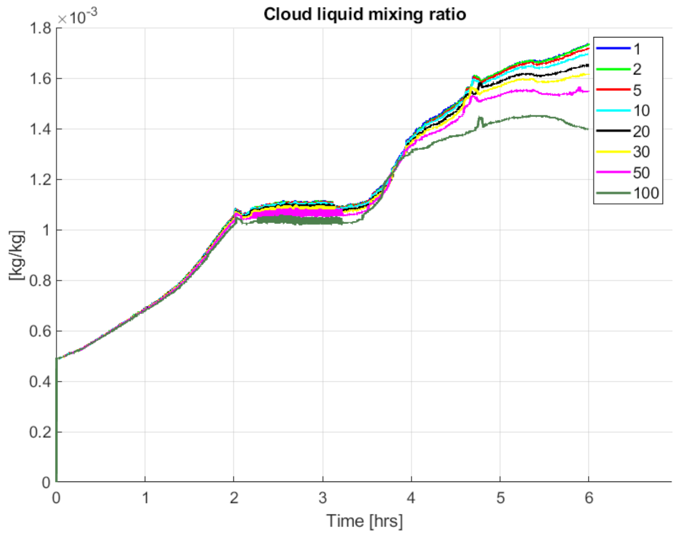

Figure 4.50: As Figure 4.46, but for the impact on cloud liquid mixing ratio [kg/kg] from perturbing the parameter RFRMIN(10). The cloud liquid mixing ratio has been summed for all 66 model layers.

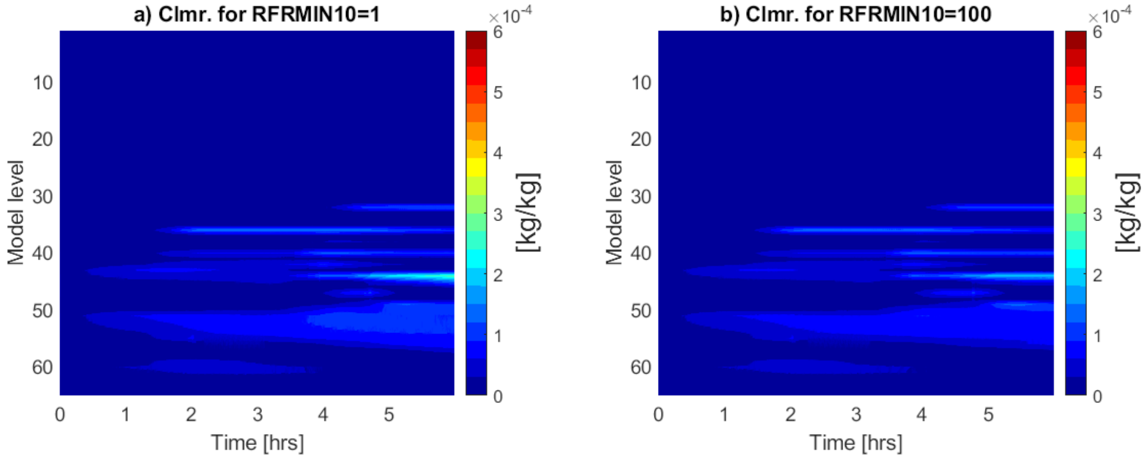

Figure 4.51: Vertical distribution of cloud liquid mixing ratio [kg/kg] from MUSC with a) RFRMIN(10)=1 and b) RFRMIN(10)=100.

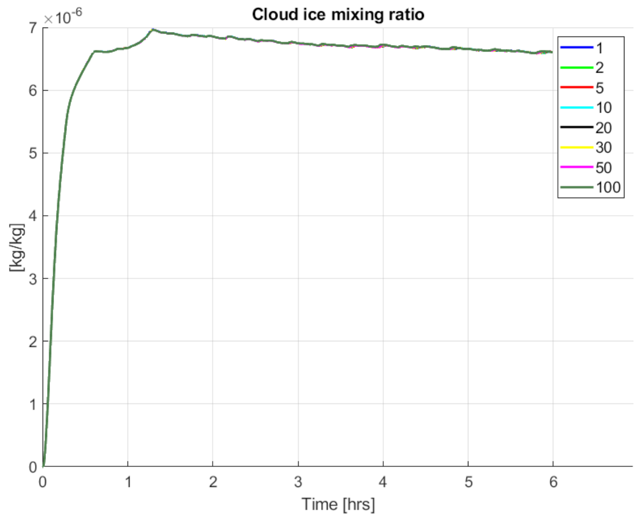

Figure 4.52: Response of cloud ice mixing ratio [kg/kg] from perturbing RFRMIN(10). All the runs have near identical values, which is why only one line is visible.

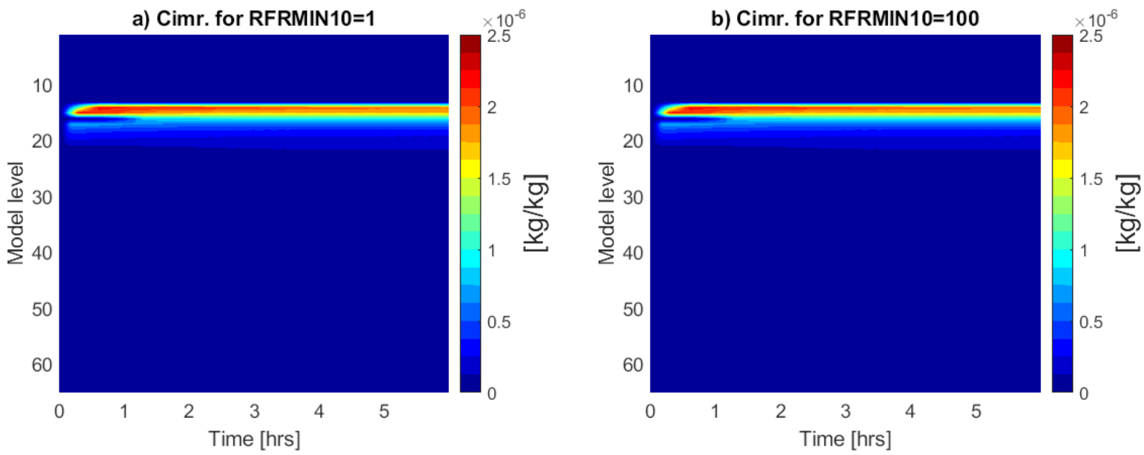

Figure 4.53: Vertical distribution of cloud ice mixing ratio [kg/kg] from MUSC with a) RFRMIN(10)=1 and b) RFRMIN(10)=100.

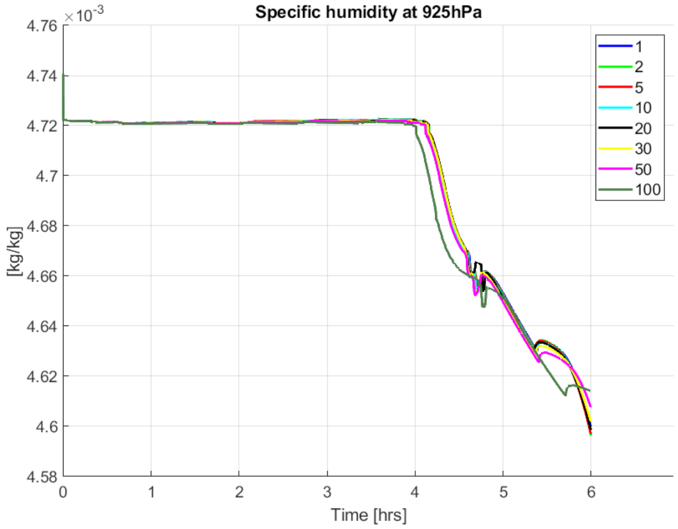

Figure 4.54: Response of specific humidity [kg/kg] at 925 hPa from perturbing RFRMIN(10).

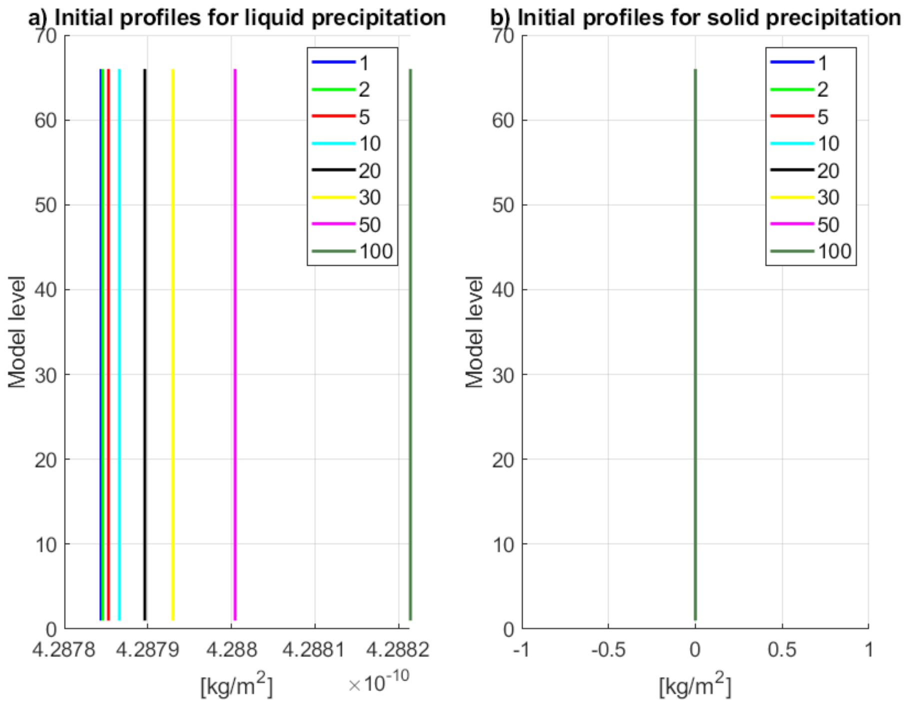

Figure 4.55: Initial vertical profiles of a) liquid precipitation [kg/m^2] and b) solid precipitation [kg/m^2]. The profiles are plotted for the first timestep of the model simulation. Only one line is visible because all the initial profiles are identical.

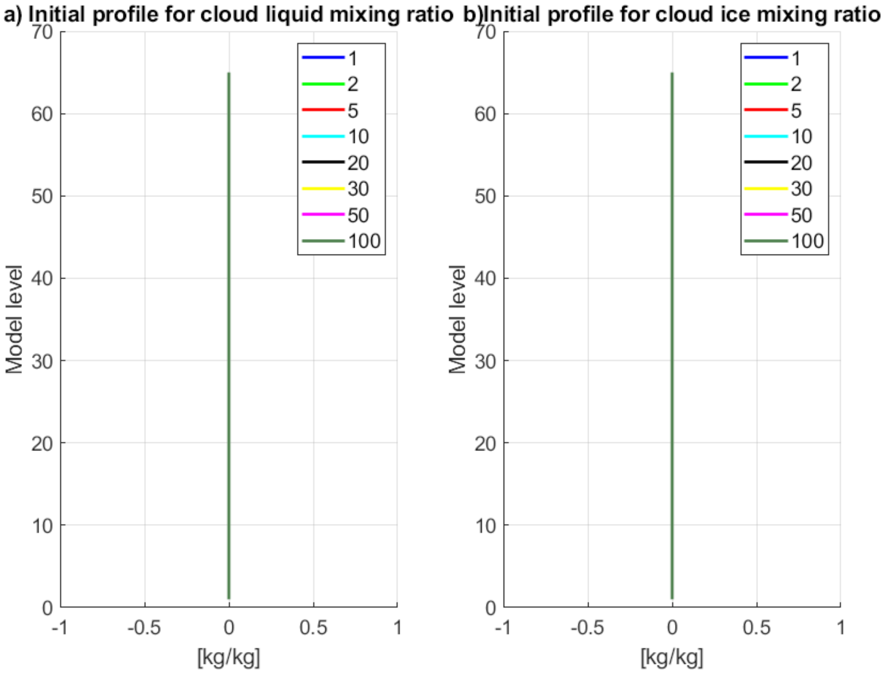

Figure 4.56: Initial vertical profiles of a) cloud liquid mixing ratio [kg/kg] and b) cloud ice mixing ratio [kg/kg]. The profiles are plotted for the first timestep of the model simulation. Only one line is visible because all the initial profiles are identical.

4.6 RFRMIN(11) (Kogan subgrid scale (cloud fraction) sensitivity)

This section presents the responses from perturbing the parameter RFRMIN(11). The values used in perturbing RFRMIN(11) can be found in Section 1.6.

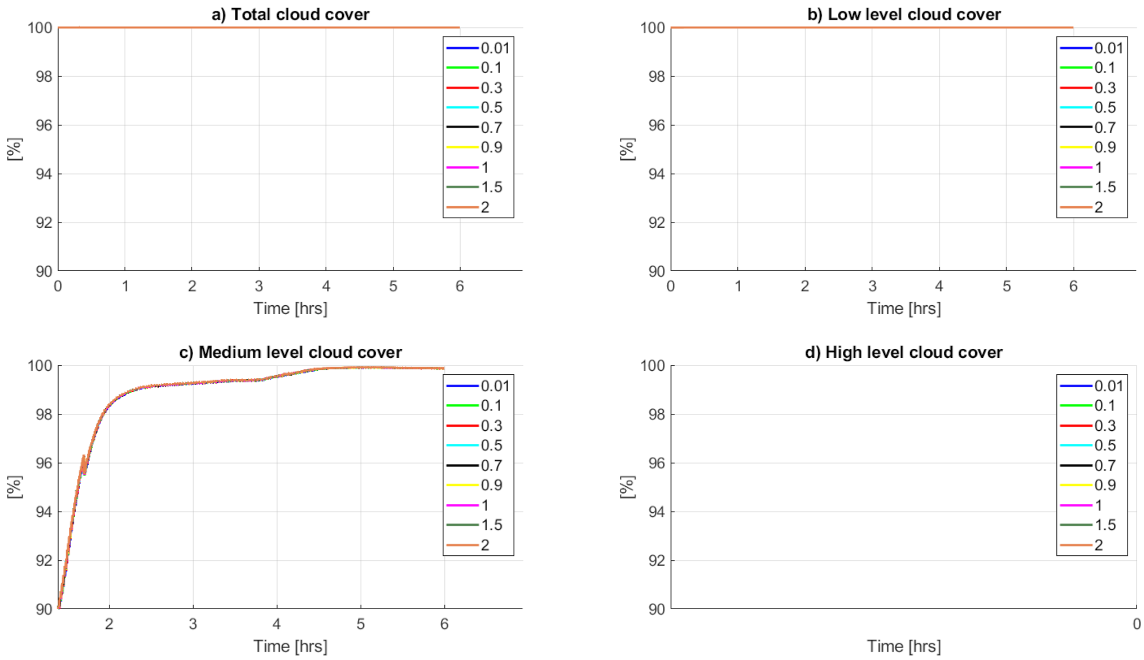

Figure 4.57: Impact on a) total cloud cover [%], b) low level cloud cover [%], c) medium level cloud cover [%] and high level cloud cover [%] from perturbing the parameter RFRMIN(11).

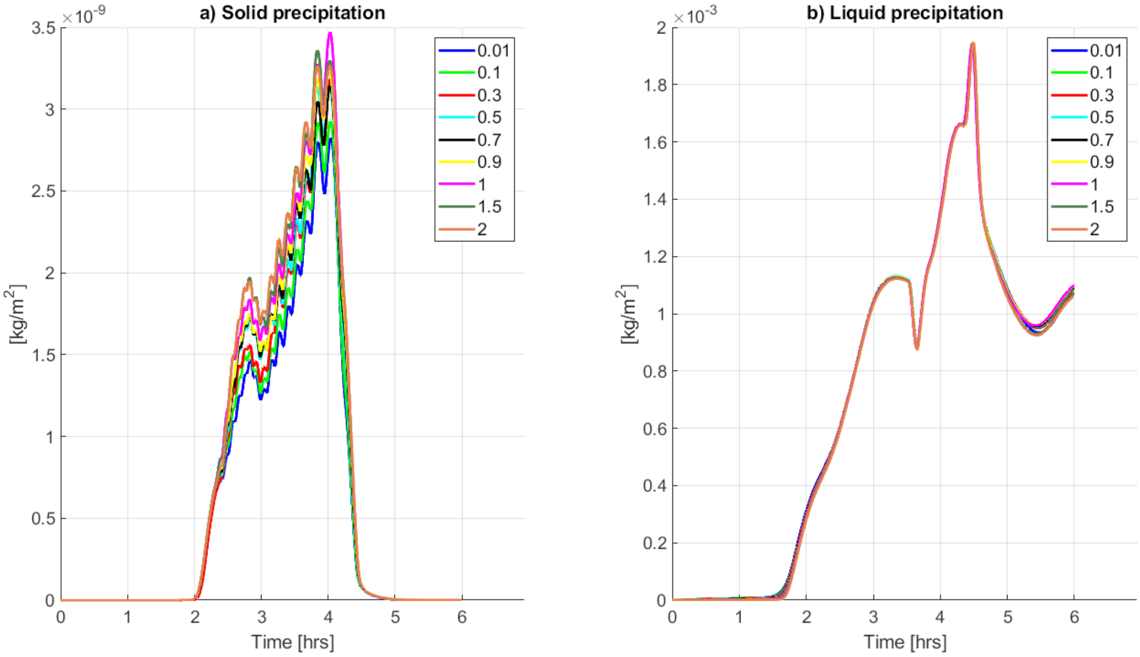

Figure 4.58: Impact of a) solid precipitation and b) liquid precipitation [kg/m^2] from perturbing the parameter RFRMIN(10). The precipitation has been summed for all 66 model layers.

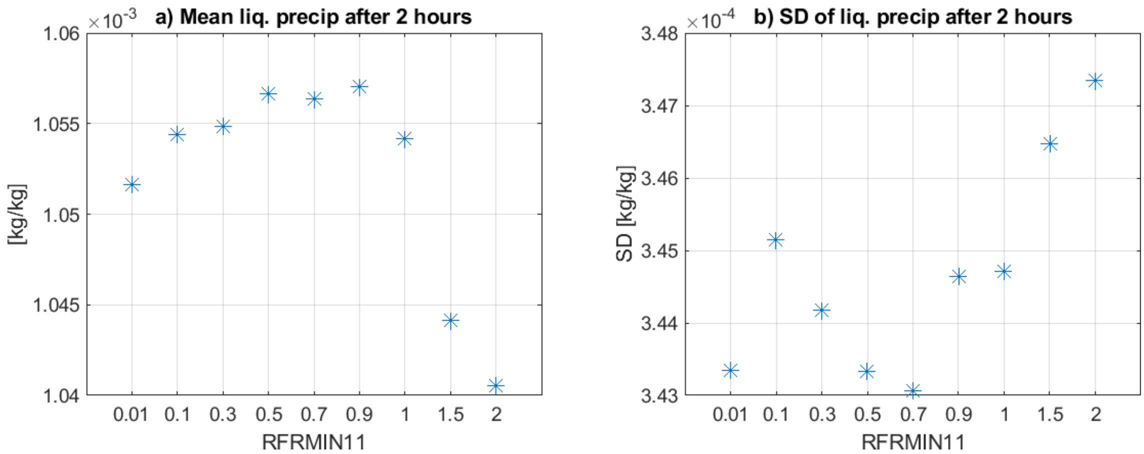

Figure 4.59: Sensitivity of a) mean of liquid precipitation during 2 to 6 hours of simulation time, and b) standard deviation of liquid precipitation during 2 to 6 hours of simulation time. After 2h, an increase in precipitation is apparent in Figure 4.58.

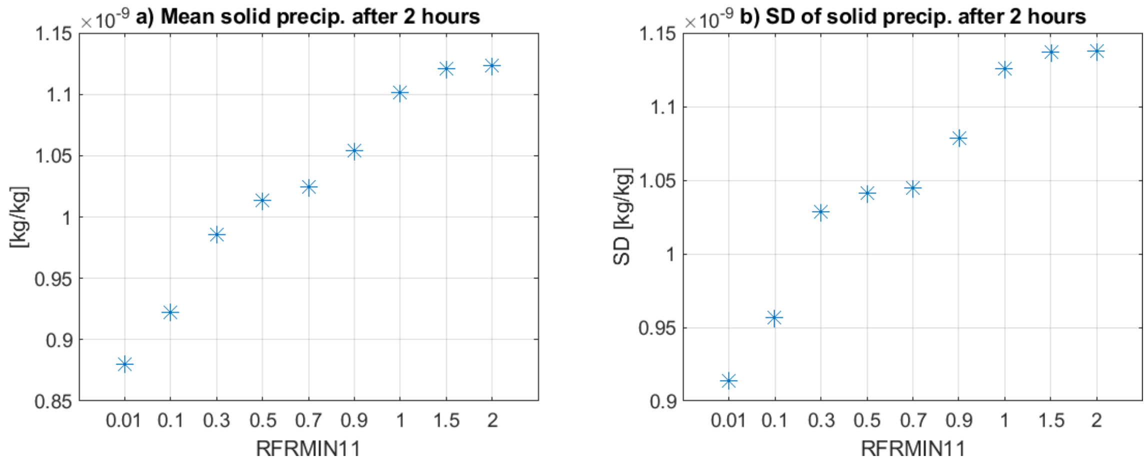

Figure 4.60: Sensitivity of a) mean of solid precipitation during 2 to 6 hours of simulation time, and b) standard deviation of solid precipitation during 2 to 6 hours of simulation time. After 2h, an increase in precipitation is apparent in Figure 4.58.

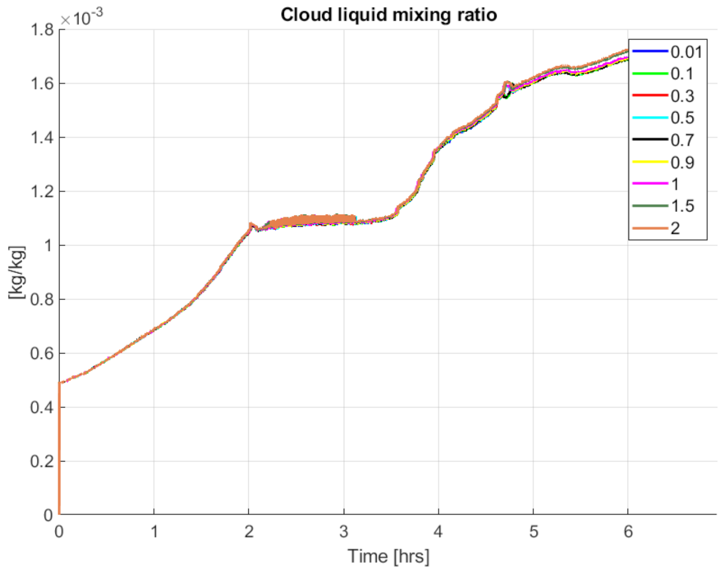

Figure 4.61: Response of cloud liquid mixing ratio [kg/kg] to perturbing the parameter RFRMIN(11). The cloud liquid mixing ratio has been summed for all 66 model layers.

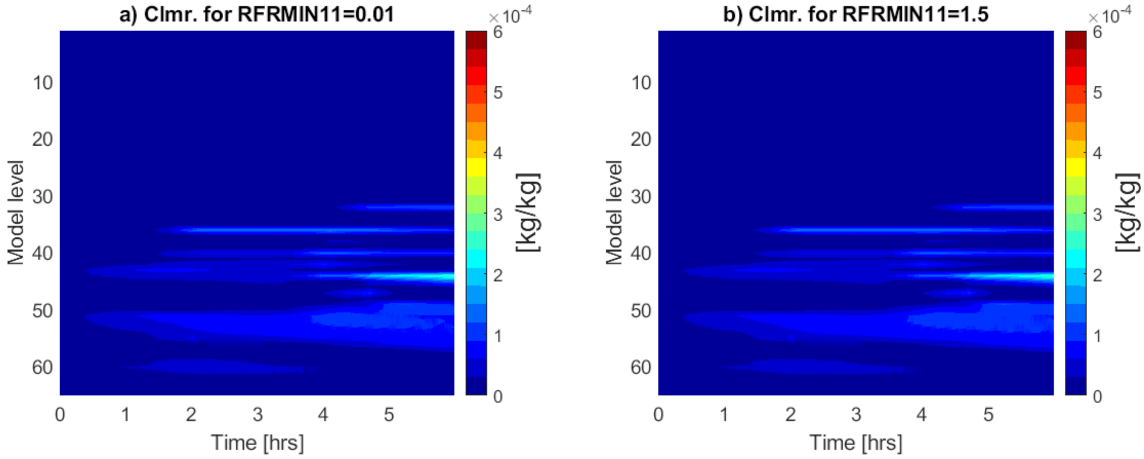

Figure 4.62: Vertical distribution of cloud liquid mixing ratio [kg/kg] from MUSC with a) RFRMIN(11)=0.01 and b) RFRMIN(11)=1.5.

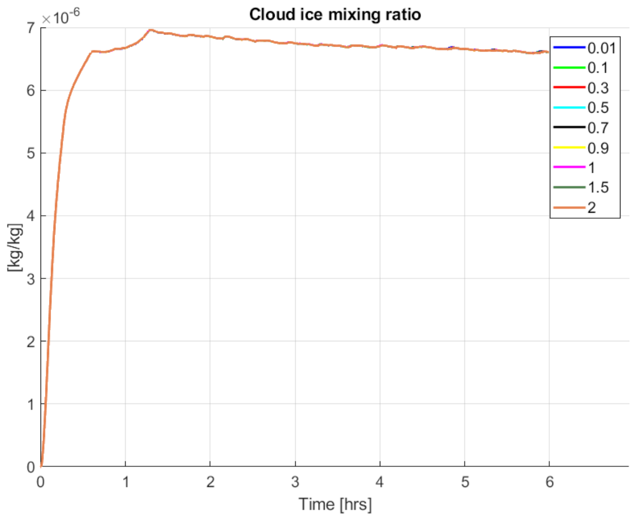

Figure 4.63: Response of cloud ice mixing ratio [kg/kg] to perturbing RFRMIN(11). All the runs have near identical values and is the reason for why only one line is visible.

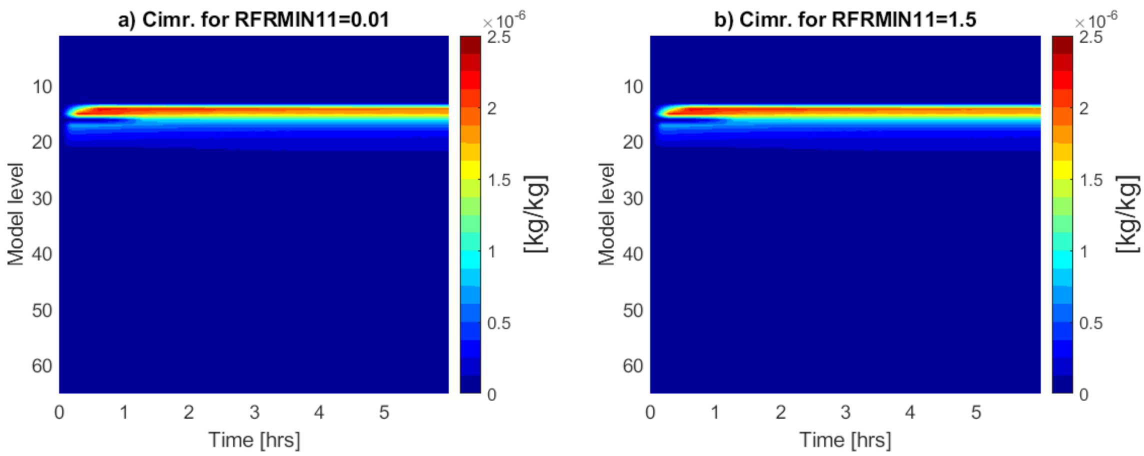

Figure 4.64: Vertical distribution of cloud ice mixing ratio [kg/kg] from MUSC with a) RFRMIN(11)=0.01 and b) RFRMIN(11)=1.5.

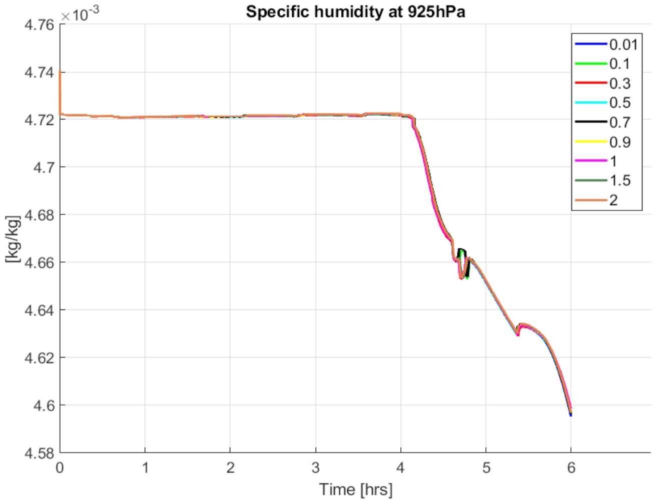

Figure 4.65: Responses of specific humidity [kg/kg] at 925 hpa to perturbing RFRMIN(11).

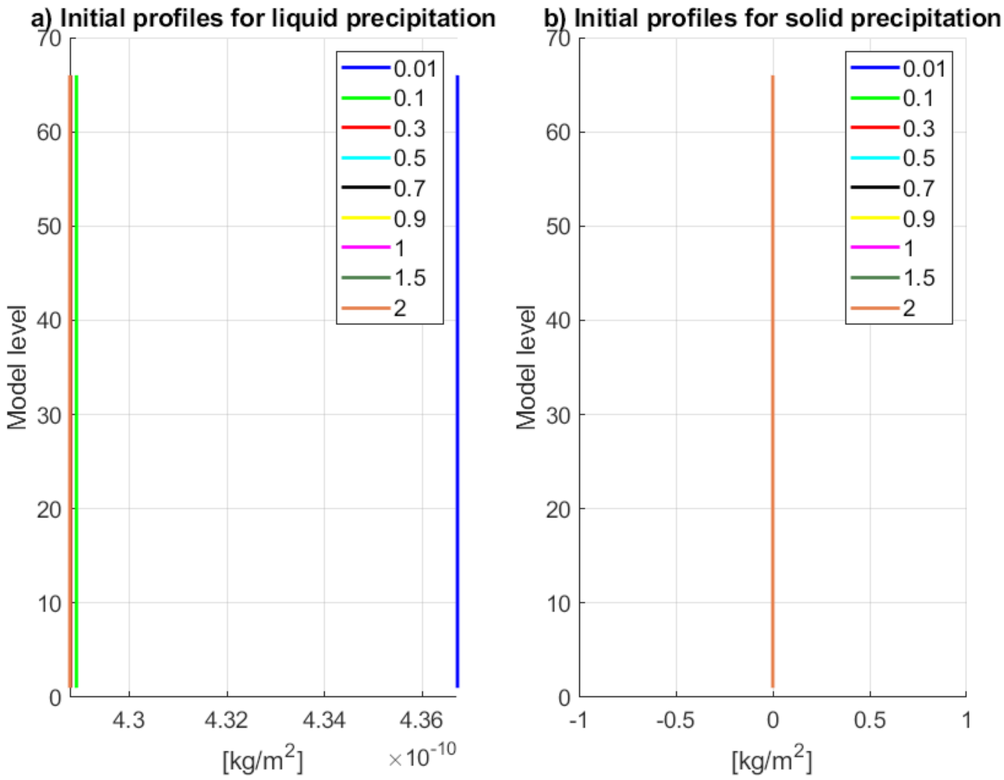

Figure 4.66: Initial vertical profiles of a) liquid precipitation [kg/m^2] and b) solid precipitation [kg/m^2]. The profiles are plotted for the first timestep of the model simulation.

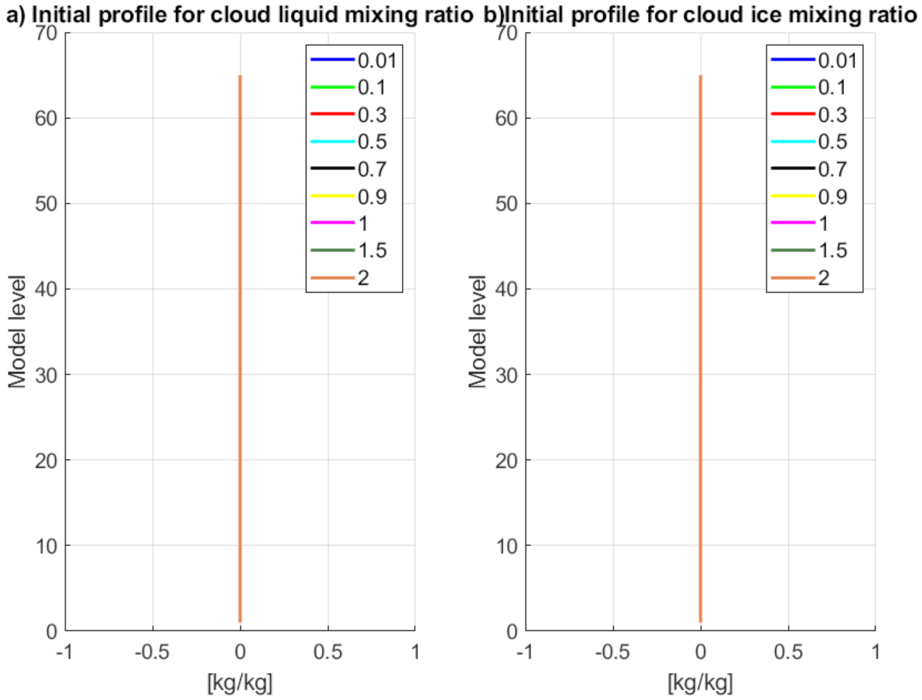

Figure 4.67: Initial vertical profiles of a) cloud liquid mixing ratio [kg/kg] and b) cloud ice mixing ratio [kg/kg]. The profiles are plotted for the first timestep of the model simulation. Only one line is visible because the profiles are near identical for each RFRMIN(11).

4.7 XCCR (rain intercept parameter)

Plots of responses on different variables by perturbing the parameter XCCR. The default value for this parameter is 8×10^6. The different values used in perturbing XCCR can be found below. XCCR is also called rain intercept parameter N0, and shifts the distribution from larger to smaller raindrops.

Parameter values:

XCCR	**8.0x10^5**	**4x10^6**	**8x10^6**	**4x10^7**	**8x10^7**	**4x10^8**	**8x10^8**	**4x10^9**	**8x10^9**

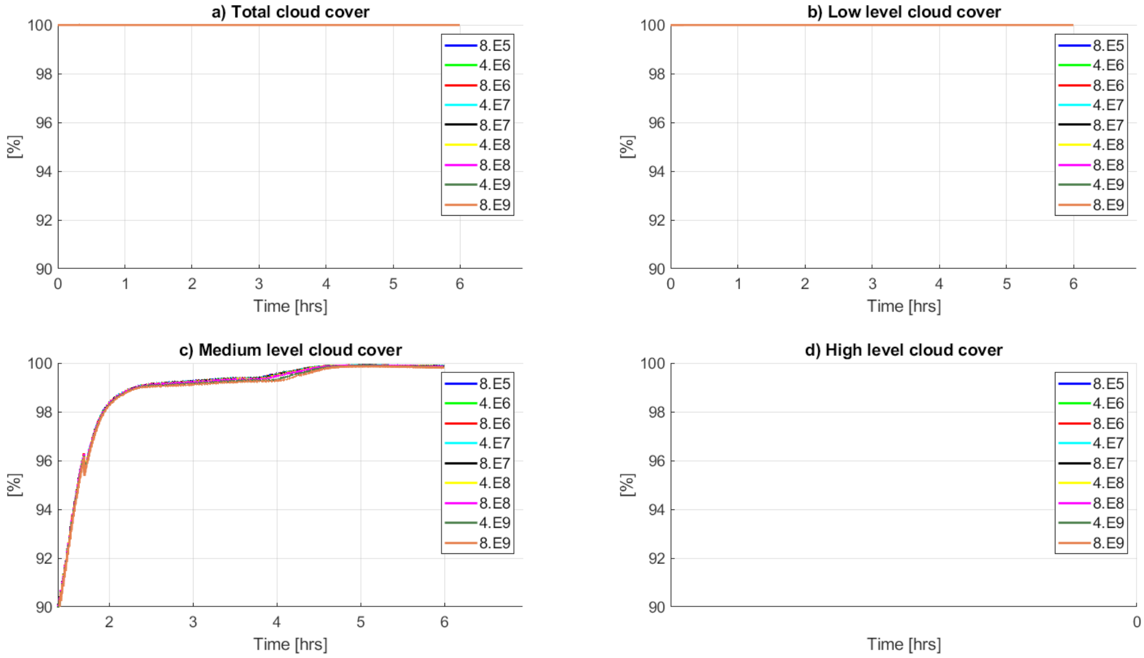

Figure 4.68: Impact on a) total cloud cover, b) low level cloud cover, c) medium level cloud cover, d) high level cloud cover [%] from perturbing the parameter XCCR. The time period is for 6 hours of simulation time and at the location 80ºN, 4ºW.

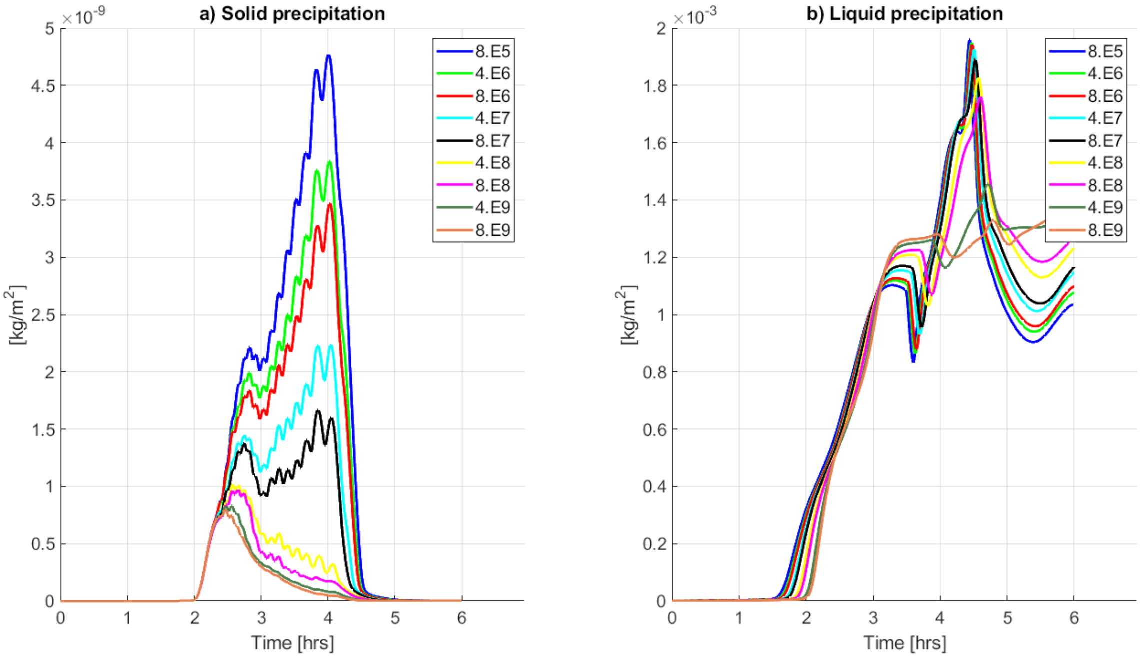

Figure 4.69: As Figure 4.68, but for the impact on a) solid precipitation and b) liquid precipitation [kg/m^2] to perturbing the parameter XCCR. The precipitation has been summed for all 66 model layers. Note the difference in scale on the y-axis on panel a) and b).

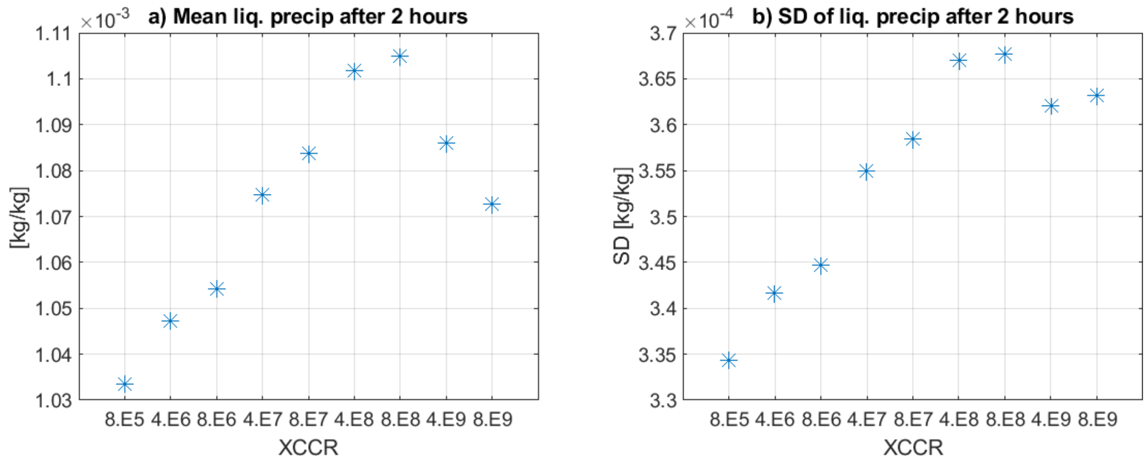

Figure 4.70: Sensitivity of a) mean of liquid precipitation during 2 to 6 hours of simulation time, and b) standard deviation of liquid precipitation during 2 to 6 hours of simulation time. After 2 h, a sudden increase in liquid precipitation is apparent in Figure 4.2.

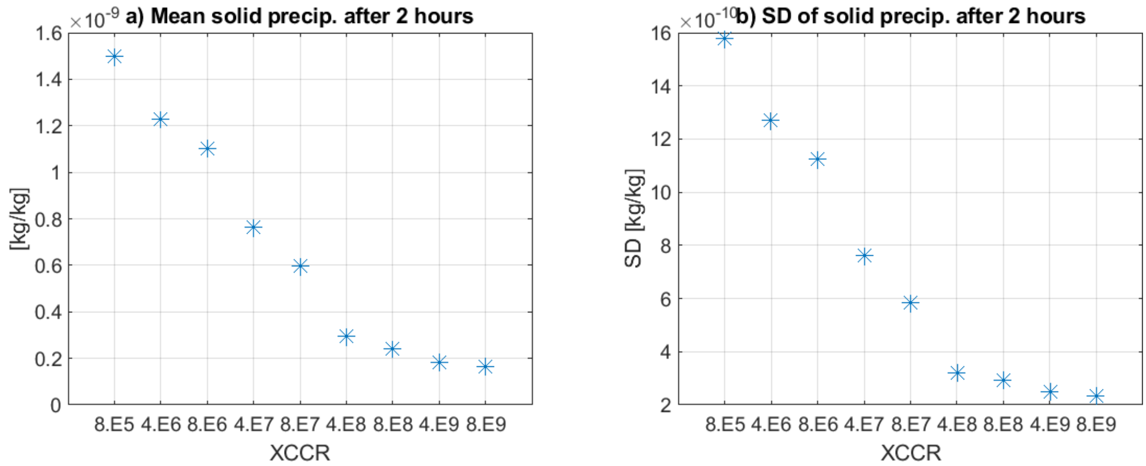

Figure 4.71: Sensitivity of a) mean of solid precipitation during 2 to 6 hours of simulation time, and b) standard deviation of solid precipitation during 2 to 6 hours of simulation time. After 2 h, a sudden increase in liquid precipitation in Figure 4.2.

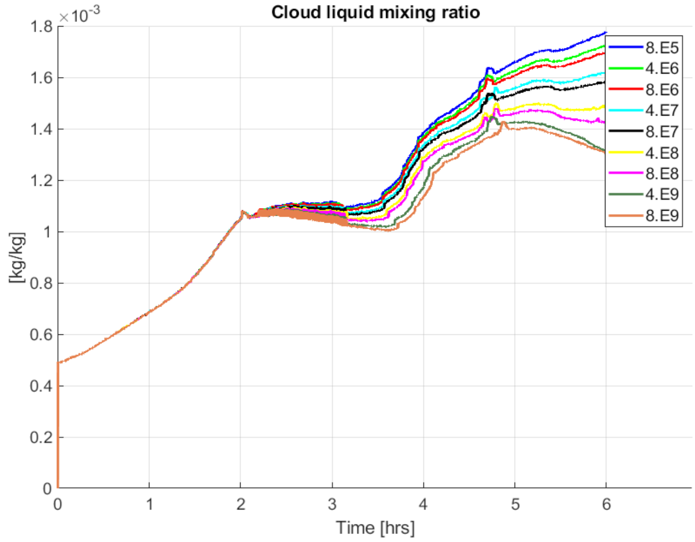

Figure 4.72: As Figure 4.68, but for the impact on cloud liquid mixing ratio [kg/kg] from perturbing the parameter XCCR. The cloud liquid mixing ratio has been summed for all 66 model layers.

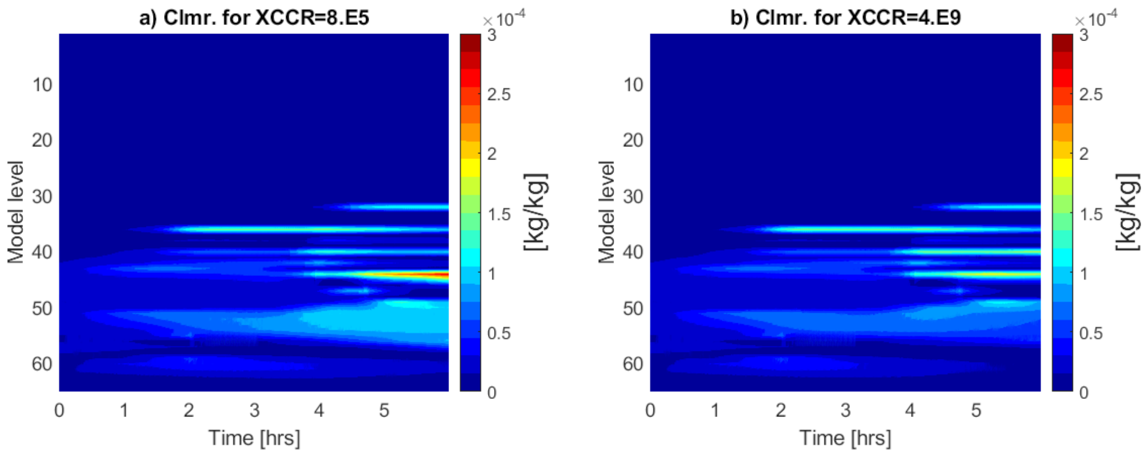

Figure 4.73: Vertical distribution of cloud liquid mixing ratio [kg/kg] from MUSC with a) XCCR = 8×10^{5} and b) XCCR = 4×10^{9}.

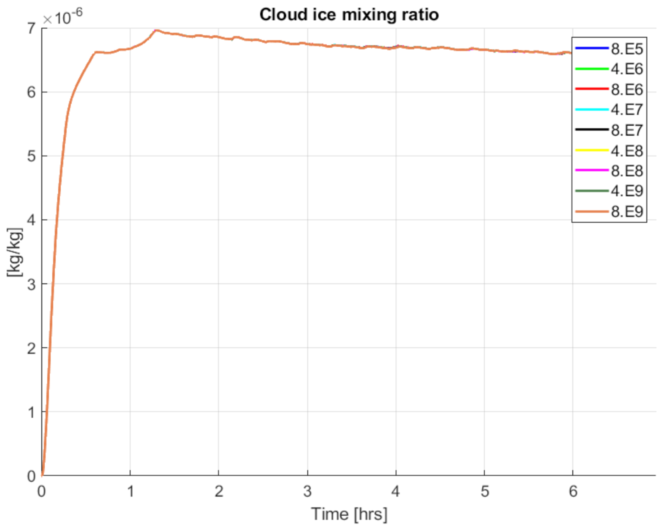

Figure 4.74: As Figure 4.68, but for the impact on cloud ice mixing ratio [kg/kg] from perturbing the parameter XCCR. The cloud ice mixing ratio has been summed for all 66 model layers. Only one line is visible because the cloud ice mixing ratio is near equal for all the runs.

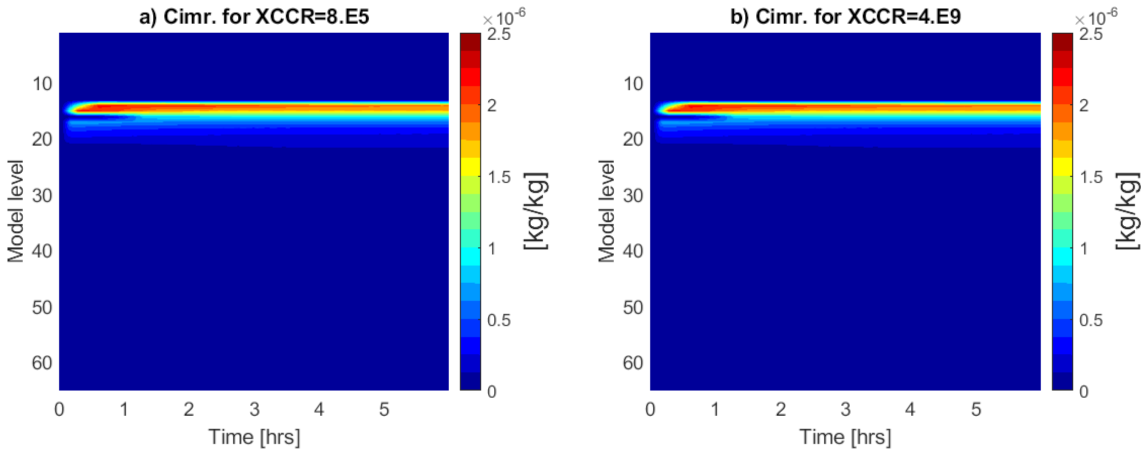

Figure 4.75: Vertical distribution of cloud ice mixing ratio [kg/kg] from MUSC with a) XCCR = 8×10^5 and b) XCCR = 4×10^9.

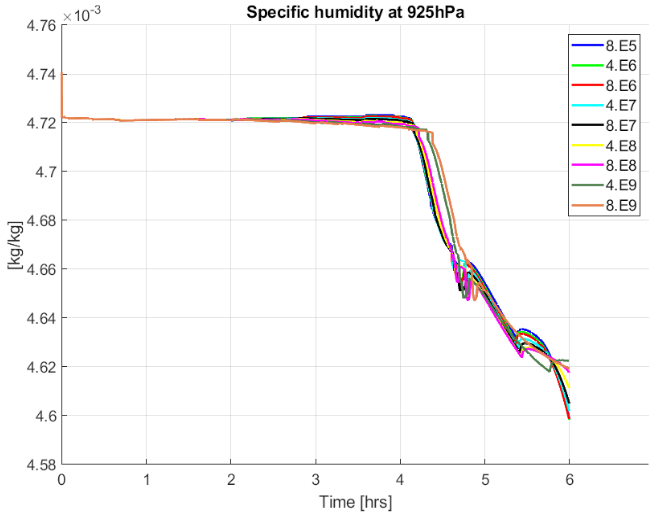

Figure 4.76: As Figure 4.68, but for the impact on specific humidity at 925 hPa [kg/kg] from perturbing the parameter XCCR.

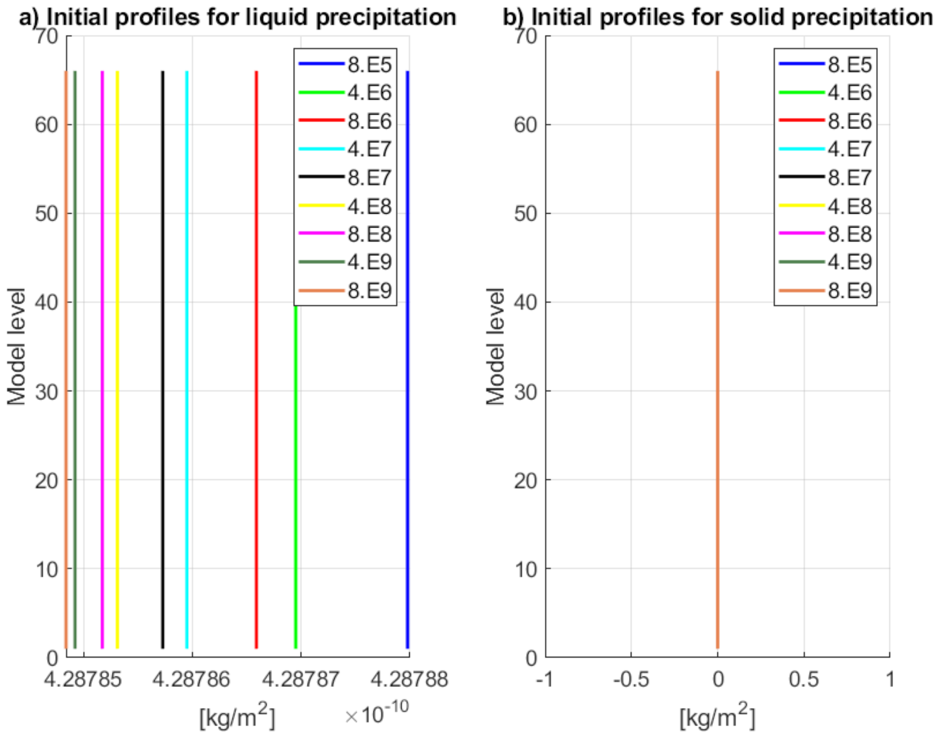

Figure 4.77: Initial vertical profiles of a) liquid precipitation [kg/m^2] and b) solid precipitation [kg/m^2] for the location 80ºN, 4ºW. The profiles are plotted for the first timestep of the model simulation. In panel b) only one line is visible because all the initial profiles are identical.

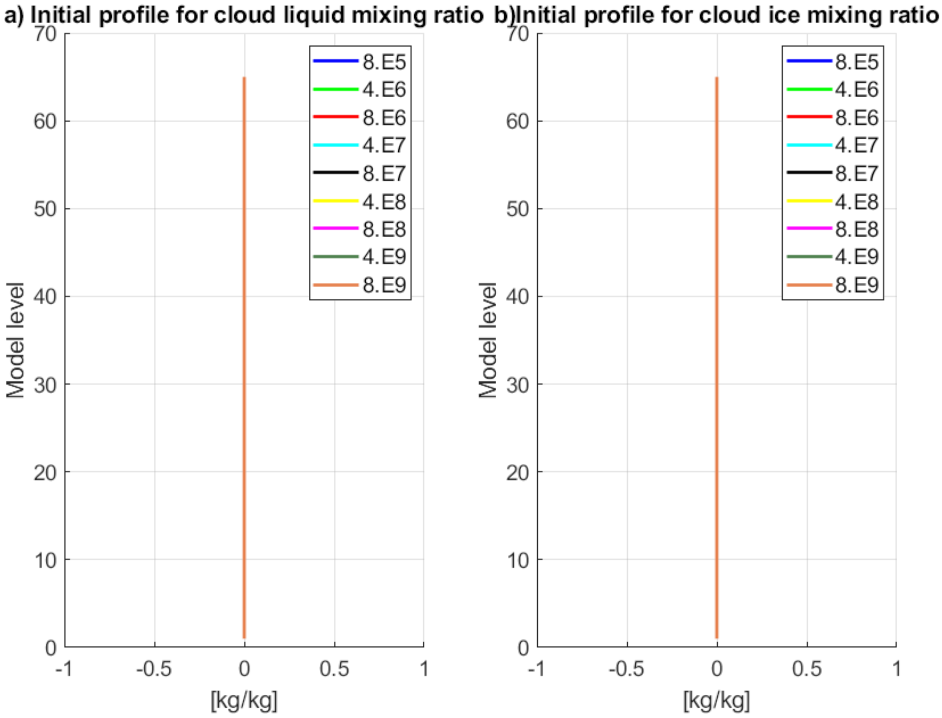

Figure 4.78: Initial vertical profiles of a) cloud liquid mixing ratio [kg/kg] and b) cloud ice mixing ratio [kg/kg] for the location 80ºN, 4ºW. The profiles are plotted for the first timestep of the model simulation. Only one line is visible because all the initial profiles are identical.

4.8 RFRMIN(21) (Cloud ice content impact on cloud thickness)

This section presents the response from perturbing the parameter RFRMIN(21). RFRMIN(21) controls the cloud ice content impact on cloud thickness. The values used in perturbing RFRMIN(21) can be found below. The default value for RFRMIN(21) is 1. Values above 2 exceed the range given by physics experts.

Parameter values:

RFRMIN(21)	**0**	**0.5**	1	**1.5**	**2**	3	4	5	6

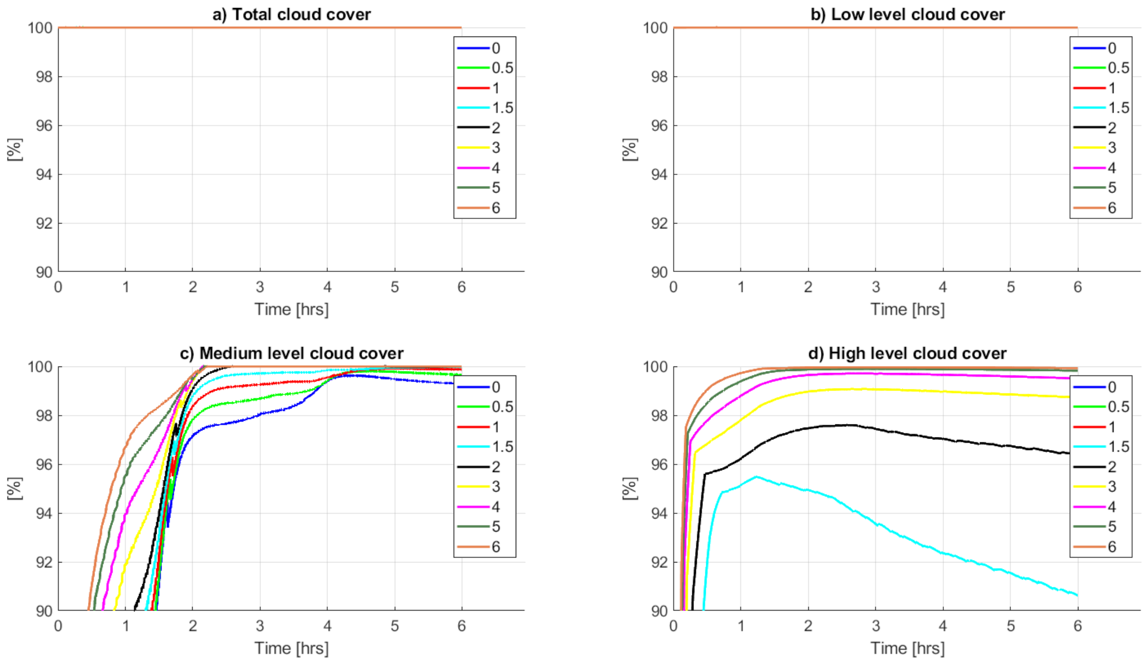

Figure 4.79: Impact on a) total cloud cover, b) low level cloud cover, c) medium level cloud cover, d) high level cloud cover [%] from perturbing the parameter RFRMIN(21). The time period is for 6 hours of simulation time and at the location 80ºN, 4ºW.

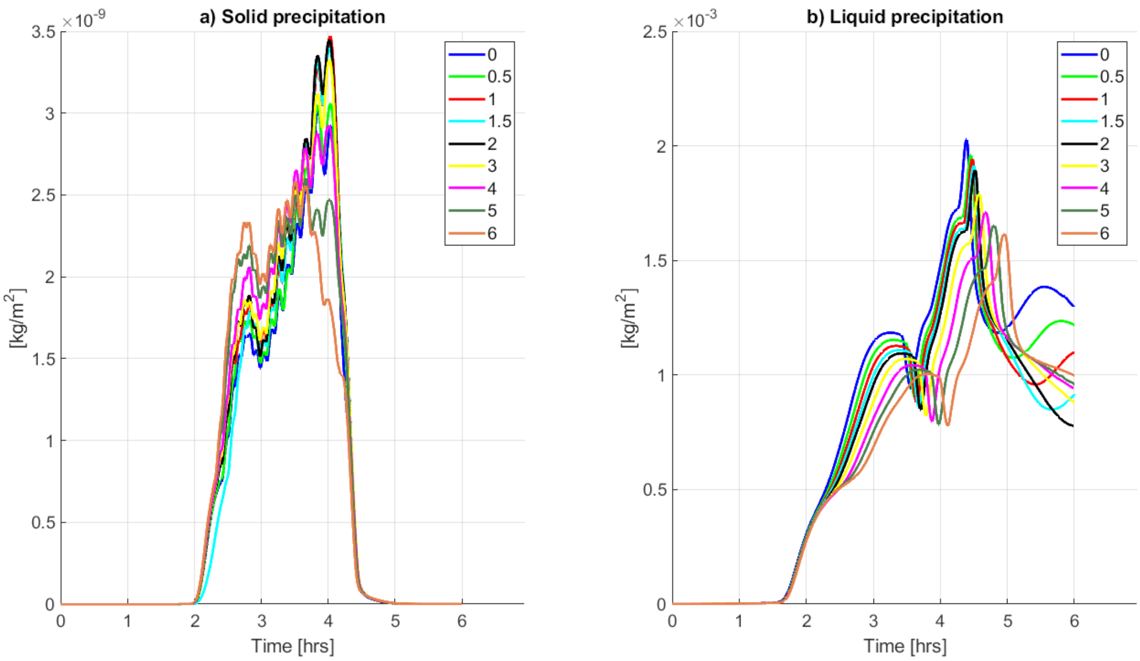

Figure 4.80: As Figure 4.79, but for the impact on a) solid precipitation and b) liquid precipitation [kg/m^2] from perturbing the parameter RFRMIN(21). The precipitation has been summed for all 66 model layers. Note the difference in scale on the y-axis in panels a) and b).

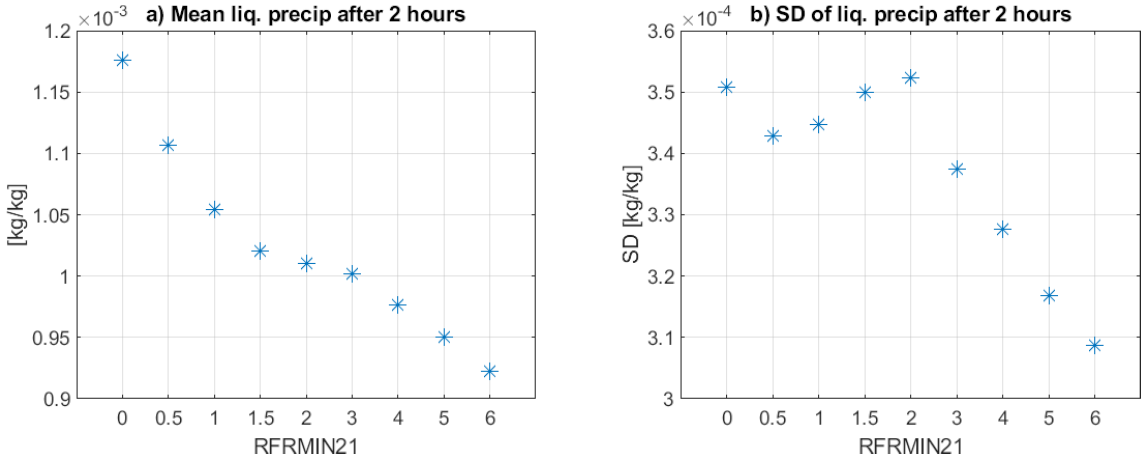

Figure 4.81: Sensitivity of a) mean of liquid precipitation during 2 to 6 hours of simulation time, and b) standard deviation of liquid precipitation during 2 to 6 hours of simulation time. After 2 h, a sudden increase in liquid precipitation is apparent in Figure 4.2.

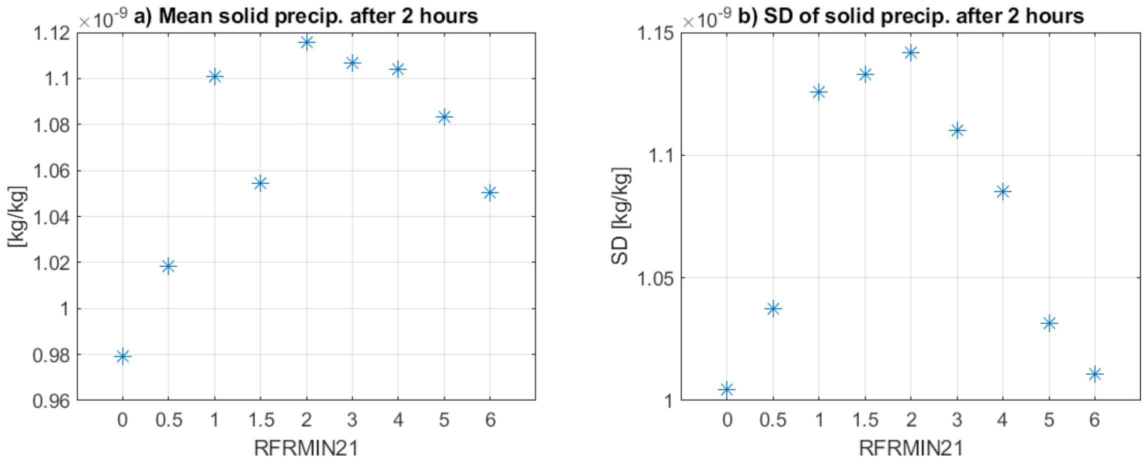

Figure 4.82: Sensitivity of a) mean of solid precipitation during 2 to 6 hours of simulation time, and b) standard deviation of solid precipitation during 2 to 6 hours of simulation time. After 2 h, a sudden increase in liquid precipitation is apparent in Figure 4.2.

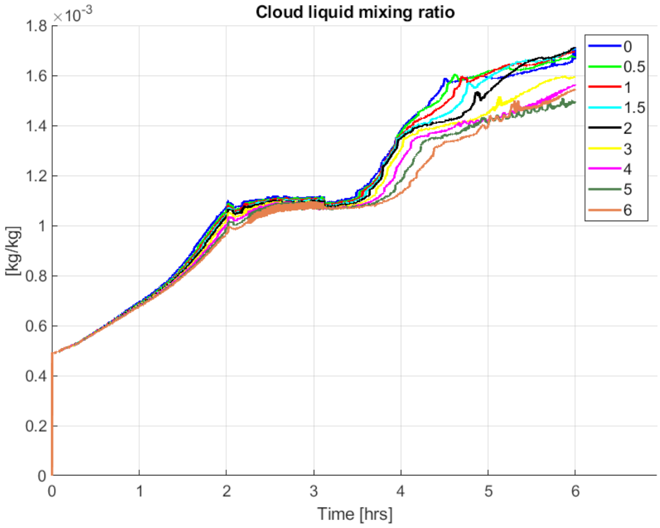

Figure 4.83: As Figure 4.79, but for the response on cloud liquid mixing ratio [kg/kg] from perturbing the parameter RFRMIN(21). The cloud liquid mixing ratio has been summed for all 66 model layers.

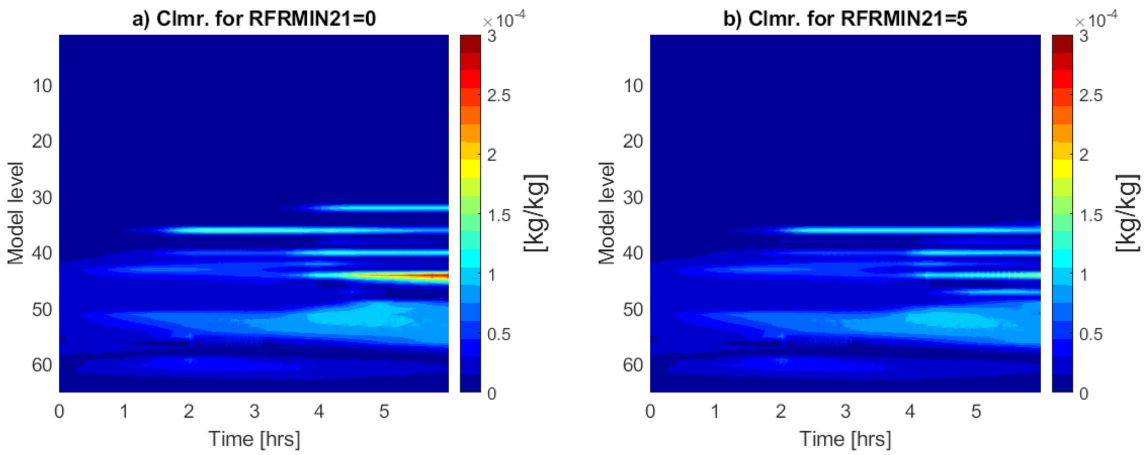

Figure 4.84: Vertical distribution of cloud liquid mixing ratio [kg/kg] from MUSC with a) RFRMIN(21) = 0 and b) RFRMIN(21) = 5.

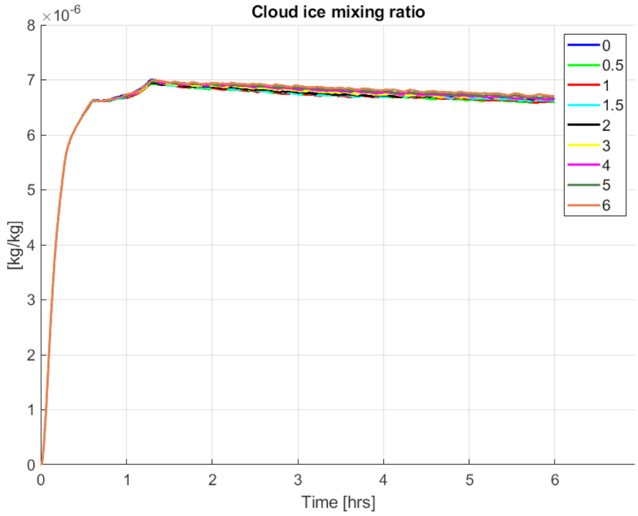

Figure 4.85: As Figure 4.79, but for the response of cloud ice mixing ratio [kg/kg] from perturbing the parameter RFRMIN(21). The cloud ice mixing ratio has been summed for all 66 model layers.

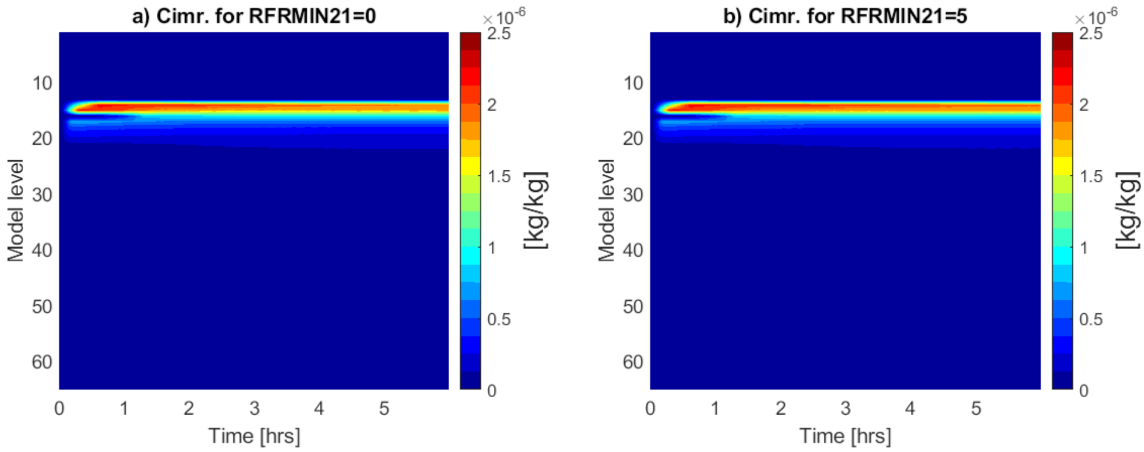

Figure 4.86: Vertical distribution of cloud Iice mixing ratio [kg/kg] from MUSC with a) RFRMIN(21) = 0 and b) RFRMIN(21) = 5.

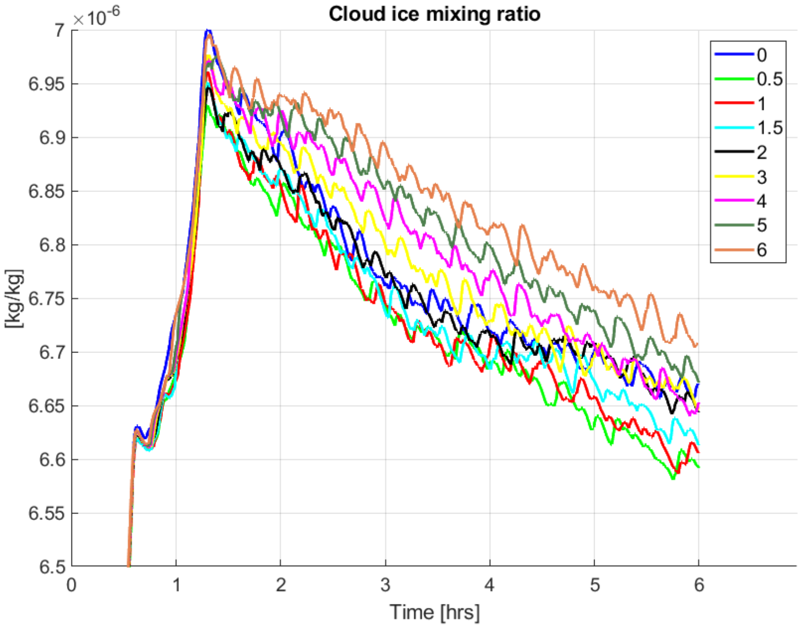

Figure 4.87: As Figure 4.85, but with the y-axis scaled for the purpose of identifying smaller differences.

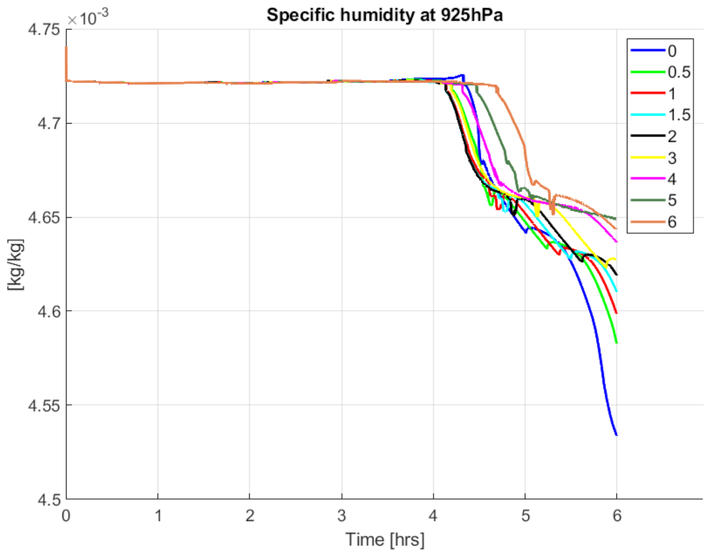

Figure 4.88: As Figure 4.79, but for impact on specific humidity at 925 hPa [kg/kg] from perturbing the parameter RFRMIN(21).

Initial profiles for liquid precipitation, solid precipitation, and cloud liquid mixing ratio are zero for all values of RFRMIN(21) (not shown).

4.9 RFRMIN(20) Threshold cloud thickness in shallow/deep convection decision

Perturbing RFRMIN(20) showed no responses on the variables investigated here.

4.10 RFRMIN(9) (Ice nuclei)

This section presents the responses from perturbing the parameter RFRMIN(9). The values used in perturbing RFRMIN(9) can be found below. This parameter has a default of 1 and a range from 0.1-10. Values above 10 exceed the range given by physics experts.

Parameter values:

RFRMIN(9)	**0.1**	**1**	**2**	**3**	**5**	**7**	**10**	**15**	**20**

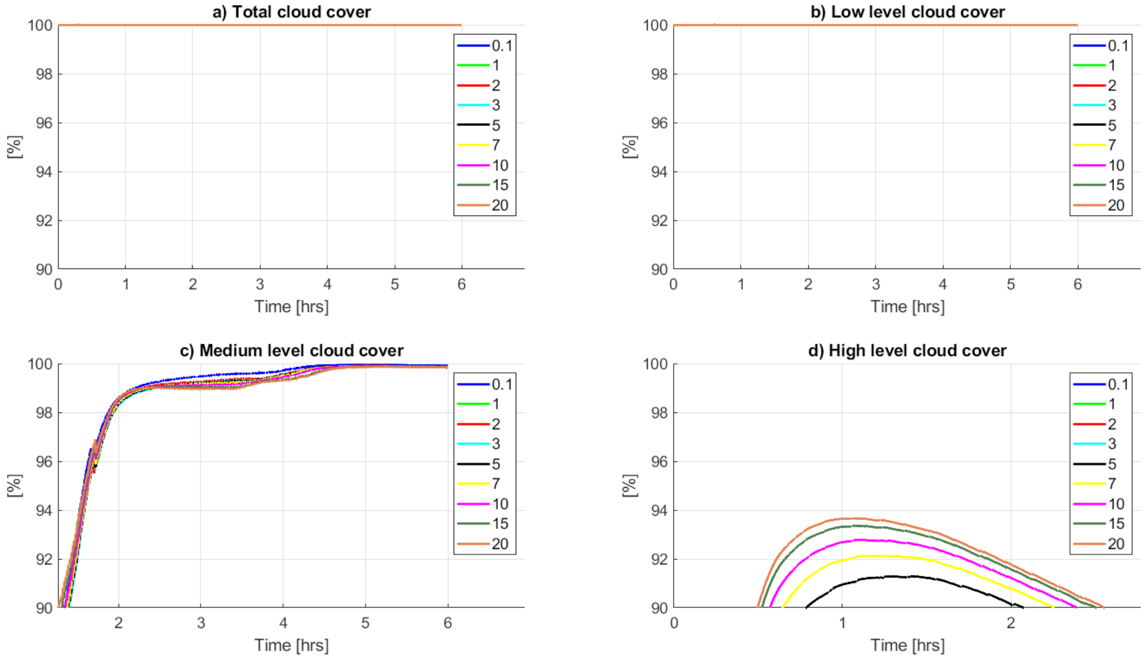

Figure 4.91: Impact on a) total cloud cover, b) low level cloud cover, c) medium level cloud cover, d) high level cloud cover [%] from perturbing the parameter RFRMIN(9). The time period is for 6 hours of simulation time and at the location is 80ºN, 4ºW.

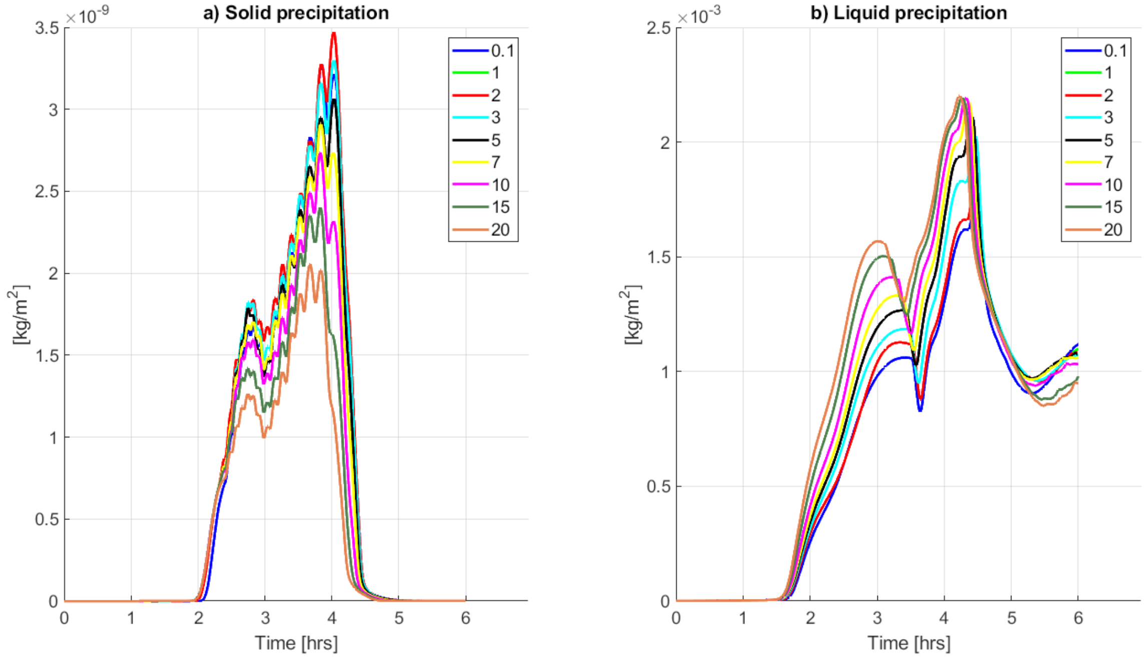

Figure 4.92: As Figure 4.91, but for the impact on a) solid precipitation and b) liquid precipitation [kg/m^2] from perturbing the parameter RFRMIN(9). The precipitation has been summed for all 66 model layers. Note the difference in scale on the y-axis on panels a) and b).

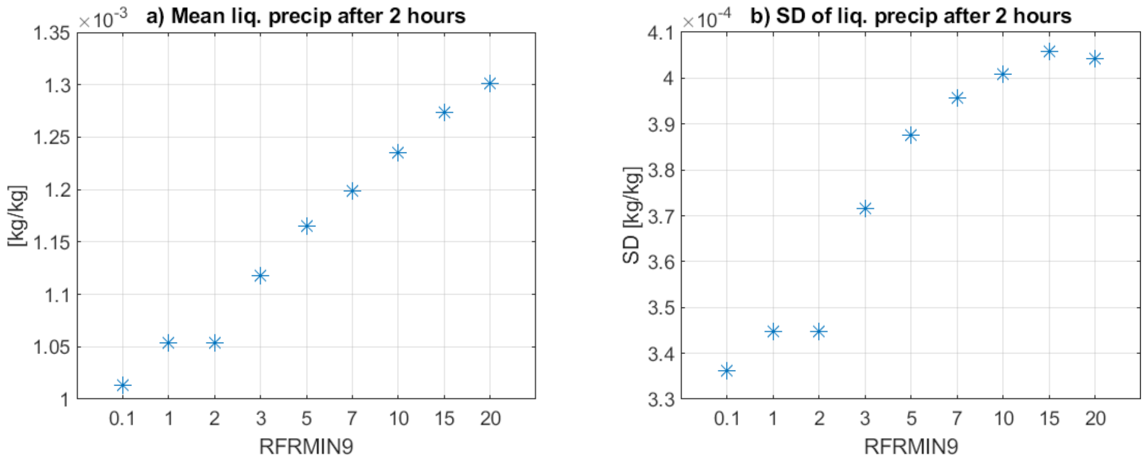

Figure 4.93: Sensitivity of a) mean of liquid precipitation during 2 to 6 hours of simulation time, and b) standard deviation of liquid precipitation during 2 to 6 hours of simulation time. After 2 h, a sudden increase in liquid precipitation is apparent in Figure 4.92.

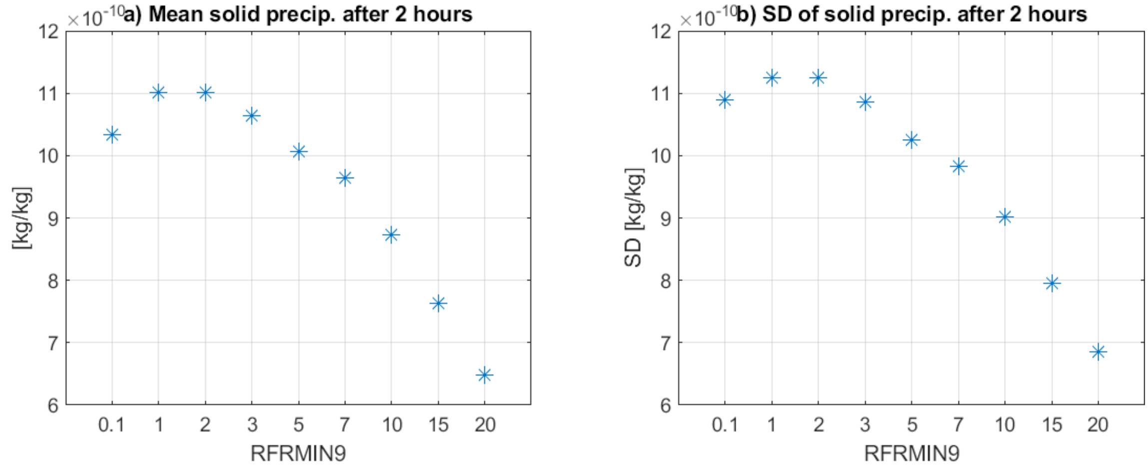

Figure 4.94: Sensitivity of a) mean of solid precipitation during 2 to 6 hours of simulation time, and b) standard deviation of solid precipitation during 2 to 6 hours of simulation time. After 2 h, a sudden increase in liquid precipitation is apparent in Figure 4.2.

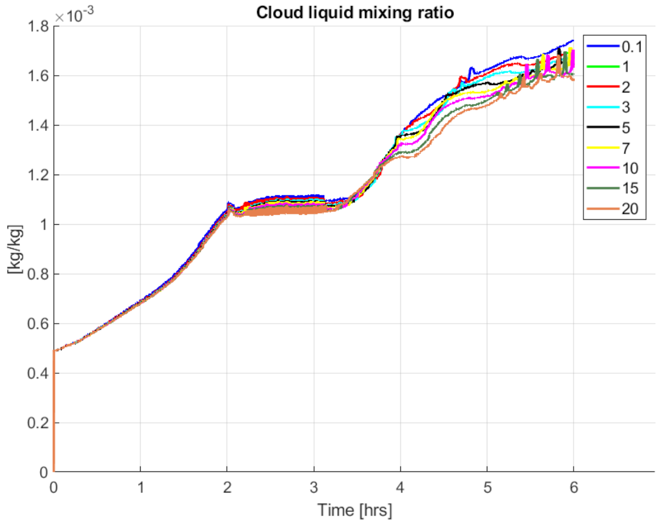

Figure 4.95: As Figure 4.91, but for the responses on cloud liquid mixing ratio [kg/kg] from perturbing the parameter RFRMIN(9). The cloud liquid mixing ratio has been summed for all 66 model layers.

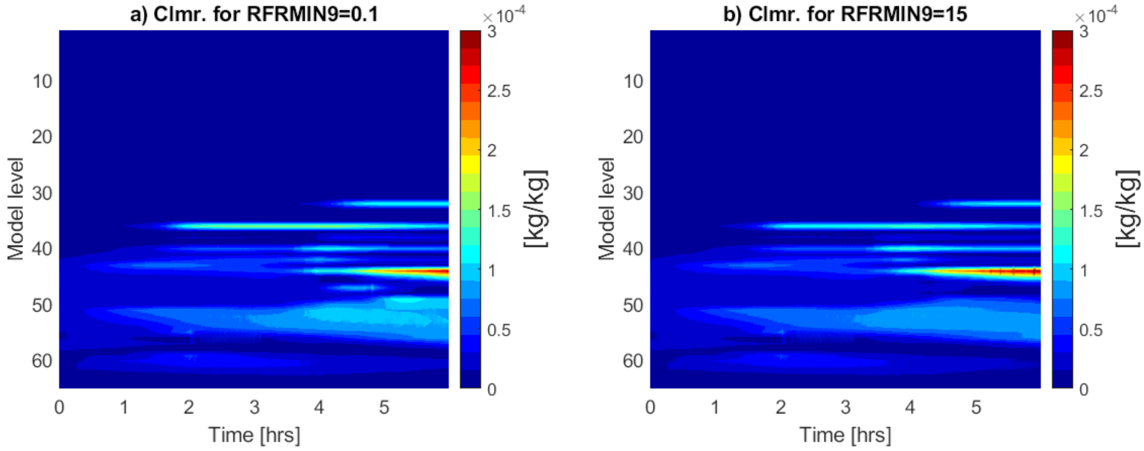

Figure 4.96: Vertical distribution of cloud liquid mixing ratio [kg/kg] from MUSC with a) RFRMIN(9) = 0.1 and b) RFRMIN(9) = 15.

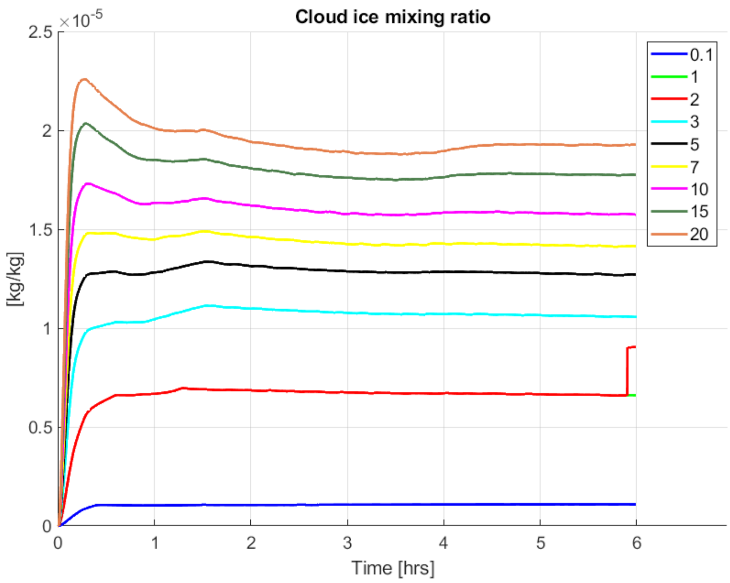

Figure 4.97: Same as Figure 4.91 but for a time series of cloud ice mixing ratio [kg/kg] from perturbing the parameter RFRMIN(9). The cloud ice mixing ratio has been summed for all 66 model layers.

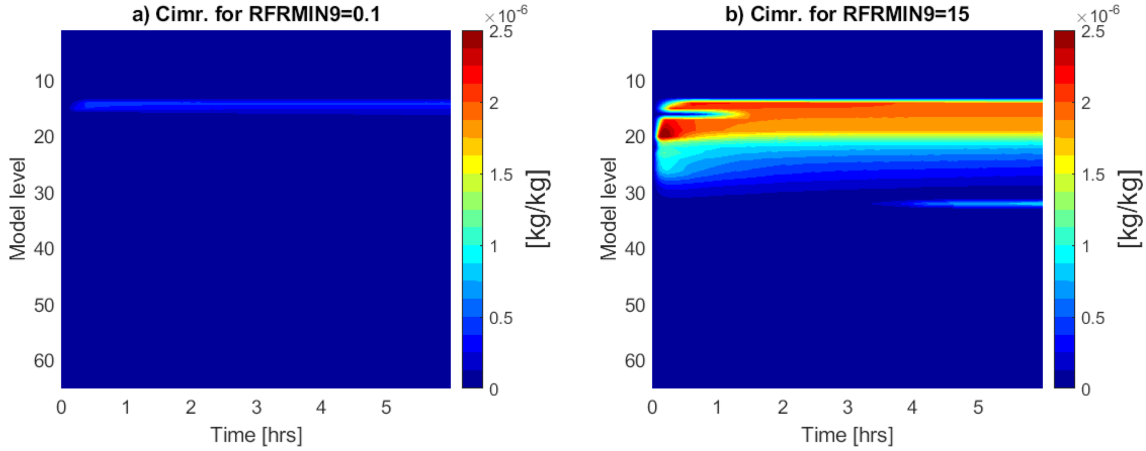

Figure 4.98: Vertical distribution of cloud lice mixing ratio [kg/kg] from MUSC with a) RFRMIN(9) = 0.1 and b) RFRMIN(9) = 15. In panel b), the cloud ice mixing ratio has greater values and in a greater vertical extent compared to panel a).

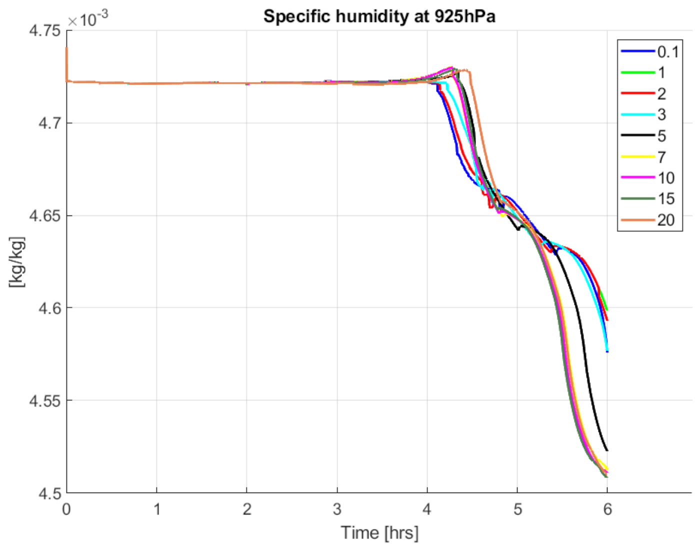

Figure 4.99: As Figure 4.91, but for the impact on specific humidity at 925 hPa [kg/kg] from perturbing the parameter RFRMIN(9).

Initial profiles for liquid precipitation, solid precipitation, and cloud liquid mixing ratio are zero for all values of RFRMIN(9) (not shown).

5 Summary table for statistical properties from perturbed variables

Tables for mean values and standard deviation for liquid precipitation, solid precipitation and ice water for the different sensitivity model runs at location N80W04 can be found in Tables 4-6 below.

Table 4: Liquid precipitation amounts from 2-6 hours (6 hour total simulation time) for location 80N04W

VSIGQSAT	0.01	0.02	0.04	0.06	0.08	0.10	0.12	0.18		
Mean(kg/kg 10^-3)	1.021	1.054	0.907	0.685	0.441	0.708	1.583	5.439		
SD(kg/kg10^-3)	0.109	0.344	0.594	0.655	0.294	0.768	2.519	10.819		
RADGR	0.1	0.3	0.5	0.7	1.0	1.5	2.0	3.0		
Mean(kg/kg 10^-3)	1.054	1.054	1.054	1.054	1.054	1.055	1.056	1.057		
SD(kg/kg 10^-3)	0.345	0.345	0.344	0.344	0.344	0.344	0.343	0.341		
RZC_H	0.11	0.13	0.15	0.17	0.20	0.23	0.25	0.40	0.60	
Mean(kg/kg10^-3)	1.054	1.047	1.046	1.047	1.068	1.078	1.069	1.040	1.033	
SD(kg/kg10^-3)	0.344	0.339	0.336	0.337	0.338	0.336	0.331	0.328	0.333	
RZL_INF	20	40	60	80	100	150	200	250	300	500
Mean(kg/kg10^-3)	1.101	1.054	1.038	1.045	1.139	1.189	1.227	1.162	1.309	1.172
SD(kg/kg10^-3)	0.392	0.344	0.341	0.372	0.469	0.511	0.525	0.386	0.552	0.392
RFRMIN(10)	1	2	5	10	20	30	50	100		
Mean(kg/kg10^-3)	1.036	1.037	1.042	1.054	1.077	1.099	1.138	1.230		
SD(kg/kg10^-3)	0.349	0.347	0.346	0.344	0.343	0.341	0.340	0.346		
RFRMIN(11)	0.01	0.1	0.3	0.5	0.7	0.9	1	1.5	2	

Mean(kg/kg10^-3)	1.051	1.054	1.054	1.056	1.056	1.057	1.054	1.044	1.040	
SD(kg/kg10^-3)	0.343	0.345	0.344	0.343	0.343	0.344	0.344	0.343	0.347	
XCCR	$8.0*10^{5}$	$4*10^{6}$	$8*10^{6}$	$4*10^{7}$	$8*10^{7}$	$4*10^{8}$	$8*10^{8}$	$4*10^{9}$	$8*10^{9}$	
Mean(kg/kg10^-3)	1.033	1.047	1.054	1.074	1.083	1.101	1.104	1.086	1.072	
SD(kg/kg10^-3)	0.334	0.341	0.344	0.345	0.358	0.366	0.367	0.362	0.363	
RFRMIN(21)	0	0.5	1	1.5	2	3	4	5	6	
Mean(kg/kg10^-3)	1.175	1.106	1.054	1.020	1.010	1.001	0.976	0.950	0.922	
SD(kg/kg10^-3)	0.350	0.342	0.344	0.349	0.352	0.337	0.327	0.316	0.308	
RFRMIN(9)	0.1	1	2	3	5	7	10	15	20	
Mean(kg/kg10^-3)	1.013	1.054	1.054	1.118	1.1655	1.198	1.234	1.273	1.301	
SD(kg/kg10^-3)	0.336	0.344	0.344	0.371	0.387	0.385	0.400	0.405	0.404	

Table 5: Solid precipitation amounts from 2-6 hours (6 hour total simulation time) for location 80N04W

VSIGQSAT	0.01	0.02	0.04	0.06	0.08	0.10	0.12	0.18		
Mean(kg/kg 10^-8)	2.469	0.101	25.654	35.560	0	0	0	0		
SD(kg/kg10^-8)	1.791	0.112	34.444	32.804	0	0	0	0		
RADGR	0.1	0.3	0.5	0.7	1.0	1.5	2.0	3.0		
Mean(kg/kg 10^-8)	0.1071	0.1098	0.1101	0.1102	0.1115	0.1093	0.1131	0.1133		
SD(kg/kg 10^-8)	0.109	0.112	0.112	0.112	0.115	0.112	0.117	0.116		
RZC_H	0.11	0.13	0.15	0.17	0.20	0.23	0.25	0.40	0.60	
Mean(kg/kg10^-8)	0.1101	0	0	0	0	0.0001	0.0001	0	0	
SD(kg/kg10^-8)	0.1056	0	0	0	0	0.0001	0.0002	0	0	
RZL_INF	20	40	60	80	100	150	200	250	300	500
Mean(kg/kg10^-8)	0.276	1.101	1.579	1.603	1.956	2.565	2.891	3.159	3.364	3.610
SD(kg/kg10^-8)	0.295	1.125	1.530	1.591	1.939	2.406	2.670	2.883	3.067	3.296
RFRMIN(10)	1	2	5	10	20	30	50	100		
Mean(kg/kg10^-8)	0.1165	0.1144	0.1121	0.1101	0.1019	0.0975	0.0862	0.0737		
SD(kg/kg10^-8)	1.208	1.157	1.137	1.125	1.054	1.015	0.933	1.001		
RFRMIN(11)	0.01	0.1	0.3	0.5	0.7	0.9	1	1.5	2	
Mean(kg/kg10^-8)	0.087	0.092	0.098	0.101	0.102	0.105	0.110	0.112	0.123	
SD(kg/kg10^-8)	0.091	0.095	0.102	0.104	0.104	0.107	0.112	0.113	0.113	
XCCR	$8.0*10^{5}$	$4*10^{6}$	$8*10^{6}$	$4*10^{7}$	$8*10^{7}$	$4*10^{8}$	$8*10^{8}$	$4*10^{9}$	$8*10^{9}$	
Mean(kg/kg10^-8)	0.150	0.122	0.110	0.076	0.059	0.029	0.024	0.018	0.016	
SD(kg/kg10^-8)	0.157	0.127	0.112	0.076	0.058	0.031	0.029	0.024	0.023	

RFRMIN(21)	0	0.5	1	1.5	2	3	4	5	6	
Mean(kg/kg10^-8)	0.097	0.101	0.110	0.105	0.111	0.110	0.110	0.108	0.105	
SD(kg/kg10^-8)	0.100	0.103	0.112	0.112	0.114	0.110	0.108	0.103	0.101	
RFRMIN(9)	0.1	1	2	3	5	7	10	15	20	
Mean(kg/kg10^-8)	0.103	0.110	0.110	0.106	0.100	0.096	0.087	0.076	0.064	
SD(kg/kg10^-8)	0.108	0.112	0.112	0.108	0.102	0.098	0.090	0.079	0.068	

Table 6: Ice water path from 2-6 hours (6 hour total simulation time) for location 80N04W

VSIGQSAT	0.01	0.02	0.04	0.06	0.08	0.10	0.12	0.18		
Mean(kg/kg 10^-3)	1.517	1.538	1.572	1.583	1.109	0.299	0.428	2.042		
SD(kg/kg10^-3)	0.019	0.016	0.006	0.015	0.014	0.023	0.226	1.374		
RADGR	0.1	0.3	0.5	0.7	1.0	1.5	2.0	3.0		
Mean(kg/kg 10^-3)	1.538	1.538	1.538	1.538	1.538	1.538	1.538	1.538		
SD(kg/kg 10^-3)	0.015	0.015	0.015	0.015	0.015	0.015	0.015	0.015		
RZC_H	0.11	0.13	0.15	0.17	0.20	0.23	0.25	0.40	0.60	
Mean(kg/kg10^-3)	1.538	1.538	1.537	1.537	1.538	1.545	1.552	1.570	1.574	
SD(kg/kg10^-3)	0.015	0.015	0.015	0.015	0.014	0.016	0.019	0.044	0.049	
RZL_INF	0.11	0.13	0.15	0.17	0.20	0.23	0.25	0.40	0.60	
Mean(kg/kg10^-3)	1.540	1.538	1.535	1.532	1.531	1.531	1.530	1.531	1.539	1.529
SD(kg/kg10^-3)	0.353	0.344	0.341	0.372	0.469	0.511	0.525	0.386	0.552	0.392
RFRMIN(10)	1	2	5	10	20	30	50	100		
Mean(kg/kg10^-3)	1.538	1.538	1.538	1.538	1.538	1.538	1.538	1.538		
SD(kg/kg10^-3)	0.015	0.015	0.015	0.015	0.015	0.015	0.015	0.015		
RFRMIN(11)	0.01	0.1	0.3	0.5	0.7	0.9	1	1.5	2	
Mean(kg/kg10^-3)	1.538	1.538	1.538	1.538	1.538	1.538	1.538	1.538	1.538	
SD(kg/kg10^-3)	0.015	0.015	0.015	0.015	0.015	0.015	0.015	0.015	0.015	
XCCR	$8.0*10^5$	$4*10^6$	$8*10^6$	$4*10^7$	$8*10^7$	$4*10^8$	$8*10^8$	$4*10^9$	$8*10^9$	
Mean(kg/kg10^-3)	1.538	1.538	1.538	1.538	1.538	1.538	1.538	1.538	1.538	
SD(kg/kg10^-3)	0.015	0.015	0.015	0.015	0.015	0.015	0.015	0.015	0.015	
RFRMIN(21)	0	0.5	1	1.5	2	3	4	5	6	
Mean(kg/kg10^-3)	1.547	1.537	1.538	1.541	1.546	1.550	1.555	1.560	1.566	
SD(kg/kg10^-3)	0.014	0.016	0.015	0.014	0.013	0.015	0.017	0.016	0.015	
RFRMIN(9)	0.1	1	2	3	5	7	10	15	20	
Mean(kg/kg10^-3)	0.247	1.538	1.551	2.470	2.962	3.291	3.655	4.089	4.407	

SD(kg/kg10^-3)	0.002	0.015	0.083	0.025	0.027	0.027	0.026	0.028	0.037	

References

Kokkvoll Engdahl, B. J. K., Thompson, G. and Bengtsson, L., 2020: Improving the representation of supercooled liquid water in the HARMONIE-AROME weather forecast model, Tellus A: Dynamic Meteorology and Oceanography, 72:1, 1-18, https://doi.org/10.1080/16000870.2019.1697603

Gleeson, E., Outten, S., Kokkvoll Engdahl, B. J., Whelan, E., Andrae, U., and Rontu, L.: HARMONIE-AROME single-column tools and experiments, Adv. Sci. Res., 17, 255–267, https://doi.org/10.5194/asr-17-255-2020, 2020.

Müller, M., Y. Batrak, J. Kristiansen, M.A. Køltzow, G. Noer, and A. Korosov, 2017: Characteristics of a Convective-Scale Weather Forecasting System for the European Arctic. Mon. Wea. Rev., 145, 4771–4787, https://doi.org/10.1175/MWR-D-17-0194.1

Acknowledgements

TV, MK and HS acknowledge support from the Norwegian Research Council through the ALERTNESS project in the POLARPROG program (Project 280573).